Title

PART I. X-RAY PHOTOELECTRON SPECTROSCOPIC STUDIES OF NITROGEN, PHOSPHORUS, BORON, AND CHROMIUM COMPOUNDS. PART II. AN INTERPRETATION OF THE PROTON MAGNETIC RESONANCE SPECTRA OF PENTAAMMINES OF COBALT (III), RHODIUM(III), AND IRIDIUM(III).

Permalink

https://escholarship.org/uc/item/5bp6c442

Author

Hendrickson, David Norman.

Publication Date

1969-08-01

$ey. 2$

PART I. X-RAY PHOTOELECTRON SPECTROSCOPIC STUDIES OF
NITROGEN, PHOSPHORUS, BORON, AND CHROMIUM COMPOUNDS

PART II. AN INTERPRETATION OF THE PROTON MAGNETIC
RESONANCE SPECTRA OF PENTAAMMINES OF COBALT(III),
RHODIUM(III), AND IRIDIUM(III)

David Norman Hendrickson
(Ph. D. Thesis)

August 1969

LAWRENCE RADIATION LABORATORY

UNIVERSITY of CALIFORNIA BERKELEY

DISCLAIMER

TABLE OF CONTENTS

TABLE OF CONTENTS (continued)

PART I.

X-RAY PHOTOELECTRON SPECTROSCOPIC STUDIES OF NITROGEN, PHOSPHORUS, BORON, AND CHROMIUM COMPOUNDS

David Norman Hendrickson

Inorganic Materials Research Division, Lawrence
Radiation Laboratory and Department of Chemistry,
University of California, Berkeley, California

ABSTRACT

Nitrogen, phosphorus, boron, and chromium compounds have been studied using x-ray photoelectron spectroscopy. Nitrogen $1s$ electron binding energies have been correlated with nitrogen atom charges calculated from CNDO and extended Hückel molecular orbital eigenfunctions. These correlations and the measured nitrogen $1s$ binding energies for sodium oxyhyponitrite ($Na_2N_2O_3$) have been used to establish the structure of the $N_2O_3^{2-}$ ion. Binding energy data for some nitrogen-containing metal-coordinated ligands have been used to characterize the bonding in these ligands. Phosphorus $2p$ electron binding energies are reported for 53 phosphorus compounds. Phosphorus atom charges, calculated for some of the compounds by means of a non-iterative as well as an iterative extended Hückel molecular orbital method, have been correlated with the measured phosphorus $2p$ binding energies. Boron $1s$ and chromium $3p$ electron binding energies have been correlated with boron and

chromium atom charges calculated by various molecular orbital methods.

It has been shown by making several approximations that it is possible to calculate, from available thermodynamic data, a "thermochemical energy" corresponding to the core-electron binding energy for an atom in a compound. For a given element, a linear relation to experimental binding energies has been established for these calculated "thermochemical energies." With this approach various thermodynamic data have been predicted from experimentally-determined binding energies.

I. INTRODUCTION

The earliest studies of the energy distribution of photo-electrons from x-radiation of solids was carried out by Robinson[1] in England and by de Broglie[2] in France from the 1910's. These early studies were somewhat discouraging and as such the field was abandoned until 1951 when Siegbahn[3] set out to overcome the initial experimental difficulties. In 1954 the first high-resolution photoelectron measurements were completed using an iron-free double-focusing electron spectrometer.[3,4] It was found that core-electron binding energies could be readily determined from a knowledge of the energy of the photoelectrons as determined in the electron spectrometer.[3]

In 1958 the first chemical shifts of core-electron binding energies were reported by Nordling et al[5] in measurements of Cu levels in Cu, Cu_2O, and CuO. Qualitatively they found that the binding energy for a particular copper core-electron increased with increasing copper oxidation state. Since this initial work, extensive studies of chemical shifts associated with atomic core-electron binding energies have been made by Siegbahn et al[3] using x-ray photoelectron spectroscopy (XPS). Core-electron binding energies have been shown to be correlated to formal oxidation states in sulfur[3,6] and chlorine[3,7] compounds and to fractional atomic charges in sulfur[3] and nitrogen[3,8] compounds. The method for calculating the fractional atomic charges was a modification of Pauling's method.[9]

Considering the empirical nature of the Pauling method for calculating fractional atomic charges, it seemed useful to secure molecular atomic charges by more sophisticated methods. A further check of the apparent correlation of XPS-measured core-electron binding energies with atomic charges would then be possible. This was one of the goals of the present work. In addition we hoped to investigate the ability of XPS to elucidate chemical structure and bonding in some inorganic systems. Development of a working under-standing of some of the factors that determine a core-electron binding energy (particularly in solids) was the ultimate goal.

In this work the results of extensive measurements of nitrogen 1$\underline{s}$, boron 1$\underline{s}$, phosphorus 2$\underline{p}$, and chromium 3$\underline{p}$ electron binding energies are reported. Atomic charges resultant from complete valence orbital basis molecular orbital calculations are correlated with these core-electron binding energies. The molecular structure of the oxyhyponitrite ion, $N_2O_3^{2-}$, as well as the bonding char-acteristics of some metal-coordinated ligands are investigated. Finally, a thermodynamic interpretation of chemical shifts in core-electron binding energies is advanced.

II. EXPERIMENTAL

The experimental aspects of the determination of inner-electron binding energies have been reviewed by Siegbahn et al.[3] In this work MgK$_\alpha$ x-radiation (1253.6 eV.) was used. The kinetic energy of the photoelectrons was measured in an iron-free, double-focusing magnetic spectrometer[4] shown schematically in Figure 1. The instrumental line width, including the contribution from the x-ray line, was about 1 eV.,[3] and the observed photoelectron lines had widths of 1.5-2.5 eV. Photoelectrons were counted[10] typically for time intervals of 12 sec. at each magnetic field setting, and the spectrometer current in the range 1.0-1.5 A was varied in increments of 0.2 mA.

The compounds studied were either purchased or prepared by standard syntheses. Many phosphorus compounds were kindly provided by Dr. J. Van Wazer. Trans-$Mn(CO)_4P(C_6H_5)_3Cl$, (cis-PP)$Mn(CO)_3I$[11], and $Mn(CO)_3(AP)I$[11] were supplied by Dr. G. Nelson, and compounds 46-50 were obtained from L. Kramer. The boron studies were aided by gifts of many compounds from Dr. M. F. Hawthorne.

Spectrometer samples were prepared by brushing the powdered material onto double-faced conducting tape attached to an aluminum plate that served as a heat and electron sink. Three measurements were made for each sample; in each case the carbon 1s line (arising from pump oil which forms a film on the samples) was recorded. The film of pump oil provides a convenient reference peak and probably also acts to remove surface charging that may arise with
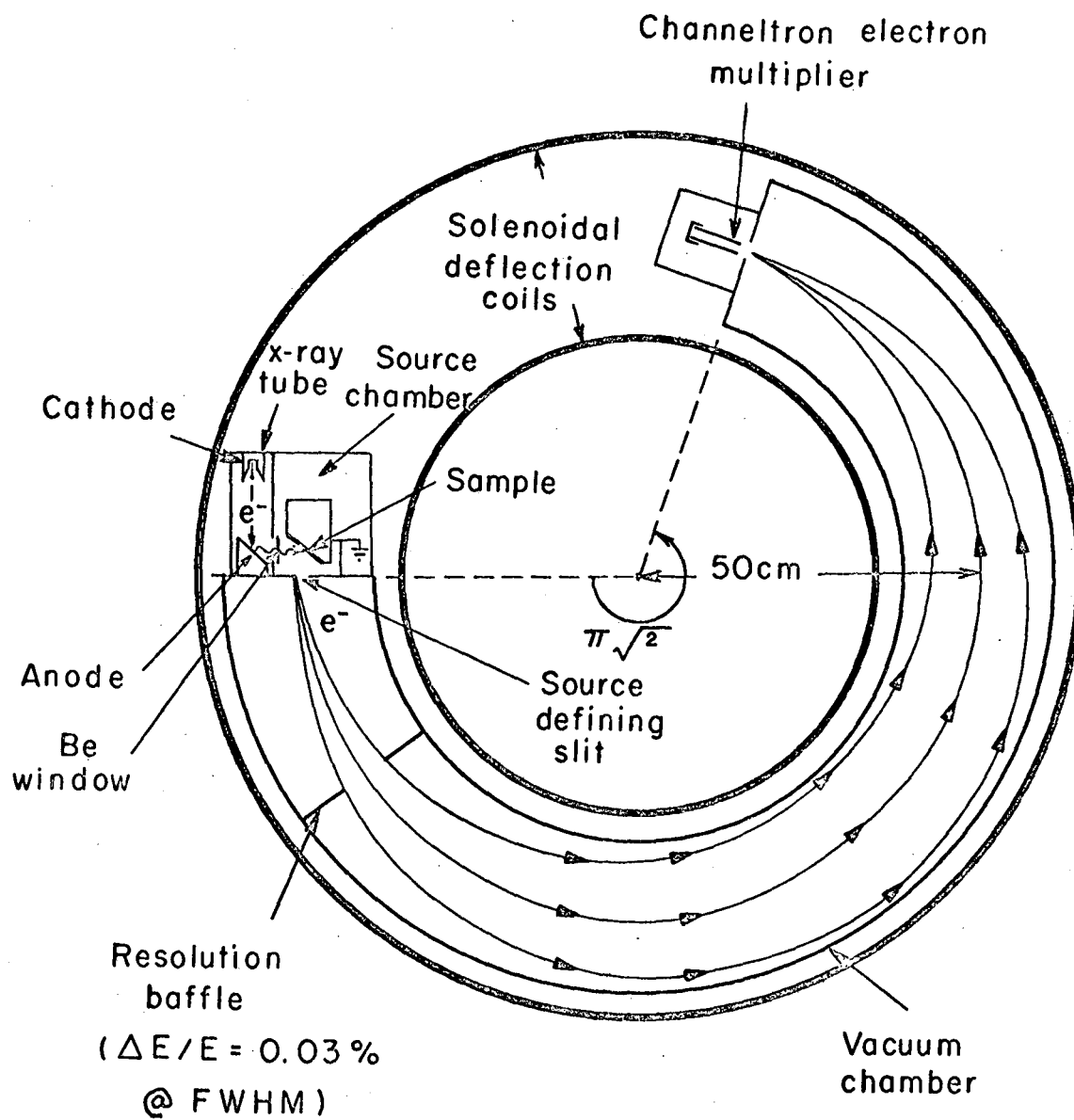
XBL694-2402

Figure 1. Schematic illustration of the experimental setup.

insulating samples. By this method it is possible to locate the photoelectron peaks reproducibly to within 0.2 eV.

In the case of three compounds it was necessary to cool the sample to prevent sublimation in the spectrometer. The compounds $(CH_3)_3NBF_3$, $B_{10}H_{14}$, and $Cr(CO)_6$ were loaded into the source house under dry nitrogen and cooled to $\approx-60°C$ before opening to the vacuum.

Photoelectrons originate from sites near the surface (i.e. a layer $\approx100Å$ thick)[3], thus it was necessary to continuously clean the surface of a piece of chromium foil in order to see a peak that could be assigned to the unoxidized metal. This was accomplished by heating the chromium foil to $\approx650°C$ for many hours in an $\approx10^{-2}$ torr hydrogen atmosphere. The disappearance of the oxide layer was monitored by the $O_{1\underline{s}}$ line. Chromium hydride formation would be negligible for the solubility of hydrogen in chromium metal at 650°C is nominal.[12]

The work function for the spectrometer material (aluminum) was assigned the value 4.0 eV. This normalization gives the best agreement of our nitrogen core-electron binding energies with previously measured values for the same compounds (in particular the nitrogen compounds[8]), and makes it possible to include some of the binding energies of Siegbahn et al[3] in the correlations with our calculated charges.

III. THEORY

Because we are dealing with measurements on solid materials, the calculated electron binding energies are referred to the Fermi levels of the solids. We calculated the electron binding energies, E_B, from the relation[3]

$$E_B = E_{x-ray} - E_{kin} - \phi_{spec} \tag{1}$$

where E_{x-ray} is the incident x-ray energy, E_{kin} is the kinetic energy of the photoelectron, and ϕ_{spec} is the work function of the spectrometer material, aluminum. The core-electron binding energies are dependent on the chemical environment, and previous discussions have shown that they are principally determined by the potential associated with the valence shell electron density and the crystal field felt by the core electrons.[3,1]

For binary salts, Siegbahn and co-workers[3,8] have formulated a relation between the electronic charge (q) removed from the valence shell of an atom and the energy shift (ΔE) of the core electrons of that atom:

$$\Delta E = \left(\frac{1}{r} - \frac{\alpha}{R}\right)q \tag{2}$$

Here r is the radius of the valence shell, and α is the contribution to the Madelung constant from the atom at the internuclear distance

R. With this classical charged-sphere model a relation is expected between the measured core-electron binding energy and the valence-electron charge density.

In order to gain some insight into the effect lattice energies would have on any attempted correlation of measured core-electron binding energy with calculated atomic charge, it is useful to consider a certain thermochemical cycle. A thermochemical cycle can be constructed for the situation where an atom is bonded in an anionic, a neutral, or a cationic molecule in a crystal. We will consider only the first two cases in this section.

For the anionic site case the following thermochemical cycle can be written (where we consider a lattice AX in which interchange of the cations and anions yields an indistinguishable lattice)

$$
\begin{array}{ccc}
A^-(\text{lattice}) & \xrightarrow{\;E_B\;} & A^*(\text{lattice}) + e^-(\text{Fermi}) \\[1em]
\Big\downarrow U & & \Big\uparrow {-E - \phi_{\text{sample}}} \\[1em]
A^-(g) + \text{hole} & \xrightarrow{\;\epsilon\;} & A^*(g) + \text{hole} + e^-(g)
\end{array}
$$
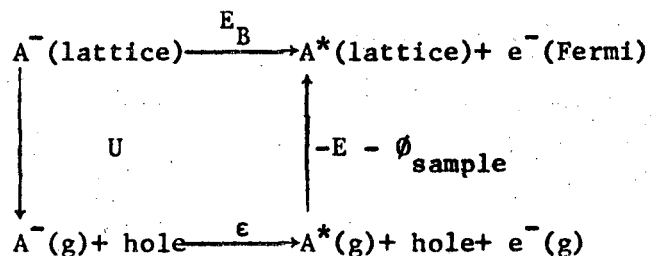
Here E_B is the measured electron binding energy referred to the Fermi level, U is the usual lattice energy, ϵ is a gas phase core-electron ionization potential (an asterisk signifies that a core-electron is missing), E is the lattice energy associated with putting A^* (g) back into the lattice, and ϕ_{sample} is the work function of the sample material. The energy $(-\phi_{\text{sample}})$ is obtained when the electron is re-referenced from the vacuum level to the Fermi

level. The binding energy in this simple model can be represented as

$$E_B(\text{anion}) = U+\epsilon-E-\phi_{\text{sample}} \qquad (3)$$

For the case of a neutral site we find using a similar thermochemical cycle that we have

$$E_B(\text{neutral}) = E_{\text{subl.}}+\epsilon'-E'-\phi_{\text{sample}} \qquad (4)$$

Here the lattice energy U has been replaced by the sublimation energy, $E_{\text{subl.}}$, for a neutral molecule.

Consider the hypothetical case of an anionic-site atom and a neutral-site atom where both atoms have the same effective valence-electron charge density. The difference in binding energies $\Delta E_B = E_B(\text{anion}) - E_B(\text{neutral})$ would be given by

$$\Delta E_B = (U-E_{\text{subl.}})+(\epsilon-\epsilon')+(E'-E)+(\phi'-\phi) \qquad (5)$$

Since we seek only a qualitative understanding of the effects of lattice potentials on measured core-electron binding energies, we will assume that the two materials have the same work functions. This is necessitated of course by the lack of available data. Since the lattice terms E and E' are expected to be small (i.e., essentially sublimation energies) and comparable we will also neglect them. The difference in binding energies then reduces to

$$\Delta E_B = (U - E_{subl.}) + (\varepsilon - \varepsilon') \qquad (6)$$

The gas phase core-electron ionization potentials ε and ε' are influenced by the valence charge density in the molecule.[14,15] If as expected, they are dependent to first order on the immediate valence-electron density for a particular atom, then in our hypothetical case $(\varepsilon - \varepsilon') \approx 0$ since we have assumed both atoms (i.e. the anionic site and neutral site atoms) have the same valence-electron density.

With all of these assumptions we conclude that E_B for the anonic-site atom would be greater than E_B for the neutral-site atom if both atoms have the same effective valence-electron density. However, extreme caution must be exercised in accepting this conclusion. Certainly the gas phase core-electron ionization potentials depend on more factors than merely the immediate valence-electron density around an atom. Many other factors will influence the core-electron binding energies. Nevertheless this thermochemical cycle approach is useful. In fact appropriate modifications of the cycle can give a cycle where a "thermochemical energy" corresponding to the core-electron binding energy for an atom in a compound can be calculated. This latter approach will be discussed in Section VII.

IV. NITROGEN 1s ELECTRON BINDING ENERGIES. CORRELATIONS WITH MOLECULAR ORBITAL-CALCULATED NITROGEN CHARGES.

A. Introduction

In this section nitrogen 1s binding energies are reported for an extensive list of compounds. This compilation of nitrogen binding energies augments and to a certain degree overlaps the nitrogen 1s binding energies of Nordberg et al.[8] Correlations are established between nitrogen atomic charges calculated from CNDO[16] and extended Hückel[17] molecular-orbital eigenfunctions. We use these correlations and the observed nitrogen 1s binding energies for sodium oxyhyponitrite ($Na_2N_2O_3$) to establish the structure of the $N_2O_3^{2-}$ ion. In addition, we use binding energy data for some nitrogen-containing metal-coordinated ligands to characterize the bonding in the ligands.

B. Calculations

Molecular orbital eigenfunctions were obtained from CNDO[16] and extended Hückel[17] calculations. In both cases computations were performed with a CDC 6400 computer using a Fortran IV program. Calculation details and required input data for the CNDO calculations are given in reference 16. In the extended Hückel calculations, the Coulomb integrals H_{ii}, were approximated by the valence state ionization potentials calculated by Hinze and Jaffe.[18] The arithmetic

mean approximation for the off-diagonal elements of the Hamiltonian matrix was used:[19]

$$H_{ij} = 1.75 \, S_{ij} (H_{ii} + H_{jj})/2 \qquad (7)$$

Here S_{ij} is the overlap integral between the ith and jth atomic orbitals.

Net atomic charges were obtained by subjecting the extended Hückel molecular orbitals to a Mulliken population analysis.[20] In the CNDO method there is no overlap population, and as such the net atomic charges are easily obtained from the appropriate diagonal elements of the charge density matrix.

Cartesian coordinates for complicated systems were obtained from program PROXYZ,[21] coupled with experimental[22] or estimated molecular parameters.

C. Results and Discussion

Correlation with Atomic Charges - Extended Hückel calculations were completed for 28 nitrogen compounds; the calculated nitrogen atom charges and the measured nitrogen $\underline{1s}$ binding energies are listed in Table I. Some binding energies determined in previous studies are also given with the corresponding calculated nitrogen charges. A linear correlation between $\underline{1s}$ nitrogen binding energies and extended Hückel-calculated nitrogen charges is demonstrated in Figure 2.

TABLE I.

Nitrogen 1s Binding Energies and Calculated Charges

Compound Number	Compound	Binding Energy, eV.	Calculated Nitrogen Atom Charge	
			CNDO	Extended Hückel[g]
1	$NaNO_3$	407.4	+0.429	+2.557
2	$NaNO_2$	404.1	+0.100	+1.273
3	$Na_2(ON\underline{N}O_2)$	403.9	+0.140	+1.749
3	$Na_2(O\underline{N}NO_2)$	400.9	-0.195	-0.090
4	$Na(N\underline{N}N)$	403.7	+0.096	+1.066
4	$Na(\underline{N}N\underline{N})$	399.3	-0.548	-1.033
5	$Na_2N_2O_2$	401.3	-0.256	+0.175
6	KCN	399.0	-0.518	-1.181
7	KOCN	398.3	-0.550	-1.572
8	$\underline{p}-HOC_6H_4NO_2$	405.3[a]	+0.353	+1.541
9	$C_6H_5NO_2$	405.1[a]	+0.347	+1.613
10	$\underline{n}-C_5H_{11}ONO$	403.7[a]	+0.288[b]	+1.323[b]
11	$N_2H_6SO_4$	402.5	+0.094	+0.184
12	$(CH_3)_3NO$	402.2[a]	+0.079	+0.520
13	$\underline{N}H_4NO_3$	402.3	+0.039	-0.145
13	$NH_4\underline{N}O_3$	407.2	+0.429	+2.557
14	$(CH_3)_4NB_3H_8$	402.2	+0.185	-0.253

Compound Number	Compound	Binding Energy, eV.	Calculated Nitrogen Atom Charge	
			CNDO	Extended Hückel
15	NH_3OHCl	402.1	+0.219	+0.612
16	$(CONH_2)_2$	400.0	−0.133	−0.550
17	$(NH_2)_2CNCN$	399.2(broad)	−0.17 to −0.31[c]	−0.71 to −1.56[c]
18	C_6H_5CN	398.4[a]	−0.226	−1.356
19	C_5H_5N	398.0[a]	−0.166	−1.098
20	KSCN	398.5		−1.672(−1.711)
21	$NH_3(s)$	398.8	−0.079	−0.914
22	S_4N_3Cl	399.6		−0.912,−1.03[d] (−0.915,−0.984)
23	NH_3SO_3	401.8		−0.262(−0.307)
24	$C_6H_5CONH_2$	399.4	−0.238	−0.236
25	$(NPCl_2)_3$	399.5		−1.718(−1.741)
26	$C_5H_5N\cdot HCl$	400.2	+0.035	−0.352
27	BN	398.2		−1.4[f]
28	$Na_3(PO_2NH)_3$	398.5		−0.971(−1.058)[e]

[a] Data of Siegbahn et al.[3]

[b] Charge calculated for CH_3ONO, the structure of which is known.

[c] The four structurally-different nitrogen atoms of this molecule bear different calculated charges.

[d] There are two different nitrogen atoms.

[e] Calculated for $r_{P-N} = 1.50Å$.

f Treated approximately, see results and discussion section.

g Number in parenthesis is for case where 3$\underline{d}$ orbitals are included.
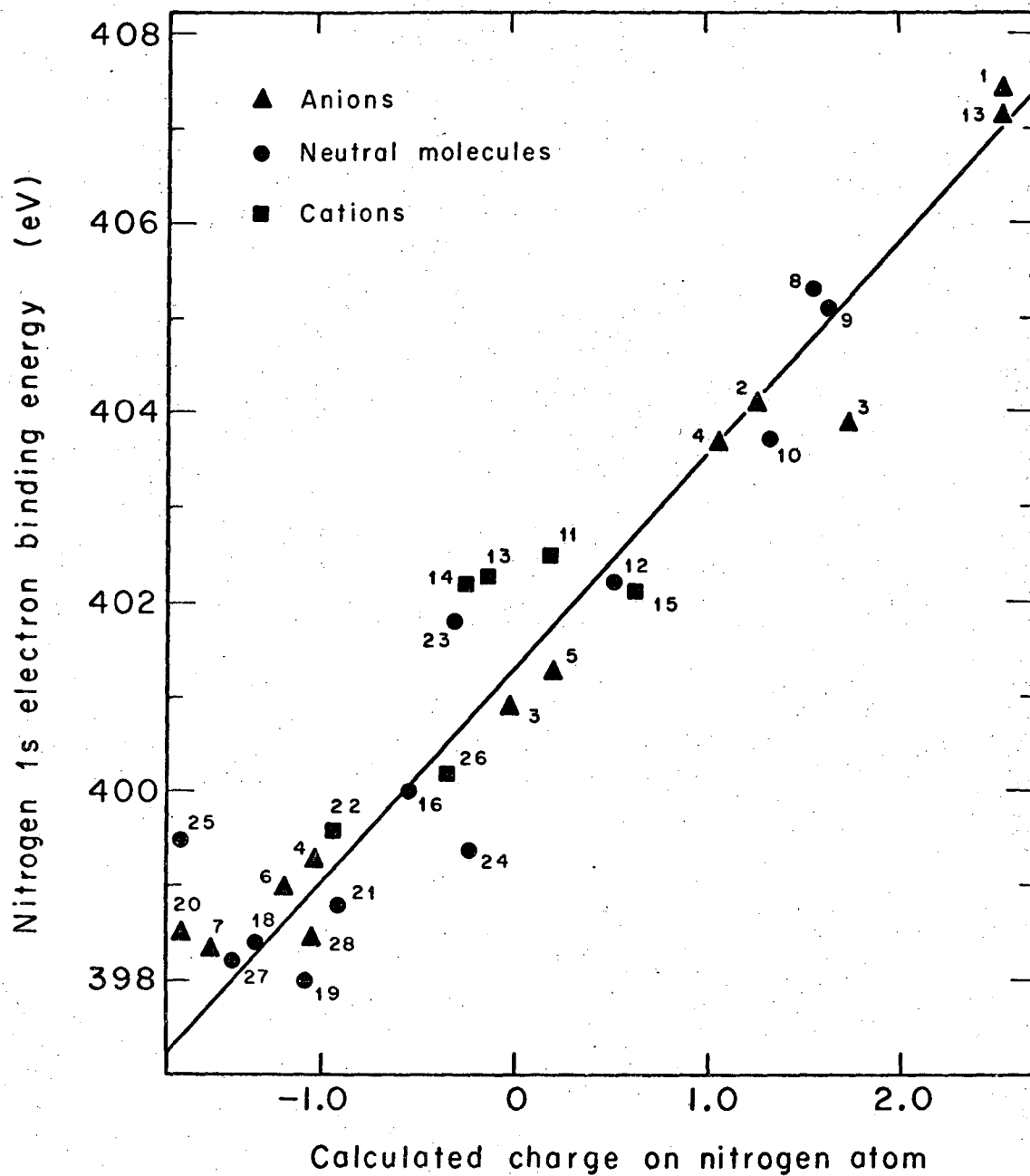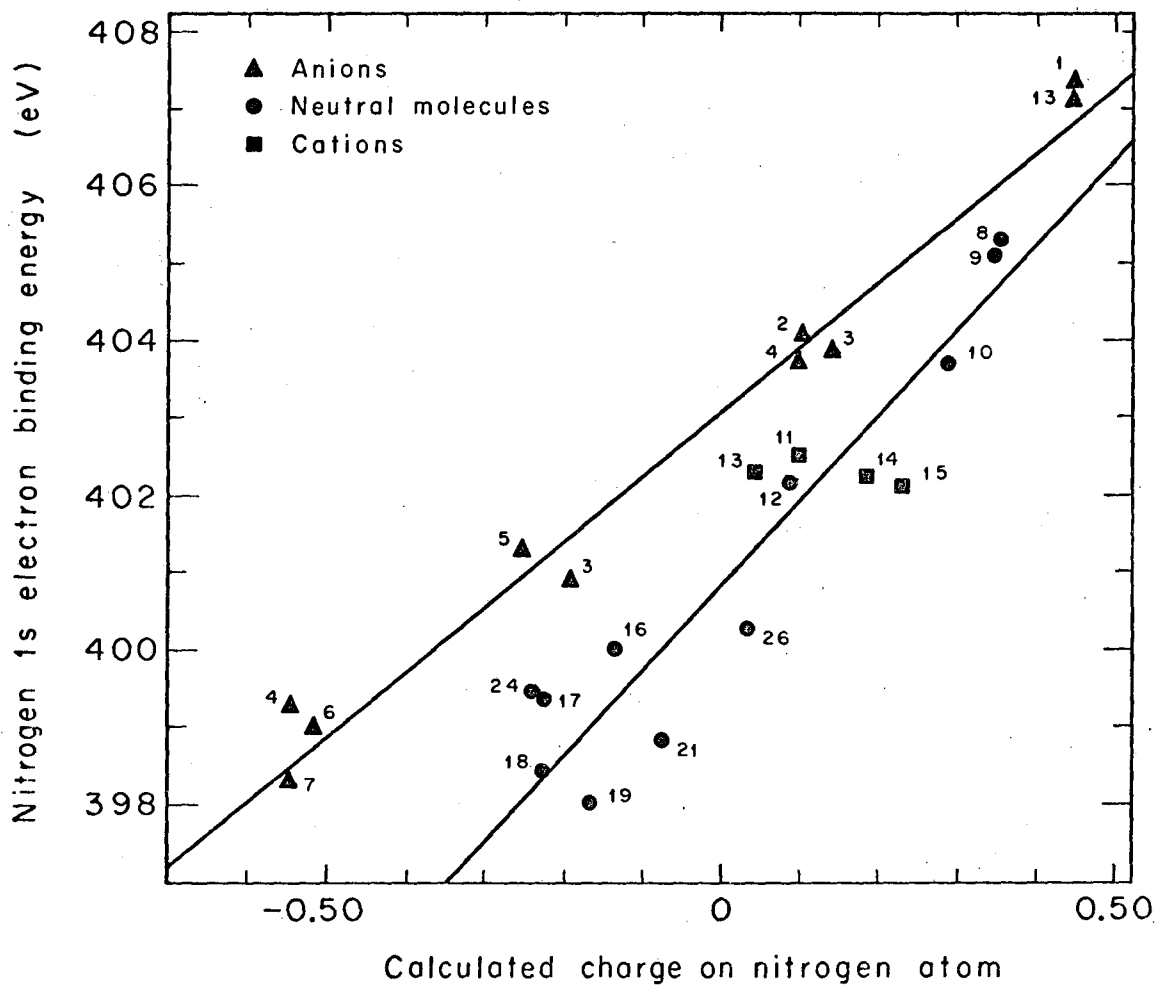
XBL695-2645

Figure 2. Plot of nitrogen 1s binding energies vs. extended Hückel-calculated charges on nitrogen atoms.

The range of nitrogen 1s binding energies covered by this correlation plot is approximately 10 eV., extending from the nitrate ion to pyridine. This is about the same range covered by Nordberg et al[8] in their correlation of nitrogen 1s binding energy with fractional atomic charge calculated by a modification of Pauling's method. In the case of our extended Hückel plot the correlation seems to be linear, whereas the correlation obtained by Nordberg et al shows curvature. In addition, the extended Hückel calculations assign charges to the nitrogens in n-amyl nitrite, nitrite ion, cyanide ion and azide ion that fit reasonably well on the line, whereas their fit on the modified Pauling plot is poor. It will be noted that the extended Hückel calculations give reasonably good fit for nitrogen molecules that contain sulfur or phosphorus atoms. In these cases it was found (See Table I) that inclusion of 3d orbitals on the sulfur or phosphorus atoms did not appreciably change the calculated nitrogen atom charges.

There are qualifications that need be stated regarding two of the compounds. In the case of boron nitride the graphite-like structure was only approximated; only 24 atoms were considered in calculating the charge on a central nitrogen atom. The crystal structure of compound 28, $Na_3(PO_2NH)_3$, has not been reported; we assumed a cyclic anion with the bond distances r_{N-H} = 1.0Å and r_{P-O} = 1.5Å, coupled with two different P-N distances, 1.5 and 1.7Å (cf 1.65Å for r_{P-N} in $(NPCl_2)_3$[22]). The calculations of the nitrogen charges gave for these two cases -0.971 and -0.984, respectively (without considering 3d orbitals on the phosphorus atoms).

The nitrogen charges obtained from the extended Hückel cal-
culations range from -1.7 to almost +2.6. This range is to be con-
trasted with the much smaller charge range calculated from the
CNDO molecular orbitals which were obtained for the same molecules
(See Table I). As noted earlier,[23] the CNDO correlation plot
(Figure 3) shows two lines - one characteristic of anions, and the
other characteristic of neutral molecules and possibly cations.
Two rationalizations can be formulated: (a) the two lines are
merely an artifact of the CNDO method due to an inherent overemphasis
of electron repulsion in the CNDO calculations of anionic molecules;
(b) the two lines are an indication of differing lattice potentials
associated with a core-electron at either an anionic or neutral site
(See Theory Section).

It is difficult at this time to indicate clearly the cause of
the two CNDO lines. The fact that the extended Hückel data show
no indication of the same behavior can probably only be taken as
evidence of the simplicity of the latter calculations, at least
insofar as this version of the extended Hückel method is concerned.
Previous work by Siegbahn and co-workers[3] have shown that the expected
differences in crystal potentials do not appear in the measured
values (i.e., S_{2p} binding energies in a series of sulfates).
This can also be seen in our N $1s$ data for the three nitrates,
compounds 1, 13, and 29. Even further evidence for this lack of
expected lattice potential influence can be seen in the data for
the series of nitrocobaltic ammines, compounds 33, 34, 36, 37,
and 47. Throughout this series the measured nitrogen $1s$ binding

Figure 3. Plot of nitrogen 1s binding energies vs. CNDO-calculated charges on nitrogen atoms.

XBL695-2642

TABLE II.

Nitrogen 1s Binding Energies

Compound Number	Compound	Binding Energy(ev)
29	$[Rh(NH_3)_6](\underline{N}O_3)_3$	407.3
30	trans $[Co(en)_2(NO_2)_2]\underline{N}O_3$	406.8
31	$p-\underline{N}O_2-C_6H_4CONH_2$	405.9
32	$[Rh(NH_3)_5\underline{N}O_2]Br_2$	404.4
33	$Co(NH_3)_3(\underline{N}O_2)_3$	404.1
34	$[Co(NH_3)_5\underline{N}O_2]Cl_2$	404.0
35	$K[Co(NH_3)_2(\underline{N}O_2)_4]$	404.0
36	$K_3Co(NO_2)_6$	404.0[a]
37	trans $[Co(NH_3)_4(\underline{N}O_2)_2]SO_4$	403.9
30	trans $[Co(en)_2(\underline{N}O_2)_2]NO_3$	403.8
38	$Na_2[Fe(CN)_5\underline{N}O]\cdot 2H_2O$	403.3
39	S_4N_4	402.1
40	$[Co(NH_3)_5\underline{N}O]Cl_2$	402.0
41	$C_6H_5NH_2NH_2\cdot HCl$	401.4[b]
42	$K_3[Cr(CN)_5\underline{N}O]$	400.7
29	$[Rh(\underline{N}H_3)_6](NO_3)_3$	400.7
43	$[Ir(NH_3)_5Cl]Cl_2$	400.6
44	N-N-B-(-N-N-)$_3$W(CO)$_2$NO	400.6[c]

Compound Number	Compound	Binding Energy(ev)
30	trans $[Co(\underline{en})_2(NO_2)_2]NO_3$	400.4
32	$[Rh(\underline{NH}_3)_5NO_2]Br_2$	400.3
45	$S_4N_4 \cdot SbCl_5$	400.2
46	S_7NH	400.2
40	$[Co(\underline{NH}_3)_5NO]Cl_2$	400.2
33	$Co(\underline{NH}_3)_3(NO_2)_3$	400.2
35	$K[Co(\underline{NH}_3)_2(NO_2)_4]$	400.0
34	$[Co(NH_3)_5NO_2]Cl_2$	400.0
47	$[Co(NH_3)_6]_2(SO_4)_3$	400.0
48	$[Co(NH_3)_5Cl]Cl_2$	400.0
37	trans $[Co(\underline{NH}_3)_4(NO_2)_2]SO_4$	399.9
49	$Cr(NH_3)_6Cl_3$	399.9
31	$p-NO_2-C_6H_4CO\underline{NH}_2$	399.6
50	$S_4N_4H_4$	399.5
51	$(NPCl_2)_4$	399.2
52	$K_3[Cr(CN)_6]$	398.6
42	$K_3[Cr(C\underline{N})_5NO]$	398.4
38	$Na_2[Fe(C\underline{N})_5NO] \cdot 2H_2O$	398.2
53	P_3N_5	397.8
54	$K_4[Fe(CN)_6]3H_2O$	397.6
55	VN	397.2[d]
56	CrN	396.6

a   A small peak attributable to nitrate impurity was observed
    at 407.0ev.

b   Very broad peak.

c   Only one relatively sharp peak observed.

d   A decomposition product peak at 401.0ev was observed.

energy for either the coordinated NH_3 or NO_2^- is approximately

constant. There is little evidence of discontinuity in the binding

energies at the transition from a neutral to an anionic site.

Character of Metal-Coordinated Ligands - The power of the

x-ray photoelectron method can be clearly seen in Figure 4, where

we give the nitrogen 1s spectrum of trans-$[Co(en)_2(NO_2)_2]NO_3$.

Measurement of the nitrogen 1s binding energy of various metal-

coordinated ligands can give insight into the character of the

ligands. The binding energies of some metal-coordinated ammonia

groups are listed in Table II. Comparison of these nitrogen binding

energies with those obtained for the free ligand and for the ammonium

ion (See Table I) as it exists in NH_4NO_3 shows that coordination

of ammonia to Co(III), Rh(III), Ir(III), and Cr(III) gives partial

ammonium-like character to the ammonia group. A similar result

has been found for the triphenylphosphine ligand; the phosphorus

2p binding energies for coordinated triphenylphosphine and for a

phosphonium ion were greater than for free triphenylphosphine

(See next section).

In the case of the nitro ligand, however, the nitrogen 1s

binding energies found for either $NaNO_2$ or for the metal-coordinated

nitrite are approximately the same. Probably this can be explained

by the metal-to-ligand π back-bonding operative in the metal-

nitrite bond. This back-bonding would tend to keep the charge on

the nitrogen atom approximately the same in the free and coordinated

ligand. Considering the more extensive back-bonding expected in

the metal-coordinated cyanide ion, it is heartening to see that
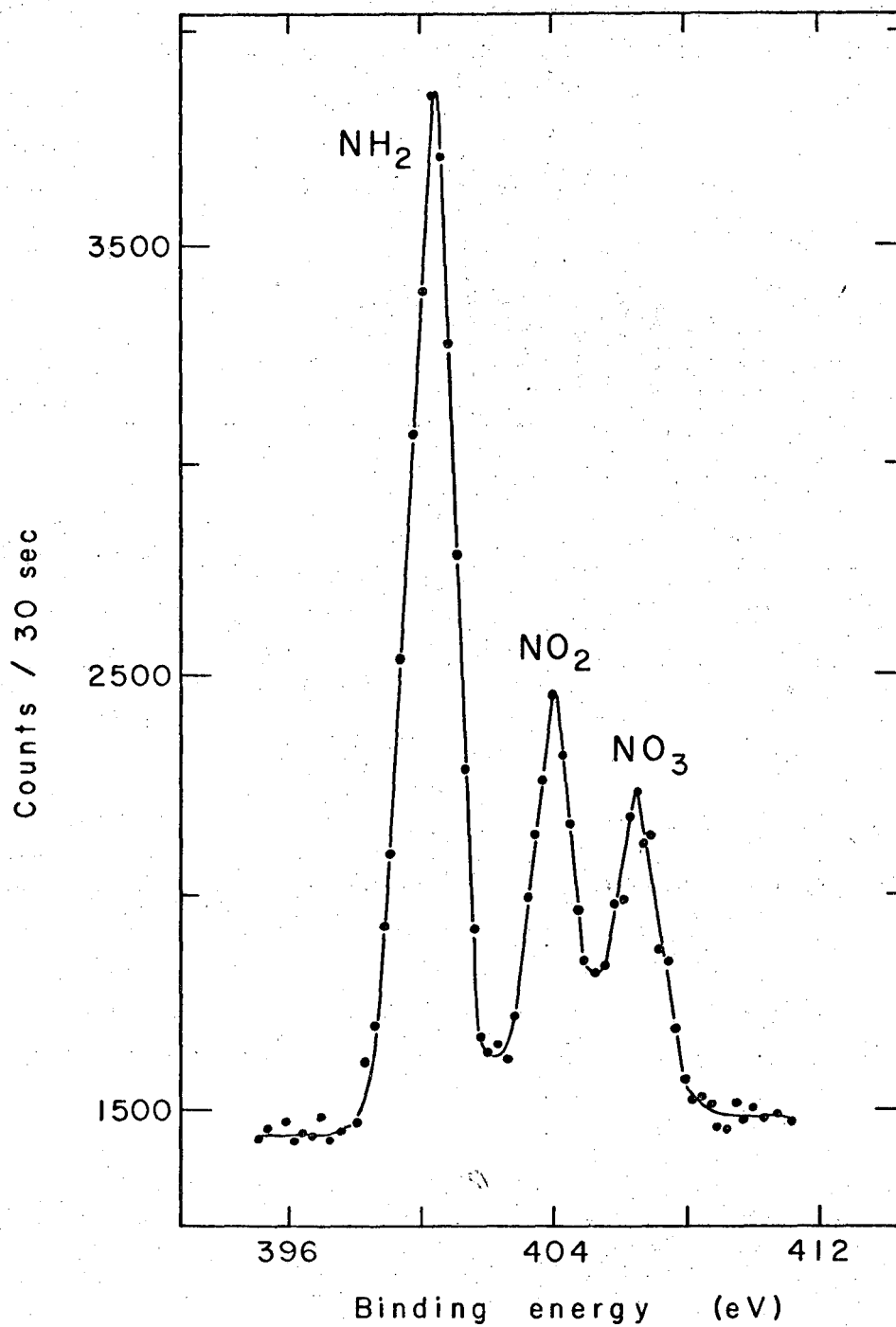
Figure 4. Nitrogen 1s photoelectron spectrum for trans-[Co(NH$_2$CH$_2$CH$_2$NH$_2$)$_2$(NO$_2$)$_2$]NO$_3$.

XBL695-2643

the nitrogen 1s binding energy is appreciably lower for the cyanide

coordinated to Fe(III), Cr(I) and Cr(III) than for the "free"

cyanide in KCN.

Another problem which can be studied by the x-ray photoelectron

method is the determination of the character of the NO group in

various metal nitrosyls.[24] There are four possible bonding situations:

(a) lone pair donation to the metal from NO^+; (b) lone pair donation

from NO with the odd electron retained by the NO; (c) lone pair

donation from NO^-; (d) bridge bonding as encountered in metal

carbonyl compounds. The majority of metal nitrosyls are believed

to be best formulated with the (a) type of bonding.

In Table II are listed the nitrogen 1s binding energies for

two metal nitrosyl cyanides, $Na_2[Fe(CN)_5NO] \cdot 2H_2O$ and $K_3[Cr(CN)_5NO] \cdot H_2O$.

It can be seen that the CN^- peak is relatively invariant to changes

in the metal, whereas the NO peak shifts appreciably. This agrees

with observations on the infrared spectra of these compounds;[25] that

is, the CN stretching frequency is relatively unchanged as opposed

to the large change for the NO stretch frequency from $1944cm^{-1}$ in

the formally Fe(II) compound to $1645cm^{-1}$ in the Cr(I) compound.[24]

Both of these compounds have been formulated as NO^+ compounds,[25]

but their NO nitrogen 1s binding energies clearly show that there

is a marked difference in nitrogen charge in these two cases. It

is a wellknown fact that the NO^+ ligand has an empty π^* orbital

available for back-bonding from the metal and further that back-

bonding is greater in compounds with metals in lower oxidation states.

The lower oxidation state in the case of the Cr(I) compound, indi-

cating greater back-bonding, would be a possible explanation for the apparently less positive NO nitrogen in $Cr(CN)_5NO^{3-}$.

However, consideration of the measured NO binding energy for the formally Co(III) compound, $[Co(NH_3)_5NO]Cl_2$ (black isomer), indicates a certain predicament. This diamagnetic compound has been found to have a monomeric structure,[26] and the Co-N bond distance is reasonable for a Co^{3+}-to-NO^- bond. The NO nitrogen is this cobalt compound would be expected then to possess the most negative nitrogen charge of these three nitrosyls, but if the binding energies are indicative, the cobalt compound is somewhat intermediate. Resolution of this problem will be best attained by carrying out more nitrogen binding energy measurements on metal nitrosyls, and possibly by studying the effective charges on the metal atoms.

Structure of the Oxyhyponitrite Ion - Perhaps the most remarkable demonstration in this study of nitrogen compounds is the clear proof of the existence of structurally different nitrogen atoms in the oxyhyponitrite ion, $N_2O_3^{2-}$. Various studies have been undertaken to differentiate between the possible structures of this ion, the three most probable structures being

$$O=N-N{\overset{\displaystyle O^-}{\underset{\displaystyle O^-}{\big<}}} \qquad\qquad O=N-O-N^-\!-O^- \qquad\qquad {}^-O-N=N-O-O^-$$
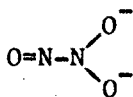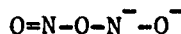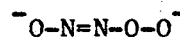
$$\text{I} \qquad\qquad\qquad\qquad \text{II} \qquad\qquad\qquad\qquad \text{III}$$

Addison et al[27] concluded that the ultra-violet absorption spectrum of $N_2O_3^{2-}$ indicated an N=N bond. Calorimetric measurements[28] have

suggested the structure I as most probable, and the infrared spectrum
has been interpreted as having bands indicative of an $-NO_2$ grouping.[29]
The nitrogen 1s photoelectron spectrum of $Na_2N_2O_3$ (See Figure 5),
with two peaks, clearly rules out structure II as a possibility.
In order to distinguish between the two remaining structures, CNDO
and extended Hückel calculations were completed for the two geometries
(varying the N-N bond distance in each case). The net nitrogen
charges obtained from the calculations are given in Table III.
Structure I is indicated by these calculations; indeed structure III
would be predicted to show only one peak, for the two different
nitrogens are predicted to have approximately the same charge.
Finally it can be seen in Figures 2 and 3 that the points representing
structure I do fit the correlation lines. Recently the oxyhyponitrite
ion has been shown by asymmetric ^{15}N-labelling to have two
structurally-different nitrogen atoms.[30]
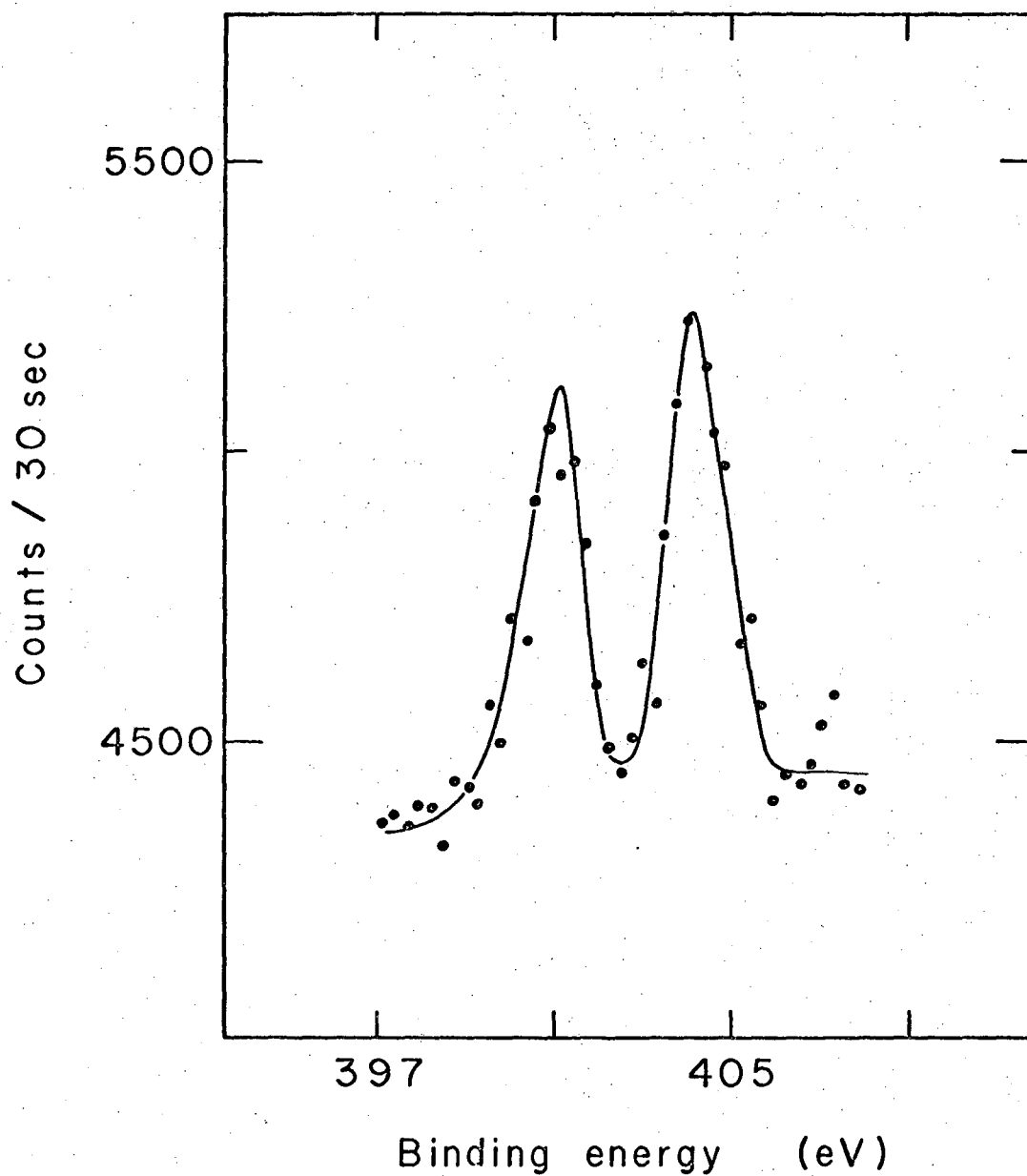
Figure 5. Nitrogen 1s photoelectron spectrum for $Na_2N_2O_3$. Sodium nitrite impurity[30] accounts for excess area in the higher binding energy peak.

TABLE III.

Calculated Nitrogen Charges for Two Asymmetric
Oxyhyponitrite Structures

Structure	r_{N-N} (Å)	Calculated Nitrogen Charges[*]			
		CNDO		Extended Hückel	
		q_1	q_2	q_1	q_2
I	1.30	0.133	−0.151	1.75	0.040
	1.50	0.147	−0.239	1.75	−0.090
III	1.30	−0.158	−0.145	0.288	0.286
	1.50	−0.181	−0.188	0.198	0.254

[*] For each molecular orbital method the net nitrogen charges, q_1 and q_2, are given for the two structurally different nitrogen atoms in each structure.

V. PHOSPHORUS 2p ELECTRON BINDING ENERGIES. CORRELATION WITH EXTENDED HÜCKEL CHARGES.

A. Introduction

Considering the extensive chemistry of phosphorus, it seemed that XPS would serve as a useful investigative tool. The successful correlation of nitrogen 1s electron binding energies with nitrogen atom charges calculated from CNDO molecular orbital[16] and extended Hückel molecular orbital[17] (EHMO) eigenfunctions prompted a similar treatment of some phosphorus compounds. Phosphorus 2p electron binding energies are reported for over fifty compounds. An attempt is made to correlate these binding energies with phosphorus atom charges calculated by the EHMO method. The simple EHMO method as well as an iterative variation[31] of the EHMO method are used to calculate the phosphorus atom charges, and the phosphorus atom input parameters are varied in an attempt to find the set which gives the best correlation of binding energy with calculated charge.

B. Calculations

Two basic modifications of the extended Hückel molecular orbital method were used. In both cases computations were performed with a CDC 6600 computer using a Fortran IV program. The first modification was that formulated by Hoffmann.[17] In the extended Hückel method no assumptions have to be made concerning hybridization.

The Coulomb integrals were approximated by valence state ionization

potentials (vsip) as determined by Hinze and Jaffe´.[18] The

ionization potential for a phosphorus $3\underline{d}$ electron was taken as

3.00 eV.[32] Orbital exponents were secured by using Slater's rules[33]

except where noted. Calculations were completed with use of three

variations for the offdiagonal Hamiltonian elements: the arithmetic

mean (Equation (8)), the geometric mean (Equation (9)), and Cusachs'

approximation[34] (Equation (10)).

$$H_{ij} = 1.75 S_{ij}(H_{ii}+H_{jj})/2 \qquad (8)$$

$$H_{ij} = 2 S_{ij}(H_{ii}H_{jj})^{1/2} \qquad (9)$$

$$H_{ij} = S_{ij}(H_{ii}+H_{jj})(2-|S_{ij}|)/2 \qquad (10)$$

Here H_{ii} is the negative of the vsip and S_{ij} is the usual overlap

integral.

The second modification of the extended Hückel method used in

this work was an iterative type.[31] The Coulomb integrals were set

equal to the negative of the appropriate neutral atom vsip's

corrected for net atomic charge q_i where K was taken as 2.00 eV.

per unit charge.

$$H_{ii} = H_{ii}^{o}-Kq_{i} \qquad (11)$$

The Slater exponents μ_i were also taken as charge dependent, assigned by an extension of Slater's rules.

$$\mu_i = \mu_i{}^o + 0.35 q_i / n^* \tag{12}$$

Here n^* is the effective principal quantum number and $\mu_i{}^o$ is the exponent for the ith orbital on a neutral atom. The net atomic charges q_i were obtained in each cycle by an application of Mulliken's population analysis.[20] In our self-consistent extended Hückel calculations we elected to use the Cusachs approximation (Equation (10)) for the off-diagonal Hamiltonian elements. The calculational procedure consisted of iterating until the atomic charges were self-consistent to at least 0.01.

Cartesian coordinates were obtained from Program PROXYZ;[21] the molecular parameters were obtained from crystal structure determinations[22, 35, 36] or from estimates.

Phosphorus atomic charges were also calculated by the simple Pauling method.[9] The ionic character (I_{AB}) of a bond between atoms A and B is taken as a function of the atom electronegativities χ_A and χ_B.

$$I_{AB} = 1.0 - e^{-0.25(\chi_A - \chi_B)^2} \tag{13}$$

The atom electronegativities can be taken as charge dependent functions, the prescription for correction of neutral atom

electronegativities being simply that the electronegativity is increased 2/3 of the way to the electronegativity of the element next in the periodic table for each unit positive charge. Hydrogen cannot be treated by this simple correction formula, but it was found that the phosphorus charges in the molecules studied in this work were affected only slightly by correcting χ_H for charge by some reasonable amount.

Within the valence-bond formalism the net charge q_A on an atom A is given by

$$q_A = Q_A + \sum_{B \neq A} I_{AB} \qquad (14)$$

where Q_A is the formal charge on atom A and the summation is over all the bonds to atom A. The calculational process is iterative because of the charge-dependent atom electronegativities; "self-consistent" atomic charges result. In no case did we use a valence bond representation indicative of 3d phosphorus orbital participation as has been done in the case of sulfur compounds.[3]

C. Result and Discussion

Correlation with Charges Obtained from Extended Hückel Molecular Orbitals. - Phosphorus 2p electron binding energies determined for over fifty compounds are listed in Tables IV and V. The range of binding energy shifts was found to be about 8 eV. In the case of

TABLE IV.

Phosphorus 2p Binding Energies and
Extended-Hückel Calculated Charges

Compound Number	Compound	Binding Energy eV.	Calculated Phosphorus Atom Charge		
			Non-Iterative[d]		Iterative[e]
			Without 3d	With 3d	With 3d
1	NH_4PF_6	137.3	3.723	3.806	2.505
2	$(NPCl_2)_3$	134.5	2.321	2.277	0.961
3	$(CH_3PS_2)_2$	133.4	1.502	1.591	0.764
4	P_4S_{10}	134.0	1.515	1.390	
5	$(C_6H_5)_3PS$	132.3		2.194	
6	$n\text{-}(C_4H_9)_4P^+Cl\text{-}$	132.3	1.173	2.525	
7	$(C_6H_5)_3P$	130.6		0.999	
8	P_4S_3	130.5[b]	0.324[c]	0.338[c]	0.303[c]
			0.048	0.148	0.122
9	P_{red}	130.1[b]	0	0	0
10	KPF_2O_2	134.8	3.578	3.547	1.956
11	$(NH_4)_2PFO_3$	134.1	3.490	3.443	1.815
12	$Na_2H_2P_2O_7$	133.9	3.387	3.387	1.767
13	KH_2PO_4	133.9		3.669	1.785
14	$(NH_4)_2CH_3PO_3$	133.8	2.905	3.041	1.435
15	$C_6H_5CH_2PO_3H_2$	133.8	2.846	3.284	
16	$HOPO(NH_2)_2$	133.6	2.832	3.083	1.465
17	$Na_4P_2O_7$	133.3	3.374	3.354	

Calculated Phosphorus Atom Charge

Compound Number	Compound	Binding Energy eV.	Non-Iterative[d] Without 3$\underline{d}$	With 3$\underline{d}$	Iterative[e] With 3$\underline{d}$
18	Na_3PSO_3	133.0	2.936	2.622	1.361
19	$Na_3(PO_2NH)_3$	133.0	2.892[a]	3.062[a]	
20	$BaHPO_3$	132.9	2.844	2.790	1.420
21	$(C_6H_5)_3PO$	132.7		2.744	
22	K_2HPO_4	132.7		3.621	2.001
23	$KH_2PO_2 \cdot H_2O$	132.4	2.236	2.201	1.189
24	Na_3PO_4	132.1	3.413	3.621	1.544
25	P_4S_7	134.3		1.370	
		132.7		0.266	

[a] Calculation with assumed $r_{P-N}=1.70\overset{\circ}{A}$.

[b] A second peak at 134.5 eV. was attributed to a decomposition product.

[c] There are two different types of phosphorus in P_4S_3; the more positive number in each case refers to the unique phosphorus atom. For purposes of plotting an average charge value was used.

[d] Completed using arithmetic off-diagonal approximation (Equation (1)).

[e] Charges are self-consistent to at least 0.01.

TABLE V.

Some Phosphorus 2p Binding Energies

Compound Number	Compound	Phosphorus 2p Electron Binding Energy eV.
26	$Mn(CO)_4P(C_6H_5)_3Cl$	131.2
27	(cis-PP)$Mn(CO)_3I$[a]	133.2
28	$Mn(CO)_3(AP)I$[b]	133.0
29	trans-$Rh(CO)Cl(P(C_6H_5)_3)_2$	131.6
30	Tris α-napthylphosphine	130.9
31	ortho-$[(C_6H_5)C_6H_5]_3P$	134.3
32	P_3N_5	133.2
33	$(NaPO_3)_3$	134.0
34	$(NaPO_3)_4 \cdot 4H_2O$	134.1
35	P_4OH	129.9[c]
		133.1
36	Phosphotungstic acid	133.0[d]
37	$(C_6H_5O)_3PO$	134.2
38	$(C_6H_5S)_3P$	134.4
39	$Na_5P_3O_{10}$ Form I	133.6
40	$NaPO_3$ glass	134.5
41	P_4S_5	132.0
		134.9(shoulder)
42	BP	129.5
43	cis-PP[a]	131.3
		132.6(shoulder)

Compound Number	Compound	Phosphorus 2$\underline{p}$ Electron Binding Energy eV.
44	PBr$_5$	138.4[e]
45	POBr$_3$	134.4
46	Riboflavin-5´-phosphate	133.5
47	O-phosphoserine (dl)	133.5
48	Barium Phosphoglyceric acid	133.5
49	O-phosphothreonine (dl)	133.7
50	O-phosphoethanolamine	134.1
51	CrP	128.8[f]
52	MnP	129.3[g]
53	$(C_6H_5CH_2)(C_6H_5)_3P^+Cl^-$	132.5

[a] The ligand cis-PP is the bidentate 2-cis-propenylphenyldiphenyl-phosphine.

[b] The ligand AP is the bidentate 2-allylphenyldiphenylphosphine.

[c] Two peaks observed for P$_4$OH in the ratio of about 2:1, the lower binding energy peak the larger. See the discussion for further particulars.

[d] A second peak at 134.2 eV. was observed, attributed to something other than starting material, for peak increased between successive scans while the 133.0 eV. peak decreased.

[e] A second larger peak was found at 134.4 eV., probably assignable to the oxidation product POBr$_3$.

[f] A second peak was observed at 133.8 eV., due probably to an oxidation product.

[g] A second peak was observed at 133.2 eV., due probably to an oxidation product.

twenty-five of these compounds, non-iterative extended Hückel molecular

orbital calculations were made by using Equation (8), both without

and with $3d$ orbitals on the phosphorus atom. The resultant phosphorus

atom charges are given in Table IV. It can be seen that the calculated

phosphorus atom charge is, except in a few cases, unaffected by

inclusion of $3d$ orbitals.

In Figure 6 the measured phosphorus $2p$ binding energies are

plotted against the non-iterative extended Hückel-calculated

phosphorus charges. The correlation of these two quantities can

be seen to be poor. This is in contrast to our nitrogen work where

a reasonably good correlation was found with the same variation of

the non-iterative extended Hückel method (i.e. the arithemetic mean

off-diagonal approximation). Extensive modifications of the input

data were tried (See Table VI). The phosphorus $3d$ orbital was

contracted by arbitrarily assigning the Slater exponent a value

of 1.6 (this value is in the range suggested by Fogleman et al).[37]

The effect of this can be seen to be negligible for the series of

molecules in Table VI.

In the second modification the phosphorus $3d$ orbital was

contracted and its vsip was changed from 3.0 eV. to 7.0 eV. (see

Column 3, Table VI). The resultant phosphorus charges were appre-

ciably changed, but the correlation was not markedly improved for

the seven compounds considered. The last two columns in Table VI

list the phosphorus charges resulting from changing the input

vsip's for the phosphorus $3s$ and $3p$ orbitals. Again, a plot of the
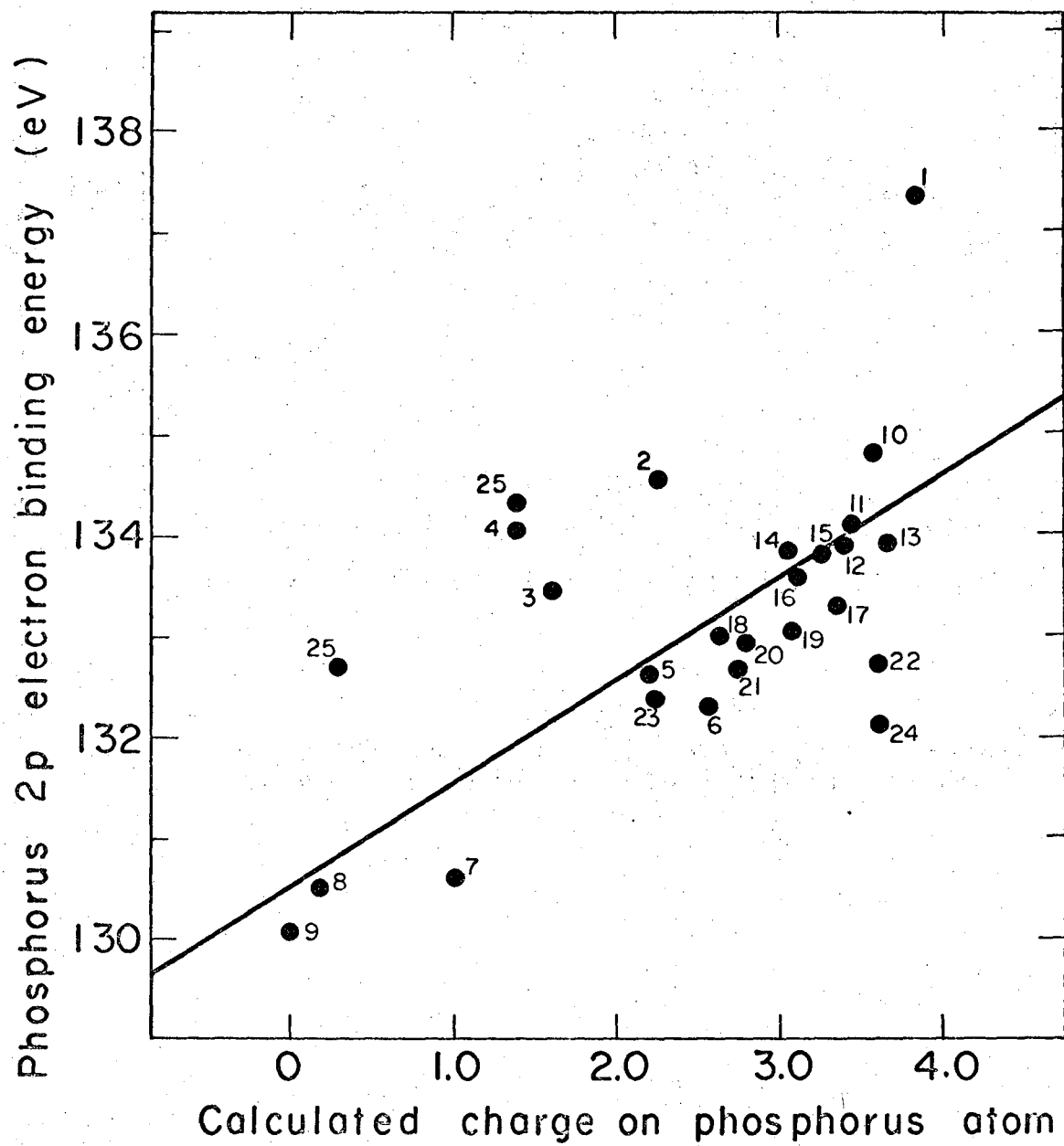
Figure 6. Plot of phosphorus 2p binding energies vs. non-iterative
extended Hückel-calculated charges on phosphorus atoms.

TABLE VI.

Non-Iterative Extended Hückel-Calculated[a]

Net Phosphorus Atom Charges Resultant From

Various Input Parameter Modifications

| | | Phosphorus Atom Charge and Input Parameter Modification | | |
| | | $\mu(P_{3\underline{d}})=1.6$ | | $vsip(P_{3\underline{s}})=16.0$ |
Molecule	$\mu(P_{3\underline{d}})=1.6$	$vsip(P_{3\underline{d}})=7.0eV.$	$vsip(P_{3\underline{s}})=17.0$	$vsip(P_{3\underline{p}})=11.5$
$PFO_3^{=}$	3.442	2.880	3.579	3.761
$PSO_3^{\equiv}$	2.746	1.943	2.881	3.096
$PF_2O_2^{-}$	3.554	3.057	3.683	3.858
$(CH_3PS_2)_2$	1.215	0.494	1.709	2.022
P_4S_3	0.260[b]	-0.181[b]	0.437[b]	0.690[b]
	0.019	-0.202	0.196	0.305
PF_6^{-}	3.792	3.259	3.933	4.086
$HPO_4^{=}$	3.524	3.054	3.810	4.017

[a] Equation (8) used for off-diagonal terms.

[b] See footnote c in Table IV.

data shows little improvement in the correlation. Finally, the character of the off-diagonal approximation used in our non-iterative extended Hückel calculations was changed to both the geometric mean (Equation (9)) and the Cusachs variation (Equation (10)). The calculated phosphorus atom charges in a series of nine compounds for both of these approaches is given in Table VII. The data obtained using the Cusachs and geometric mean approximations showed essentially the same correlation as found in Figure 6.

It seemed at this point that the inability to obtain even a moderate correlation of measured phosphorus 2$\underline{p}$ binding energy with non-iterative extended Hückel-calculated phosphorus charge was a manifestation of some inherent problem(s) in the calculational method. This belief was nurtured, as stated above, by our success with nitrogen 1$\underline{s}$ data as well as with boron 1$\underline{s}$ data (See next section). Concerning the reality of phosphorus atom charges obtained from this simple extended Hückel method, Sichel and Whitehead[38] have found a good linear correlation of the phosphorus nuclear magnetic resonance chemical shifts of the methylphosphines with calculated charges on phosphorus. Unfortunately this is not a diversified series of phosphorus compounds. An attempt to correlate the phosphorus charges given in Table IV with reported phosphorus chemical shifts[39] was a marked failure. This failure could be attributed either to some inadequacy in the non-iterative extended Hückel method (applied to phosphorus compounds) or more probably to differing average electronic excitation energies[40] throughout the series of molecules.

TABLE VII.

Non-Iterative Extended Hückel-Calculated

Net Phosphorus Atom Charges Resultant From

Two Off-Diagonal Approximations

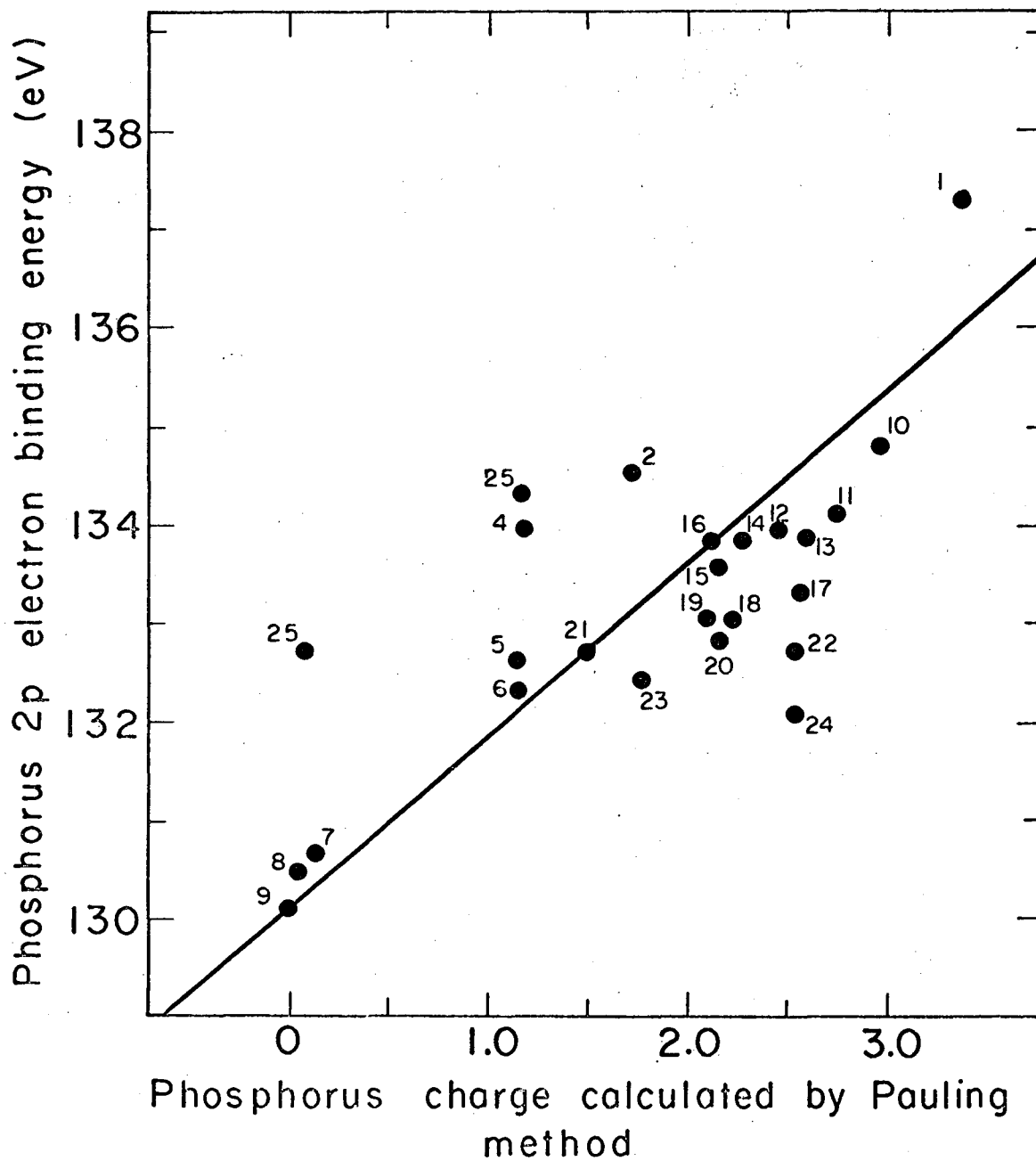| Molecule	Phosphorus Atom Charge	
	Geometric H_{ij} [a]	Cusach's H_{ij} [b]
$PF_2O_2^-$	4.191	3.739
$PFO_3^=$	4.131	3.676
$PSO_3^{\equiv}$	3.610	3.205
$(CH_3PS_2)_2$	2.963	2.182
P_4S_3	0.993[c]	0.870
	0.464	0.276
PF_6^-	4.574	4.198
$HPO_4^=$	4.402	4.068
$PO_4^{\equiv}$	3.727	3.305

[a] Equation (9).

[b] Equation (10).

[c] See footnote c in Table IV.

Considering the distribution of points in Figure 6, it is interesting to note that compounds 10-24 are molecules containing P-O bonds. Perhaps the simple extended Hückel method has tended to overemphasize the polarity of these P-O bonds and as such has assigned excessive positive charge to the phosphorus atoms. It does seem unrealistic that the phosphates 13, 22, and 24 should have essentially the same net phosphorus charges as that obtained for the hexafluorophosphate ion (1). Some support for this proposal of overemphasis of P-O bond polarity can be gained by reverting to two variations of the Pauling method[9] of calculation of net atomic charges.

In analogy with our non-iterative extended Hückel calculations, phosphorus charges for the compounds in Figure 6 were obtained by a straightforward application of Equations (11) and (12), using neutral-atom electronegativities. The resultant charges are plotted in Figure 7 $\underline{vs}$. the phosphorus $2\underline{p}$ binding energies. The similarity of distribution of points in Figures 6 and 7 is striking. If the other modification of the Pauling method is invoked we would expect this iterative "self-consistent" method to accomplish two goals: 1) overall decrease in all net charges, and 2) reduction in tendency to overemphasize particular bond polarities. In Figure 8 we can clearly see that the first expectation is met; the phosphorus charge range is essentially halved from that in Figure 7. The improved correlation depicted in Figure 8 tends to support the second expectation.

Figure 7. Plot of phosphorus 2p binding energies vs. phosphorus atom charges calculated by Pauling method using neutral atom electronegativities.
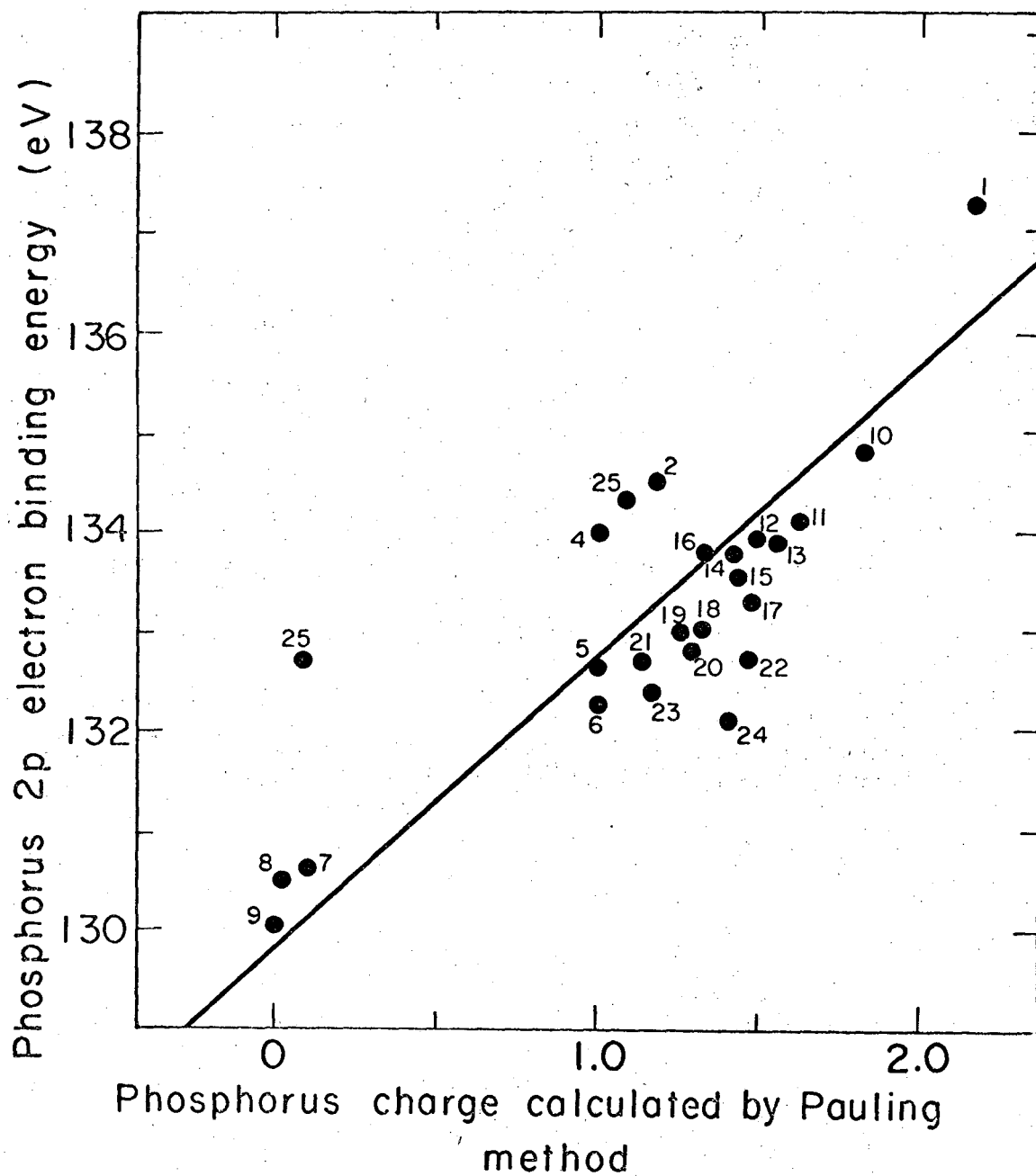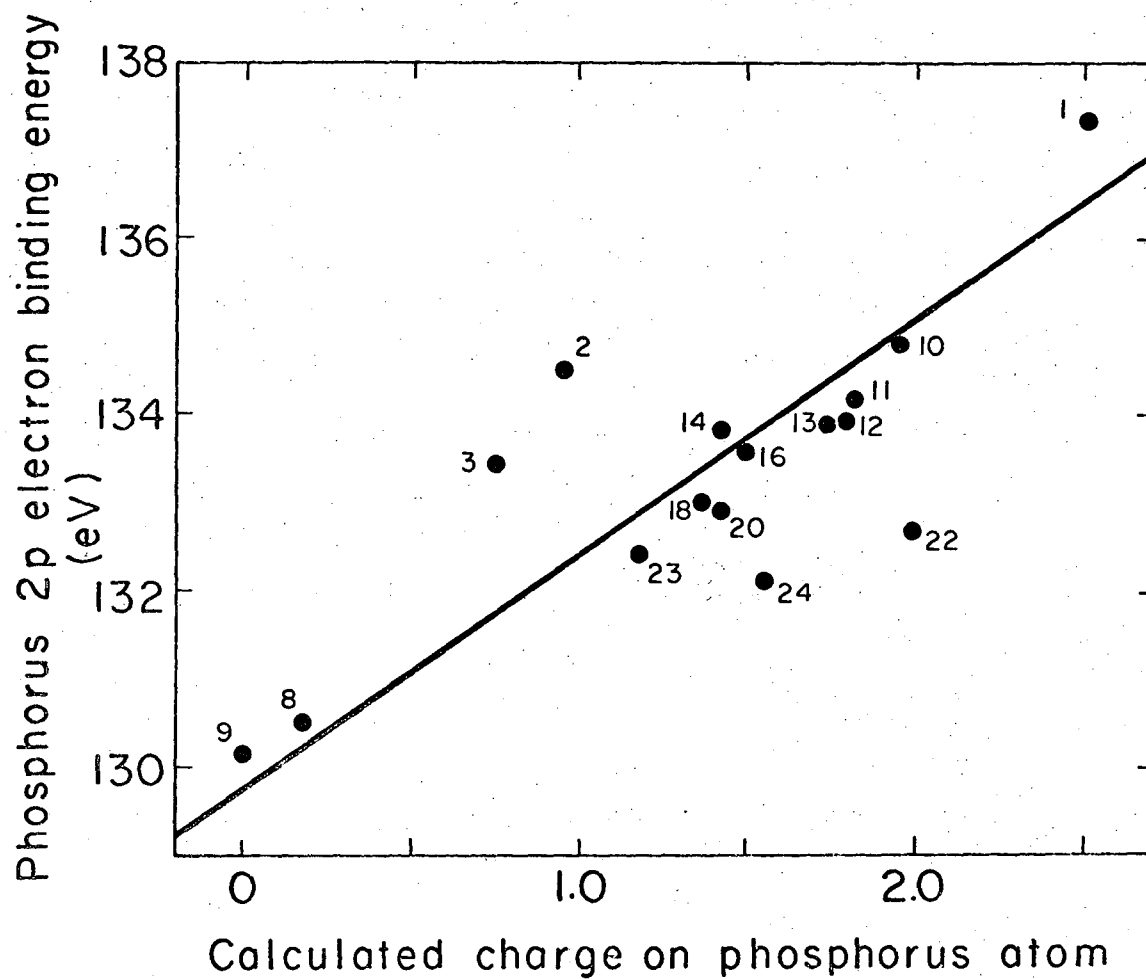
XBL696-2989

XBL696-2988

Figure 8. Plot of phosphorus 2p binding energies vs. phosphorus atom charges calculated by Pauling method using charge-dependent atom electronegativities.

Having accepted this interpretation of the lack of correlative ability, it seemed reasonable that a more modern version of the extended Hückel method would be warranted, a version where the Hamiltonian is charge dependent.[31] Using charge-dependent valence state ionization potentials (Equation (11)) coupled with the Cusachs approximation (Equation (10)) for the off-diagonal Hamiltonian terms, we obtained the phosphorus charges given in Table IV. All phosphorus charges are appreciably reduced when using this iterative extended Hückel method. In fact the same order of reduction occured in this case as with the simple Pauling method. Unfortunately, these self-consistent extended Hückel-calculated phosphorus charges gave little improvement in the correlation with phosphorus 2p binding energies (see Figure 9).

Although at this point one might tend to lose hope of obtaining a good correlation, it must be remembered that the iterative extended Hückel method used here still contains a gross approximation. The charge correction of all vsip's by the same factor seems unrealistic. A better approach would be to use valence orbital ionization potentials, which have been tabulated for the atoms as a function of charge and configuration.[41]

Electronic Structure of Phosphonitrilic Chloride Trimer. - As a by-product of this study we obtained an extended Hückel description of the cyclic phosphonitrilic chloride trimer $(NPCl_2)_3$. Calculations were completed with use of a planar structure for $(NPCl_2)_3$ coupled with known molecular dimensions.[22] Two different

Figure 9. Plot of phosphorus 2p binding energies vs. iterative
extended Hückel-calculated charges on phosphorus atoms.

descriptions have been given for the electronic pi system above and below the plane of the ring. Dewar et al[42] concluded that there are "islands" of π character, each involving three-centered π-bonds centered at a nitrogen atom. Craig and Paddock[43] suggested unequal participation of the $3d_{xz}$ and $3d_{yz}$ (the molecular plane is the x-y plane) orbitals would result in a continuous pi molecular orbital around the ring.

The π type (e'' and a_2'' in D_{3h}) molecular orbitals resulting from both the non-iterative and iterative extended Hückel treatments showed unequal $3d_{xz}$ and $3d_{yz}$ participation, in agreement with the suggestion of Craig and Paddock. The $3d$ participation was somewhat greater in the iterative case. In both cases the molecular orbital ordering was found to be $\cdots\cdots e'(2)e''(2)a_2''(2)a_2''{}^*a_1'{}^* \cdots\cdots$. The ionization potential of $(NPCl_2)_3$ has been determined to be 10.26 eV.,[44] which compares with the eigenvalue of the highest filled orbital, a_2'' (-12.00 eV. in the iterative calculation). The electronic spectrum of $(NPCl)_3$ has a broad peak at 199mμ(6.23 eV.).[45] The iterative calculations predict an ^1E ($a_2''\xleftarrow{\ *\ } e''$) transition at 8.77 eV. consisting essentially of the transition of a nitrogen $2p_z$ electron into the phosphorus $3d$ orbitals.

Decompositions. In the case of some of the compounds studied two peaks were observed in the P_{2p} spectrum where only a single peak was expected. It was usually easy to assign the peak arising from the compound under study, either by peak position or by observing a change in the relative areas of the two peaks. Both

elemental red phosphorus and tetraphosphorus trisulfide (see Table IV)
gave a second peak at 134.5 eV. in addition to their assigned peaks.
In each case the assignment was made on the basis of peak position,
since little time dependence was noted in the spectrum. For red
phosphorus the decomposition peak was the larger, whereas the opposite
was found for P_4S_3. This probably parallels their reactivities with
water vapor; red phosphorus reacts slowly with water vaper and oxygen
at normal temperatures, while under "ordinary conditions" P_4S_3 is
unaffected by exposure to the atmosphere.[46] In fact the red phosphorus
oxidation is accelerated markedly by small concentrations of silver
(we used silver-based conducting tape!).[47] The decomposition
product in each of these cases is then a mixture of the oxyacids
of phosphorus, which probably had formed on the surface before we
loaded the samples into the spectrometer.

The appearance of two peaks (see Table V) in the spectra of
the metal phosphides CrP and MnP is not easily explained. Hydrolysis
of a phosphide should give only gaseous phosphine, but apparently
there was some surface oxidation.

Two phosphorus peaks would be expected for the compound P_4OH
probably in the ratio of 3:1.[48] As noted in Table V a sample of
P_4OH (1 day old) gave two peaks in the ratio of 2:1 with binding
energy values of 129.9 and 133.1 eV, respectively. A portion of
the same sample was stored for a week in a capped bottle and the
phosphorus spectrum rerun. Two peaks were again found, still in the
ratio of 2:1. The smaller peak, however, had moved to a binding

energy of 134.0 eV while the larger peak remained fixed. The
sample was then kept in air overnight and the phosphorus spectrum
rerun. This spectrum showed peaks at 130.0 and 134.0 eV binding
energy in the ratio of 1:1. Apparently we were observing initially
the P_4OH 3:1 pattern with some surface (or bulk?) impurity.

Applications. The effect of metal coordination on the charge
of a ligand atom can be studied by this method. From the measurements
on triphenylphosphine, the triphenylphosphine coordinated complexes
(Table V, compounds 26 and 29), and the phosphonium salt, compound
53, it can be seen that coordination of the triphenylphosphine ligand
decreases the charge on the phosphorus atom. This is analogous to
results obtained for the NH_3 ligand (See previous section).

Unfortunately it does not seem that at present phosphorus
photoelectron spectroscopy on biological compounds will be definitive,
at least insofar as the type of phosphorus atom is concerned. This
can be seen by the small changes in binding energy for the compounds
46-50 in Table II.

VI. MISCELLANEOUS CORE-ELECTRON BINDING ENERGIES.

A. Introduction

Reasonably good core-electron binding energy vs. molecular orbital-calculated atom charge correlations were established in Section IV for nitrogen compounds, whereas only limited success was found in a similar treatment of phosphorus $2p$ electron binding energies (see Section V). In this section we report boron $1s$ electron and chromium $3p$ electron binding energies and an attempt is made to establish correlations between these core-electron binding energies and boron and chromium atom charges calculated by various molecular orbital methods. A CNDO correlation plot is also generated for some carbon $1s$ electron binding energies that were determined recently.[49]

B. Calculations

Boron and carbon atom charges were calculated by the CNDO and EHMO methods in the same manner as outlined for nitrogen compounds (see Section IVB).

Simple iterative extended Hückel molecular orbital calculations were completed for a few chromium molecules. Coulomb integrals for ligand orbitals were set equal to the negative of the appropriate neutral atom vsip's,[18] corrected in each cycle for net atomic

charge q_i.

$$H_{ii} = H_{ii}^{o} - (2.0 \text{ eV/charge})q_i \tag{11}$$

Metal coulomb integrals (except where noted) were calculated for a neutral chromium atom in a d^5p configuration[41] — charge correction of these values was completed using equation (11)on each iterative cycle. Both the metal and ligand orbital exponents were taken as neutral atom orbital values, μ_i, (assigned by Slater's rules[33]) corrected for charge.

$$\mu_i = \mu_i + 0.35 \ q_i/n^* \tag{12}$$

Here n^* is the effective principal quantum number. The off-diagonal Hamiltonian elements were assigned by Cusachs' approximation[34]

$$H_{ij} = S_{ij} (H_{ii} + H_{jj})(2 - |S_{ij}|)/2 \tag{10}$$

Net atomic charges q_i were obtained in each cycle by an application of Mulliken's population analysis.[20] Iterations were made on the chromium compounds until the atomic charges were self-consistent to at least 0.05.

Program PROXYZ[21] was used to obtain cartesian coordinates when necessary; the molecular parameters were obtained from crystal structure determinations[22] or from estimates.

C. Results and Discussion

Boron Compounds. Boron 1s electron binding energies have
been measured for some 25 compounds and are listed in Tables VIII
and IX. The range of boron 1s shifts is 8.4 eV., which is comparable
to the observed phosphorus 2p shift range (≈8.5 eV., see last section).
Larger shift ranges have been observed for nitrogen (≈10.8 eV., see
Section IV), carbon (≈15.9 eV.),[49] and sulfur (≈15 eV.).[1,50]

Simple extended Hückel molecular orbital (EHMO) calculations
were completed for 12 of the boron compounds. A reasonably good
correlation between measured boron 1s electron binding energy and
boron atom charge resultant from the EHMO eigenfunctions is depicted
in Figure 10. The tetramethylammonium salt of the octahydrotriborate
ion ($B_3H_8^-$) with two geometrically-different borons gave a single
boron 1s peak with no structure (peak was broad) and as such only
a single point represents this ion in Figure 10. The boron atom
charges (via the EHMO method) range from near neutrality in the
borohydrides to almost +2.4 in BF_4^-.

In our nitrogen studies we found that the EHMO method tended
to overemphasize charge separations in molecules. The CNDO nitrogen
atom charge range was 4-5 times smaller than that obtained by the
EHMO method for a series of nitrogen compounds. CNDO calculations
were completed for some of the boron compounds treated by the EHMO
method. The results are given in Table VIII. Again the calculated
CNDO atom charge range is 4 times smaller than that obtained using

TABLE VIII.

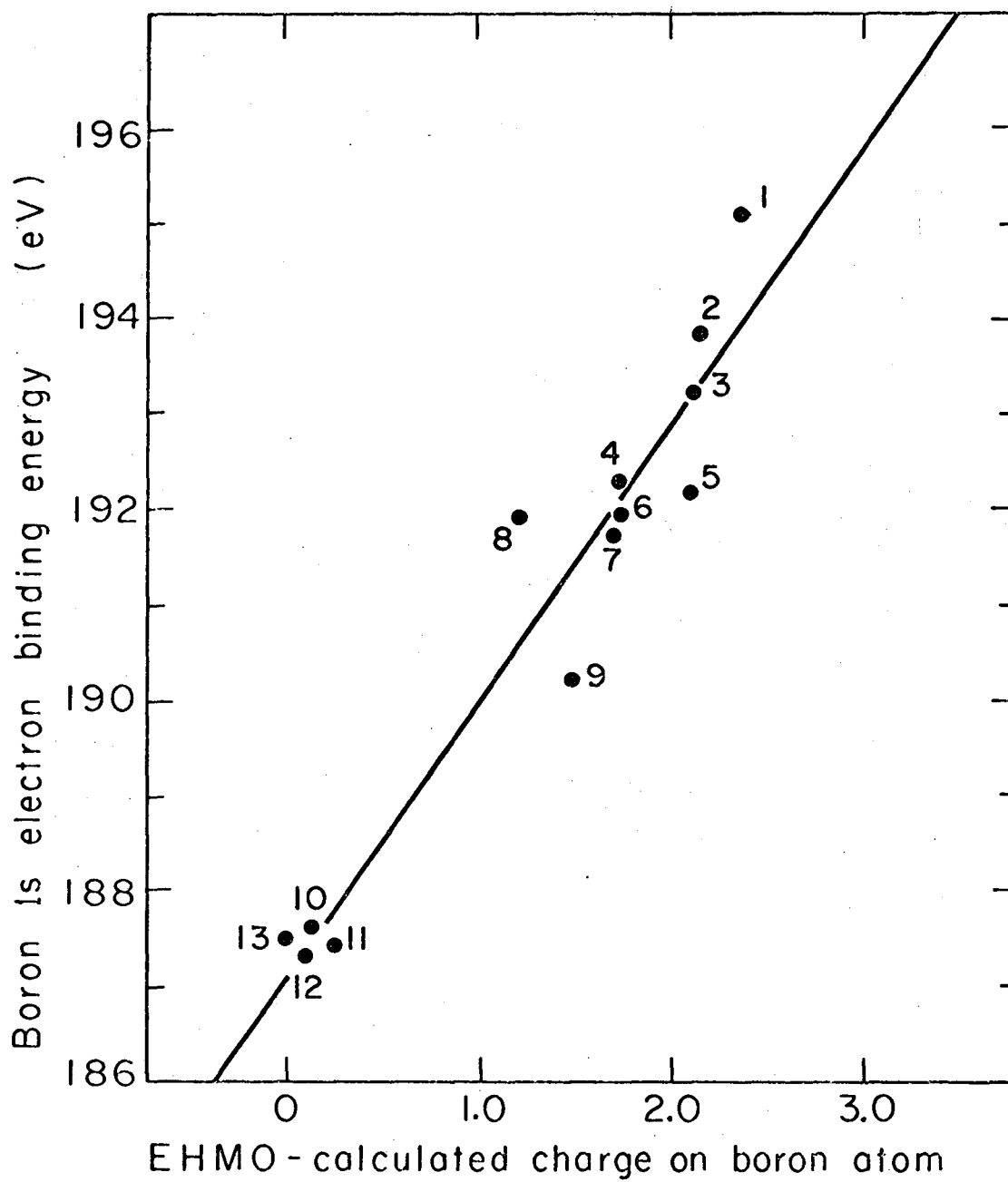### Boron 1s Binding Energies and Calculated Charges

Number	Compound	Binding Energy, eV.	Calculated Boron Atom Charge	
			CNDO	Extended Hückel
1	$NaBF_4$	195.1	+0.754	+2.361
2	$(CH_3)_3NBF_3$	193.8	+0.756	+2.161
3	$B(OH)_3$	193.2	+0.651	+2.122
4	$NaBH(OCH_3)_3$	192.3	+0.404	+1.724
5	$Na_3B_3O_6$	192.2	+0.321	+2.098
6	$p-F-C_6H_4B(OH)_2$	191.9	+0.498	+1.715
7	$p-Cl-C_6H_4B(OH)_2$	191.9		+1.713
8	$[C_2H_5B-(\underset{N-N}{\bigcirc})_3-BC_2H_5]PF_6$	191.9		+1.228
9	BN	190.2		+1.48
10	$K_2BH_3CO_2$	187.5	-0.024	
11	$(CH_3)_4NB_3H_8$	187.4	+0.165[a] -0.007	+0.518[a] +0.078
12	$NaBH_4$	187.4	0.000	+0.138
13	$B_{amor.}$	187.5	≡0	≡0

[a] There are two structurally-different B atoms in the $B_3H_8^-$ ion; the first boron charge refers to the unique boron. For purposes of plotting a weighted average was used.

TABLE IX.

Boron 1s Binding Energies

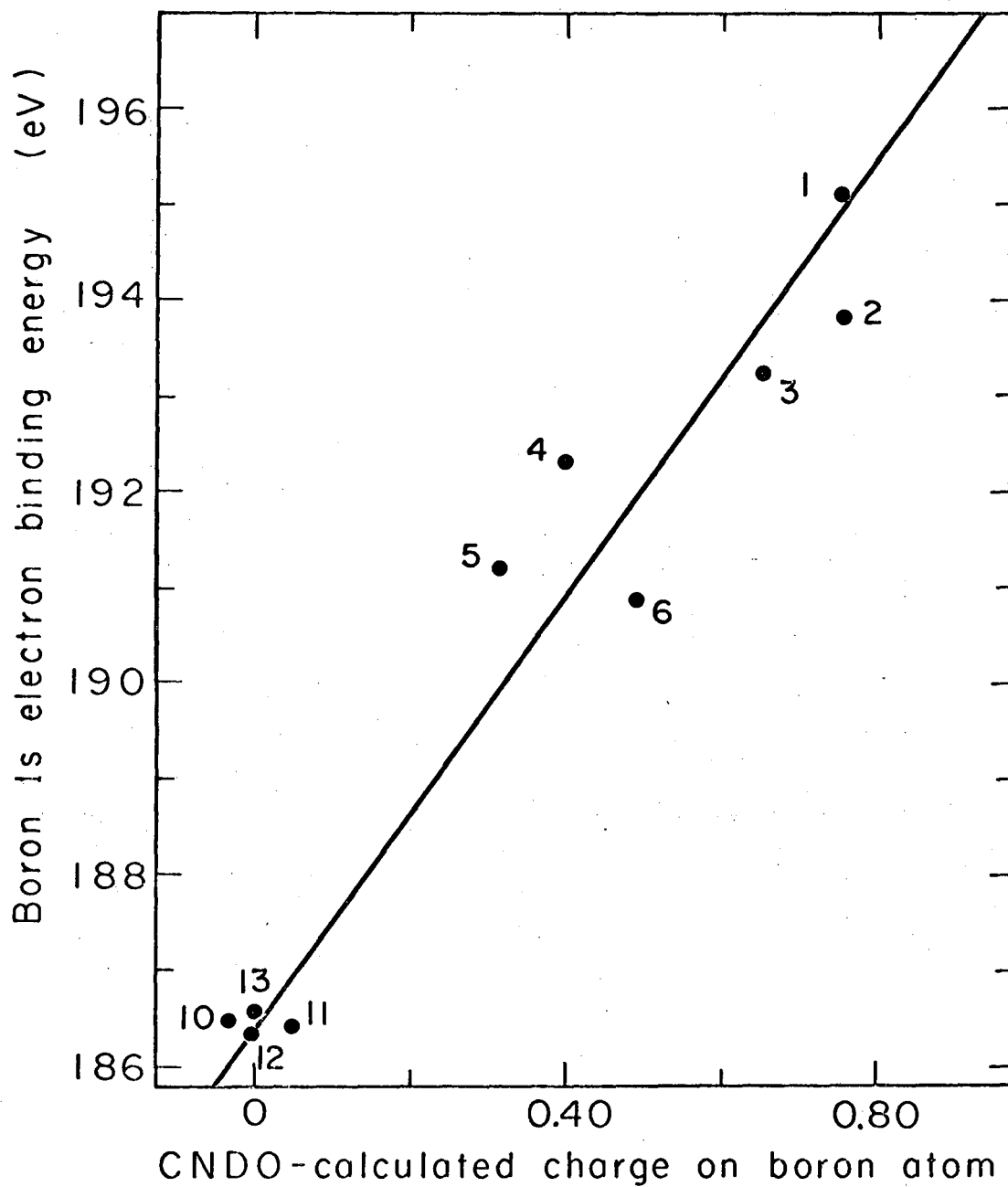| Compound Number	Compound	Binding Energy, eV.
14	$Na_2B_4O_7 \cdot 10H_2O$	192.8
15	N–N–B–(N–N)$_3$–W(CO)$_2$(NO)	191.9
16	$(CH_3)_4N[(8,9,12-Br_3-1,2-B_9C_2H_8)_2Co]$	189.5
17	$Cs[Co(1,2-B_9C_2H_{10}-8-S)_2]$	188.9
18	$Rb[Co(1,2-B_9C_2H_{11})B_8C_2H_{10}]$	188.4
19	$C_2B_9H_{11} \cdot C_5H_5N$	188.4
20	$Cs[(1,2-B_9C_2H_{11})_2Co]$	188.2
21	$B_{10}H_{14}$	188.0
22	$Na_2B_{12}H_{12} \cdot xH_2O$	187.7
23	$NaB(C_6H_5)_4$	187.7
24	$Cs_2B_{10}H_{10}$	187.6
25	B_4C	186.7

Figure 10. Plot of boron 1s binding energies vs. extended Hückel-calculated charges on boron atoms.

the simple EHMO method are probably the result of using charge
independent Coulomb integrals.

A good correlation exists between the measured boron $1s$ binding
energies and the CNDO-calculated boron charge as can be seen in
Figure 11. Using this CNDO correlation line and the boron binding
energy for BN we infer a boron charge of +0.29. The measured
nitrogen $1s$ binding energy for BN correlates with (using neutral
CNDO line) a nitrogen charge of -0.25. This is good indication of
internal consistency. Unfortunately, not enough boron compounds
were secured to enable completion of a sufficient number of CNDO
calculations to check for two lines (one characteristic of anionic
and the other neutral molecules) as had been observed in our nitrogen
work. It is interesting to note in Figure 11 that the three neutral
molecules (2, 3, and 6) fall below the line. Perhaps the boron
binding energy given for amorphous boron is too high due to surface
oxidation.

For all of the compounds listed in Table IX it was possible to
detect only a single relatively sharp boron peak. The carboranes
(compounds 16-20) have geometrically different boron atoms, but in
an unsubstituted carborane (as in compound 20 where two 1,2-dicar-
bollide ions are bound to a single cobalt atom) delocalization of
charge would be expected to eliminate any divergence of boron
charges. It can be seen that as we substitute one S atom for a
H atom on the 1,2-dicarbollide ion (as in compound 17) the boron
$1s$ binding energy is increased appreciably. Substitution of three

Figure 11. Plot of boron 1s binding energies vs. CNDO-calculated charges on boron atoms.

bromines for three hydrogens on this same cage increases the boron

binding energy even more. Still only one sharp peak can be found

for compound 16; the conclusion must be that delocalization of

charge is operative in this 1,2-dicarbollide cage.

Carbon Compounds. Nordberg et al[49] have recently reported

carbon 1s binding energies. They found that the carbon binding

energies correlated with carbon fractional atomic charges calculated

by a modification of Pauling's method and with carbon atom charges

secured from simple EHMO eigenfunctions. In an attempt to remove

some of the scatter observed in their EHMO correlation, Nordberg et al

took account of the potential afforded the carbon 1s electron by

neighboring atom charges. An improved correlation was obtained.

However, various objections can be raised to this procedure. The

carbon atom charges from the EHMO method are unrealistic and as such

could easily introduce scatter in any expected correlation with

measured binding energies. In fact the theoretical justification of

the core-electron binding energy vs. ground state valence charge

correlation has not been adequately developed. All of the factors

influencing the core-electron binding energy of a particular solid

are not known. Surely Koopman's theorem[51] does not hold and the

molecular orbitals of the ionized molecule are not those of the

parent molecule. Correlation of a ground state property (i.e. atom

charge) with a measured solid state (or even gaseous) core-electron

ionization potential is not obvious.

CNDO calculations were completed for some of the compounds

treated by Nordberg et al. The results are given in Table X.

The carbon 1s binding energies for these compounds are plotted vs.

the CNDO-calculated carbon charge in Figure 12. In the cases of

CF_4 and CHF_3 the binding energies obtained by Prof. D. Thomas

(measured both vs. Xe as well as in mixtures with CH_4)[52] were

found to fit the correlation and as such were used in place of

the values given by Nordberg et al. Two points can be made.

First, the CNDO carbon charges seem more realistic than those

obtained by the EHMO method. Second, a somewhat different dis-

tribution of points results in the CNDO correlation plot. Only

two points fall off the line (i.e. not within experimental uncertainly),

the points for KCN and Na_2CO_3. The seemingly improved correlation

using CNDO charges needs to be checked by completing further

calculations on more molecules.

Chromium Compounds. Chromium 3p electron binding energies are

given in Table XI for a series of chromium compounds. Qualitatively

the chromium 3p binding energy increases with increasing oxidation

state, the exception being $Cr(CO)_6$. These chromium 3p binding

energies are somewhat more difficult to obtain than nitrogen, carbon,

phosphorus or boron core electron binding energies. The lower

energies associated with ionization of a chromium 3p electron gives

a lower photoionization cross section when using the same x-radiation.[3]

Perhaps even more troublesome is the asymmetric background due probably

to bremstrahlung (inelastically scattered electrons).

Some preliminary iterative extended Hückel calculations, (see

TABLE X.

Carbon 1s Binding Energies and Calculated Charges

Compound Number	Compound	Binding Energy, eV.[a]	CNDO-Calculated Carbon Atom Charge
1	CF_4	300.7 (296.1[b])	+0.831
2	CF_2O	294.1	+0.720
3	CF_3H	295.1 (293.5[b])	+0.656
4	$\underline{C}F_3COCH_3$	292.8	+0.637
5	CO_2	292.5	+0.576
6	$\underline{C}F_3CO_2Na$	292.3	+0.569
7	$NaHCO_3$	290.2	+0.409
8	Na_2CO_3	289.7	+0.226
9	$CH_3\underline{C}O_2Na$	289.1	+0.437
6	$CF_3\underline{C}O_2Na$	289.1	+0.401
10	$CH_3\underline{C}O_2Na$	288.8	+0.320
4	$CF_3\underline{C}OCH_3$	288.7	+0.363
11	NH_4HCO_2	288.6	+0.318
12	$CH_3\underline{C}OCH_3$	288.0	+0.302
13	CH_2O	287.9	+0.329
10	$\underline{C}H_3CO_2Na$	285.0	+0.072
14	CH_4	285.0	+0.098
15	KCN	285.0	-0.482
12	$\underline{C}H_3COCH_3$	284.9	+0.098
9	$\underline{C}H_3CO_2H$	284.8	+0.125

[a] Binding energies taken from reference 49 except where noted.

[b] Professor D. Thomas (Princeton University), unpublished work.
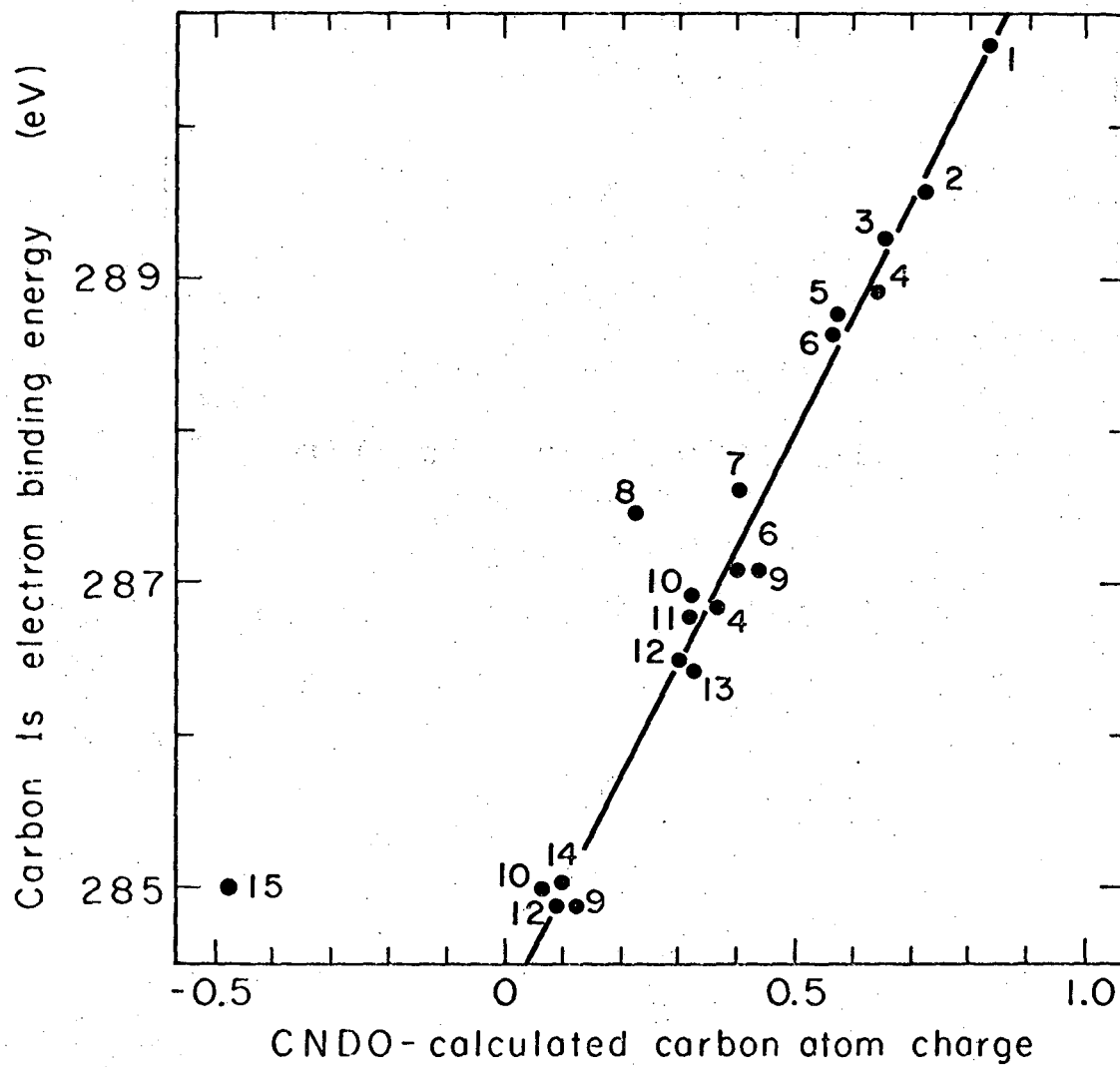
Figure 12. Plot of carbon 1s binding energies vs. CNDO-calculated charges on carbon atoms.

TABLE XI.

Chromium 3p Binding Energies

Compound	Binding Energy, eV.
$K_2Cr_2O_7$	48.7
CrO_3	48.2
$Na_2CrO_4 \cdot 4H_2O$	47.9
$Cr_2(SO_4)_3 \cdot xH_2O$	46.9
$Cr(CO)_6$	45.8
$[Cr(H_2O)_6](NO_3)_3 \cdot 3H_2O$	45.4
$CrCl_3 \cdot 6H_2O$	45.4
$[Cr(H_2O)_5Cl]Cl_2$	45.2
$K_3[Cr(CN)_6]$	44.8
$K_3[Cr(CN)_5NO]$	44.8
$Cr(NH_3)_6Cl_3$	44.7
$Cr_2O_3 \cdot xH_2O$	44.6
trans-$[Cr(H_2O)_4Cl_2]Cl$	44.5
$Cr_2(CH_3CO_2)_4(H_2O)$	44.5
Cr foil(unreduced)	43.9
Cr_2O_3	43.5
CrN	43.2
Cr foil(reduced)	43.2

calculation section) were completed for a few of the chromium com-
pounds; the results are given in Table XII. In all cases the
configuration of the chromium atom was assumed and the calculations
were iterated until all atom charges in the molecule were self-
consistent to within 0.05. Two modifications of the metal input
parameters were considered — one using Slater orbital exponents
coupled with neutral atom chromium valence orbital ionization
potentials for d^5p configuration (see reference 41) and the other
where essentially the metal orbital exponents were changed. In
both cases (see Figure 13) only a moderate correlation between
chromium 3$\underline{p}$ binding energy and calculated chromium atom charge was
found. Ultimately this type of correlation should be useful for
many aspects of transition metal chemistry. Similar studies of
iron compounds[53] are currently in progress, with particular emphasis
being placed on elucidating the character of iron in certain
biologically-important molecules.

The chromium 3$\underline{p}$ binding energies of $K_3[Cr(CN)_6]$ and $K_3[Cr(CN)_5NO]$
are the same and as such one would favor considering the later
compound as a formally Cr(III) compound contrary to the usual.[54]
Balance of charge would require a formally NO^- group. This agrees
with our nitrogen 1$\underline{s}$ work where we found the charge on the NO-nitrogen
in $K_3[Cr(CN)_5NO]$ to be too negative to be considered formally
as NO^+.

TABLE XII.

Iterative Extended Hückel-Calculated

Chromium Atom Charges

Molecule	Calculated Chromium Atom Charges	
	d^5p configuration[a]	modified d^5p configuration[b]
$Cr_2O_7^{2-}$	2.526	2.741
CrO_4^{2-}	2.430	2.618
$Cr(CN)_6^{3-}$	2.055	1.598
$Cr(CO)_6$	1.500	1.400

[a] Slater exponents used, H_{ii} for metal: 3d(-8.40 eV.), 4s(-8.01 eV.), and 4p(-3.52 eV.) as per reference 11 for neutral-atom d^5p configuration.

[b] Metal orbital exponents: 3d(2.22), 4s and 4p (0.733). H_{ii} for metal: 3d(-8.40 eV.), 4s(-9.27 eV.), and 4p(-3.52 eV.).
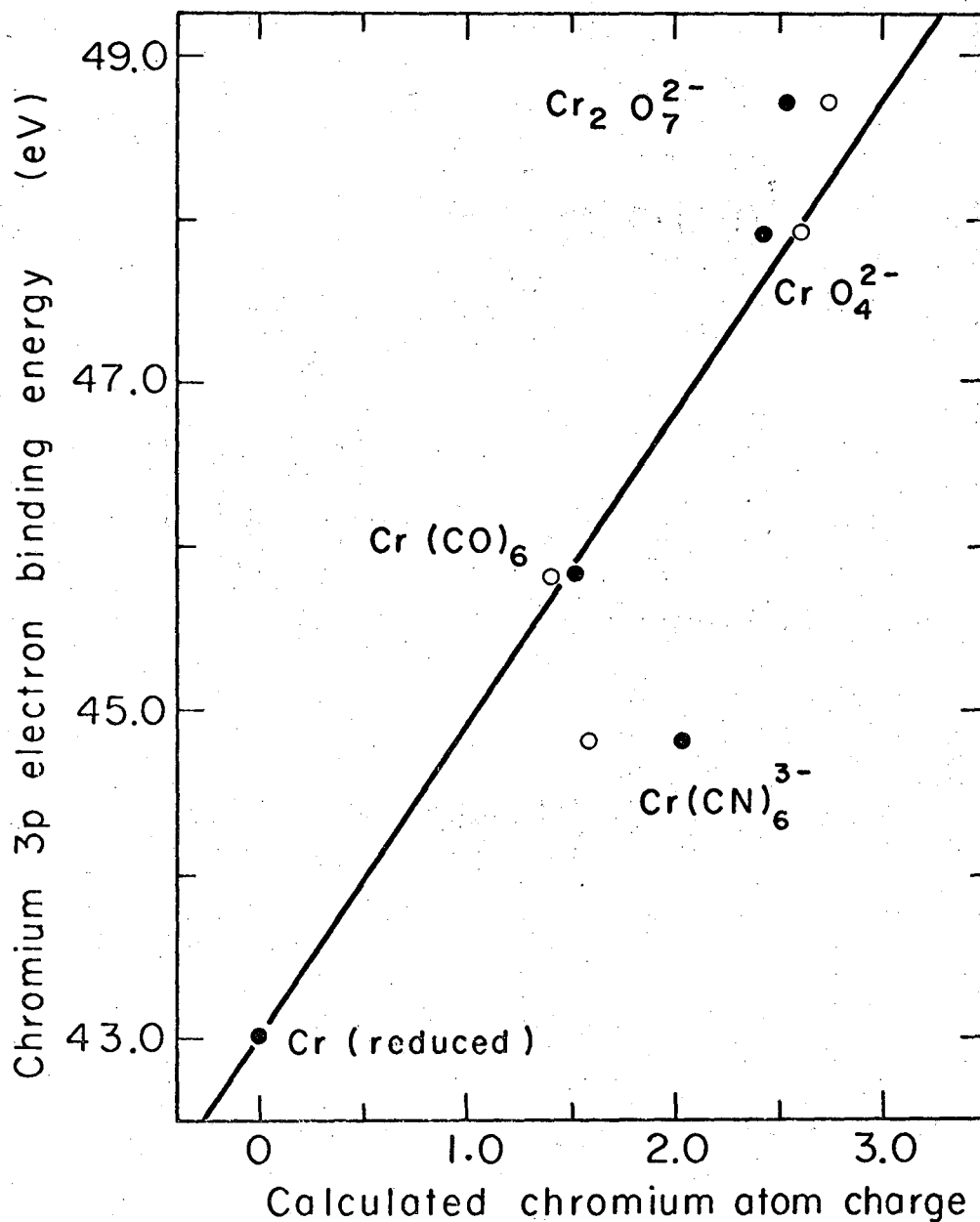
Figure 13. Plot of chromium 3p binding energies vs. iterative extended
Hückel-calculated charges on the chromium atoms. The
symbols o and o refer to the two different sets of input
data as given in footnotes a and b, respectively in Table
XII.

XBL 697-3248

REFERENCES TO PART I, SECTIONS I - VI.

(1)   H. Robinson and W. F. Rawlinson, Phil. Mag., 28, 277 (1914);
       H. Robinson, Proc. Roy. Soc., 104, 455 (1923); H. Robinson,
       Phil. Mag., 50, 241 (1925).

(2)   M. De Broglie, C. R., 172, 274 (1921).

(3)   K. Siegbahn, C. Nordling, A. Fahlman, R. Nordberg, K. Hamrin,
       J. Hedman, G. Johansson, T. Bergmark, S.-E. Karlsson, I. Lindgren
       and B. Lindberg, "ESCA Atomic Molecular and Solid State Structure
       Studied by Means of Electron Spectroscopy," Almquist and
       Wiksells AB, Stockholm (1967).

(4)   J. M. Hollander, M. D. Holtz, T. Novakov, and R. L. Grahm,
       Arkiv Fysik, 28, 375 (1965); T. Yamazaki, and J. M. Hollander,
       Nuclear Physics, 84, 505 (1966).

(5)   C. Nordling, E. Sokolowski, and K. Siegbahn., Arkiv Fysik, 13,
       483 (1958).

(6)   A. Fahlman, K. Hamrin, J. Hedman, R. Nordberg, C. Nordling,
       and K. Siegbahn, Nature, 210, 4 (1966).

(7)   A. Jahlman, R. Carlsson, and K. Siegbahn, Arkiv Kemi, 25,
       301 (1966).

(8)   R. Nordberg et al, Nature, 214, 481 (1967); R. Nordberg et al,
       Arkiv Kemi, 28, 257 (1968).

(9)   L. Pauling, "The Nature of the Chemical Bond," 3rd ed.,
       Cornell Univ. Press, Ithaca, N. Y. (1966), p. 97.

(10)   A Bendix curved channel-multiplier ("Channeltron") was used
       as the electron detector.

(11) Cis- PP and AP are the bidentate olefin phosphine ligands 2-
Cis- propenylphenyldiphenylphosphine and 2-allylphenyldiphenyl-
phosphine, respectively, see G. Nelson and L. Interrante,
Inorg. Chem., 7, 2059 (1968).

(12) D. P. Smith, "Hydrogen in Metals," University of Chicago Press,
Chicago, 1948.

(13) C. S. Fadley, S. B. M. Hagström, J. M. Hollander, M. P. Klein,
and D. A. Shirley, Science, 157, 1571 (1967); C. S. Fadley,
S. B. M. Hagström, M. P. Klein, and D. A. Shirley, J. Chem.
Phys., 48, 3779 (1968).

(14) R. Manne, J. Chem. Phys., 46, 4645 (1967).

(15) Tae-Kyu Ha and C. O'Konski, Chem. Phys. Letters, in press.

(16) J. A. Pople, D. S. Santry, and G. A. Segal, J. Chem. Phys.
43, S129, S136 (1965). A modified CNDO 1 version involving
empirically evaluated repulsion integrals was used as per
P. M. Kuznesof and D. F. Shriver, J. Am. Chem. Soc., 90,
1683 (1968).

(17) R. Hoffmann, J. Chem. Phys., 39, 1397 (1963).

(18) J. Hinze and H. H. Jaffe', J. Am. Chem. Soc., 84, 540 (1962).

(19) M. Wolfsberg and L. Helmholz, J. Chem. Phys., 20, 837 (1952).

(20) R. S. Mulliken, J. Chem. Phys., 23, 1833, 1841, 2338, 2343
(1955).

(21) P. M. Kuznesof, Quantum Chemistry Program Exchange (Indiana
University), QCPE 94 (1966).

(22) "Tables of Interatomic Distances," S. E. Sutton ed., Special
Publication No. 11, The Chemical Society, Burlington House,

London, 1958, and No. 18, Supplement, 1965.

(23) J. M. Hollander, D. N. Hendrickson, and W. L. Jolly, _J_. _Chem_. _Phys_., _49_, 3315 (1968).

(24) For review, see B. Johnson and J. McCleverty, "Nitric Oxide Compounds of Transition Metals" in _Progress_ _in_ _Inorganic_ _Chemistry_, _7_, 277 (1966).

(25) J. Lewis, R. J. Irving and G. Wilkinson, _J_. _Inorg_. _Nucl_. _Chem_., _7_, 32 (1958).

(26) D. Hall and A. A. Taggart, _J_. _Chem_. _Soc_., 1359 (1965); D. Dale and D. C. Hodgkin, _J_. _Chem_. _Soc_., 1364 (1965).

(27) C. C. Addison, G. A. Gamlen, and R. Thompson, _J_. _Chem_. _Soc_., 338 (1952).

(28) H. R. Hunt, J. R. Cox, and J. D. Roy, _Inorg_. _Chem_., _1_, 938 (1962).

(29) R. D. Feltham, _Inorg_. _Chem_., _3_, 900 (1964).

(30) D. N. Hendrickson and W. L. Jolly, _Inorg_. _Chem_., _8_, 693 (1969).

(31) P. C. Van der Voorn and R. S. Drago, _J_. _Am_. _Chem_. _Soc_., _88_, 3255 (1966).

(32) D. P. Santry and G. A. Segal, _J_. _Chem_. _Phys_., _47_, 158 (1967).

(33) J. C. Slater, _Phys_. _Rev_., _36_, 57 (1930).

(34) L. Cusachs, _J_. _Chem_. _Phys_., _43_, S160 (1965); L. Cusachs, _J_. _Chem_. _Phys_., _44_, 835 (1966).

(35) For $(C_6H_5)_3P$ see J. Daly, _J_. _Chem_. _Soc_., 3799 (1964).

(36) For P_4S_{10} and P_4S_7 see A. Vos and E. Wiebenga, _Acta_ _Cryst_., _8_, 217 (1955).

(37) W. W. Fogleman, D. J. Miller, H. B. Jonassen, and L. C. Cusachs, _Inorg_. _Chem_., _8_, 1209 (1969).

(38) J. M. Sichel and M. A. Whitehead, _Theoret. Chim. Acta_ (Berl.) _5_, 35 (1966).

(39) J. W. Emsley, J. Feeney, and L. H. Sutcliffe, "High Resolution Nuclear Magnetic Resonance Spectroscopy," Vol. 2, Pergamon Press, 1139 -54 (1966).

(40) J. A. Pople, _J. Chem. Phys._, _37_, 53 (1962).

(41) H. Basch, A. Viste, and H. B. Gray, _Theoret. Chim. Acta_ (Berl.) _3_, 458 (1965).

(42) M. J. S. Dewar, E. A. C. Lucken, and M. A. Whitehead, _J. Chem. Soc._, 2423 (1960).

(43) D. P. Graig and N. T. Paddock, _Nature_, _181_, 1052 (1958).

(44) C. E. Brion, D. J. Oldfield, and N. L. Paddock, Chem. Comm., 226 (1966).

(45) N. L. Paddock, _Quart. Rev._, 18, 168 (1964).

(46) J. Van Wazer, "Phosphorus and Its Compounds," Vol. 1, Interscience Publishers, Inc., New York, 118, 297 (1958).

(47) M. Silverstein, G. Nordblom, C. Ditlrich, and J. Jakabein, _Ind. Eng. Chem._, _40_, 301 (1948).

(48) H. Harnisch, _Z. Anorg. U. all. Chemie_, _300_, 261 (1959).

(49) R. Nordberg, U. Gelius, P. F. Hedén, J. Hedman, C. Nordling, K. Siegbahn, and B. J. Lindberg, submitted to _Arkiv för Kemi_.

(50) K. Hamrin, G. Johansson, A. Fahlman, C. Nordling, K. Siegbahn, and B. Lindberg, _Chem. Phys. Letters_, _1_, 557 (1968).

(51) T. Koopmans, _Physica_, _1_, 104 (1934); C. C. J. Roothaan, _Rev. Mod. Phys._, _23_, 61 (1951).

(52) D. Thomas (Princeton University), unpublished results.

(53) L. Cramer, M. Klein, and M. Calvin, Chemical Biodynamics
      Division of Lawrence Radiation Labs., Berkeley, unpublished
      results.

(54) This conclusion has also been reached by B. Feltham (University
      of Arizona) on the basis of bond lengths, etc., private
      communication.

VII. Paper: "Thermodynamic Interpretation of Chemical
               Shifts in Core-Electron Binding Energies"

Thermodynamic Interpretation of Chemical Shifts

in Core-Electron Binding Energies

William L. Jolly and David N. Hendrickson

Contribution from the Department of Chemistry,
University of California, and the Inorganic
Materials Research Division of the Lawrence
Radiation Laboratory, Berkeley, California 94720

Abstract: By making several approximations, it is possible to
calculate, from available thermodynamic data, a "thermochemical
energy" corresponding to the core-electron binding energy for an
atom in a compound. For a given element, such calculated "thermo-
chemical energies" are linearly related to experimental binding
energies. Thus it is possible to estimate thermodynamic data from
binding energies, and vice versa. The principal approximation
made in these calculations is that atomic cores which have the same

charge are chemically equivalent. The relatively small shifts in core-electron binding energy observed for an atom in a particular cation or anion in a series of salts are explicable in terms of lattice energy considerations.

I. Introduction

Atomic core-electron binding energies for solid compounds can be measured by x-ray photoelectron spectroscopy with a precision of ±0.2 eV. and, for a given element, have been shown to change as much as 15 eV. with changes in chemical environment.[1] The binding energies correlate with the oxidation states of the element or, better, with the estimated atomic charges: the higher the effective charge on an atom, the higher the binding energy. This correlation is intuitively reasonable because one would expect that it would be easier for an electron to leave an atom which has a negative charge than one which has a positive charge. Inasmuch as several fairly simple methods are available for estimating atomic charges, correlations of this type are easily made and have been used to infer structural information about compounds.[1-4] However there are at least two deficiencies in the use of these atomic charge-binding energy correlations.

First, in plots of core electron binding energy vs. estimated atomic charge, the points are scattered fairly widely from a smooth curve or straight line, suggesting that there is not an exact one-to-one correspondence between binding energy and atomic charge.[5] The fit of the points in such plots is only slightly improved by using more sophisticated methods for estimating atomic charges. This slight improvement can be seen by comparing the plots of nitrogen 1s binding energies vs. nitrogen atom charges calculated

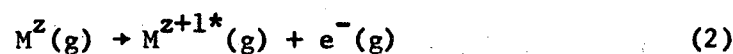by Pauling's method, by an extended Hückel MO method, and by the CNDO method.[1,2,4]

Second, the available approximate methods for estimating atomic charges (including those mentioned above) yield markedly different values. Thus, although a rough correlation can be obtained using charges consistently calculated by any one method, and although that empirical correlation can be very useful in structural studies, one obviously cannot attach fundamental or quantitative significance to "experimental" atomic charges derived from measured binding energies.

In this paper we shall consider several ways of splitting up the x-ray photoelectric process into constituent steps. We shall show that for one of these ways the estimated energies of certain steps correlate closely with the experimental binding energies.

II. The Inadequacy of the Concept of Fractional

Atomic Charge

Let us consider the promotion of a core electron from a particular atom, M, in a crystalline solid to the Fermi level of that solid. Let us assume that we are able to calculate for this atom a charge, z, which in general will be a non-integer. The core-electron binding energy of a gaseous atom possessing a charge z is a quantity which is a smooth function of z and which can be estimated fairly accurately.[6] However, this gas-phase binding energy is just one of

several energy terms which must be summed in order to evaluate the binding energy for the atom in the solid. The sum of the following processes corresponds to the desired process.

$$M^z(\text{lattice}) \rightarrow M^z(g) \tag{1}$$

$$M^z(g) \rightarrow M^{z+1*}(g) + e^-(g) \tag{2}$$

$$M^{z+1*}(g) \rightarrow M^{z+1*}(\text{lattice}) \tag{3}$$

$$e^-(g) \rightarrow e^-(\text{Fermi}) \tag{4}$$

$$\overline{M^z(\text{lattice}) \rightarrow M^{z+1*}(\text{lattice}) + e^-(\text{Fermi})} \tag{5}$$

In these equations, the asterisk indicates that the atom is lacking one core electron, and e^-(Fermi) refers to an electron at the Fermi energy level in the solid. As we have pointed out, the energy of process 2 is calculable. The energy of process 4 corresponds to the work function of the solid and is a difficult quantity to estimate. Probably the best one can do is to assume (or to hope) that the work function is relatively small and that it does not change much on going from one solid compound to another.

The energies of processes 1 and 3 are large "lattice energies" of a rather unusual type, and at present it is almost a hopeless task to estimate these quantities with an accuracy comparable to that of

the experimental binding energies.[7] Fadely et al[6] assumed that "lattice energies" of this type could be calculated by considering only coulombic interactions. They essentially adjusted the atomic charges so that the calculated energies for processes 1, 2 and 3 were consistent with the experimental binding energies.

For the atoms of a given element in a random set of compounds (e.g., for the nitrogen atoms in NH_4Cl, $NaNO_2$, pyridine, etc.) these "lattice energies" for processes 1 and 3 are not simply related to the magnitude of z, the charge on the atom. In fact if one were to find two entirely different compounds in which the nitrogen atoms had almost identical charges, it is probable that the combined energies of processes 1 and 3 would be quite different for the compounds. Thus, although the energy of process 2 correlates with z, there is no reason to expect anything better than a rough correlation between the energy of process 5 (the binding energy) and z.

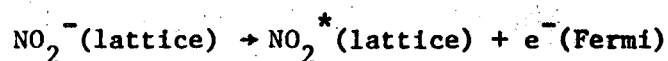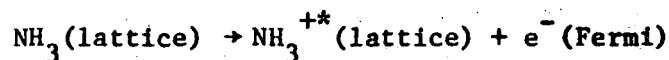### III. A Scheme Involving Neutral and Integrally-Charged Species

Let us now consider another general method for dividing up the process corresponding to the promotion of a core electron to the Fermi level in a solid. In this method the atom in question is either assigned an integral charge or is considered as part of a neutral molecule or an integrally-charged ion. We can use the same set of equations (1-5) that was used when considering fractionally-charged atoms, except that now z must be zero or a positive or

negative integer and now M^z can represent a molecule or ion.

In process 1 we remove the molecule or ion from its site in the crystal lattice. In process 2 the core electron of the atom in question is ejected from the gaseous species. (as before, the asterisk indicates a core-electron hole in the atom.) Then in process 3 we insert the M^{z+1*} group into the lattice site previously occupied by the M^z group, and in process 4 we place the electron into the Fermi level of the solid. The energy of process 5 is the experimental binding energy.

Our aim is to devise a general method for estimating the energies of the four processes which comprise process 5 in the hope that the sum of these estimated energies is a quantity that correlates well with experimental binding energy for a given element in a series of compounds.

It will be noted that process 4 has exactly the same significance that it had in the preceding scheme for dividing up the x-ray photo-electric process. Again, because of our inability to predict the Fermi energy levels in a wide variety of solids, we are forced to assume that the energy of process 4 (the work function for the substance) does not markedly vary on going from one compound to another. In the following paragraphs we shall describe a general method for estimating the sum of the energies of the three remaining processes (1, 2 and 3). We shall use, as illustrative examples, the process corresponding to the removal of nitrogen 1s electrons from ammonia and sodium nitrite.

$$NH_3(\text{lattice}) \rightarrow NH_3^{+*}(\text{lattice}) + e^-(\text{Fermi})$$

$$NO_2^-(\text{lattice}) \rightarrow NO_2^*(\text{lattice}) + e^-(\text{Fermi})$$

Process 1. – Our estimate of the energy of process 1 depends on whether M^z is situated in the bulk of the crystal lattice or near the surface. In view of the absorption of x-rays by matter, the x-ray photoelectric process might be expected to occur principally near the surface of the solid. However, Siegbahn et al.[1] have shown that x-ray photoelectrons are emitted in solids from a surface layer about 100 Å thick. Photoelectron emission is clearly not limited to the outer few ångströms, because if that were the case then the contribution of process 1 to the binding energy would be expected to range from one-half the lattice energy (for transitions at the surface) to almost the full lattice energy (for transitions within the crystal). Consequently the spectra would be expected to consist of broad bands, with half-widths as great as 10 eV. Inasmuch as relatively sharp spectra are actually observed, we believe that most of the transitions occur in the bulk of the crystal.
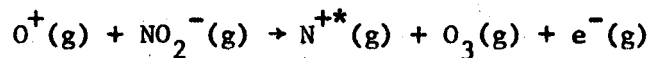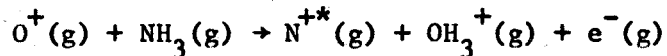
If M^z is a neutral molecule, the energy of process 1 is twice the sublimation energy of the compound. If M^z is an ion in a crystal lattice with counter-ions of charge $-z$, the energy of process 1 is the lattice energy of the compound.[9] Therefore we write the following equations for this process for NH_3 and $NaNO_2$.

$$2NH_3(s) \rightarrow 2NH_3(g)$$

$$NaNO_2(s) \rightarrow Na^+(g) + NO_2^-(g)$$
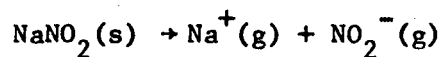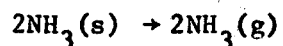
Process 2 and the Concept of "Equivalent Cores". - We assume that when the core electron of the atom in question is ejected from the species M^z in process 2, the valence electrons adjust to the increase in charge of the atom's core. (Later we shall consider the justification for this assumption in detail.) Now if we make the approximation that <u>cores</u> <u>which</u> <u>have</u> <u>the</u> <u>same</u> <u>charge</u> <u>are</u> <u>chemically</u> <u>equivalent</u>, then we conclude that the increase in the atom's core charge by one unit corresponds to the replacement of the atomic nucleus by a nucleus of the next element in the periodic table. In the particular cases under discussion, the practical result of this approximation is the realization that the radicals $NH_3^{+}*$ and NO_2* are equivalent to the species OH_3^+ and O_3, respectively, as far as the valence electrons are concerned. On this basis we assume that the energies of the following processes are zero.

$$O^+(g) + NH_3^{+*}(g) \rightarrow N^{+*}(g) + OH_3^+(g)$$

$$O^+(g) + NO_2^*(g) \rightarrow N^{+*}(g) + O_3(g)$$
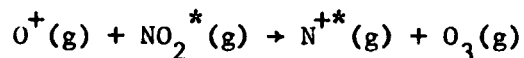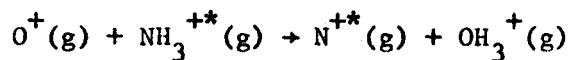
Thus we may write the following equations in place of process 2.

$$O^+(g) + NH_3(g) \rightarrow N^{+*}(g) + OH_3^+(g) + e^-(g)$$

$$O^+(g) + NO_2^-(g) \rightarrow N^{+*}(g) + O_3(g) + e^-(g)$$

Process 3. - When $z = 0$, process 3 corresponds to the condensation of a radical cation into a hole in a latice of neutral molecules. We shall assume that the energy of this process is unchanged when we replace the cation by the corresponding neutral species. In the case when M^z is NH_3, we write for process 3,

$$2NH_3(g) \rightarrow 2NH_3(s)$$

When $z = -1$, process 3 corresponds to the condensation of a neutral radical into a hole in an ionic lattice. We shall use the concept of "equivalent cores" discussed above and shall assume that in process 3 the species M^{z+1*} may be replaced with the appropriate neutral molecule and that the hole in the ionic lattice may be replaced with a hole in the corresponding lattice of neutral molecules. Thus in the case of $NaNO_2$ we assume that the energy of process 3 is the same as that for the condensation of O_3 into a hole in a lattice of solid O_3. We write
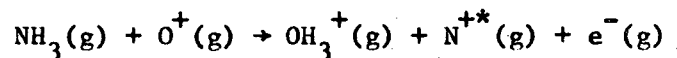
$$2O_3(g) \rightarrow 2O_3(s)$$
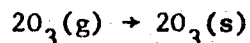
Fortunately the energy of this type of process is not large, and

so even this crude approximation does not introduce much error.
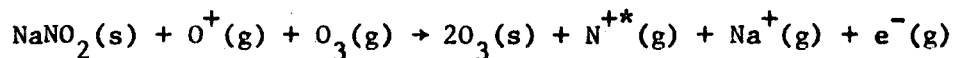
When z is other than 0 or -1, it is relatively difficult to estimate the energy of process 3 (and sometimes process 1). For example, consider the ejection of a core electron from sulfur in Na_2S. Here the energy of process 1 (the removal of sulfide ion from the lattice) is not readily calculable from the lattice energy of Na_2S without a detailed consideration of Madelung energies. The energy of process 3 (the insertion of S^{-*} into a sulfide vacancy in Na_2S) is even more difficult to estimate. Therefore we shall now limit ourselves to compounds where z = 0 or -1.

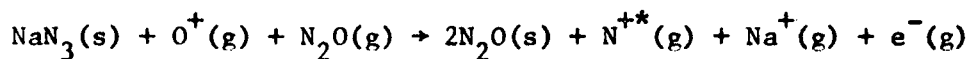"Thermochemical Energies." - By adding the equation corresponding to processes 1, 2 and 3, we obtain the following results. For $NH_3(s)$,

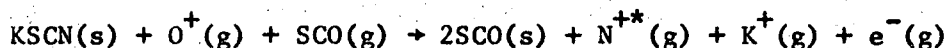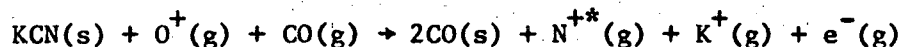$$NH_3(g) + O^+(g) \rightarrow OH_3^+(g) + N^{+*}(g) + e^-(g)$$

for $NaNO_2(s)$,
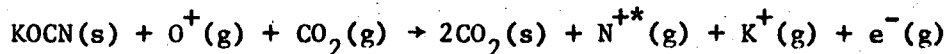
$$NaNO_2(s) + O^+(g) + O_3(g) \rightarrow 2O_3(s) + N^{+*}(g) + Na^+(g) + e^-(g)$$

We may similarly write, for other nitrogen compounds whose x-ray photoelectron spectra have been obtained, the following equations.

$$NaN_3(s) + O^+(g) + N_2O(g) \rightarrow 2N_2O(s) + N^{+*}(g) + Na^+(g) + e^-(g)$$

$$KOCN(s) + O^+(g) + CO_2(g) \rightarrow 2CO_2(s) + N^{+*}(g) + K^+(g) + e^-(g)$$

$$KCN(s) + O^+(g) + CO(g) \rightarrow 2CO(s) + N^{+*}(g) + K^+(g) + e^-(g)$$

$$KSCN(s) + O^+(g) + SCO(g) \rightarrow 2SCO(s) + N^{+*}(g) + K^+(g) + e^-(g)$$

We shall refer to the preceding six reactions as _thermo-equivalent_ reactions, because they are supposed to be thermodynamically equivalent to the core-electron emission processes for the compounds on the left sides of the equations. It will be noted that the energies of these thermo-equivalent reactions can, in principle, be evaluated from thermodynamic data. Inasmuch as the species $N^{+*}(g)$ and $O^+(g)$ appear in all these reactions, the energies of formation of these species contribute equally to the energies of the reactions. Consequently _differences_ in the energies of the reactions are unaffected by ignoring the species $O^+(g)$ and $N^{+*}(g)$, and we have done so for simplicity in calculation. We shall refer to the simplified calculated energies as _thermochemical energies_, E_T. These energies and the corresponding experimental 1s binding energies for nitrogen compounds are presented in Table I. The data, when plotted as in Figure 1, clearly show that the binding energy, E_B, is a linear function of the thermochemical energy, E_T. The scatter of the points is considerably less than that found in plots of E_B against estimated nitrogen atom charges.[2,4] In fact, inasmuch as the slope of the straight line in Figure 1 is unity, we may

Table I.

Nitrogen 1s Binding Energies (E_B) and the Corresponding Thermochemical Energies (E_T).

Compound	E_B, kcal/mole	E_T, kcal/mole[a]
$NaNO_2$	9318	261
$AgNO_2$	9305	284
KNO_2	9298	240
Na[N-N-N]	9208	150[b]
NaCN	9203	138
KCN	9201	120
NH_3	9196	151[b]
KSCN	9189	128
KOCN	9185	115

[a] E_T values were calculated from data in reference 22 except where otherwise indicated.
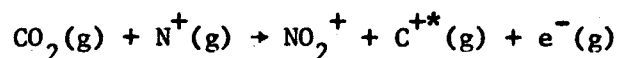
[b] See Section IX.
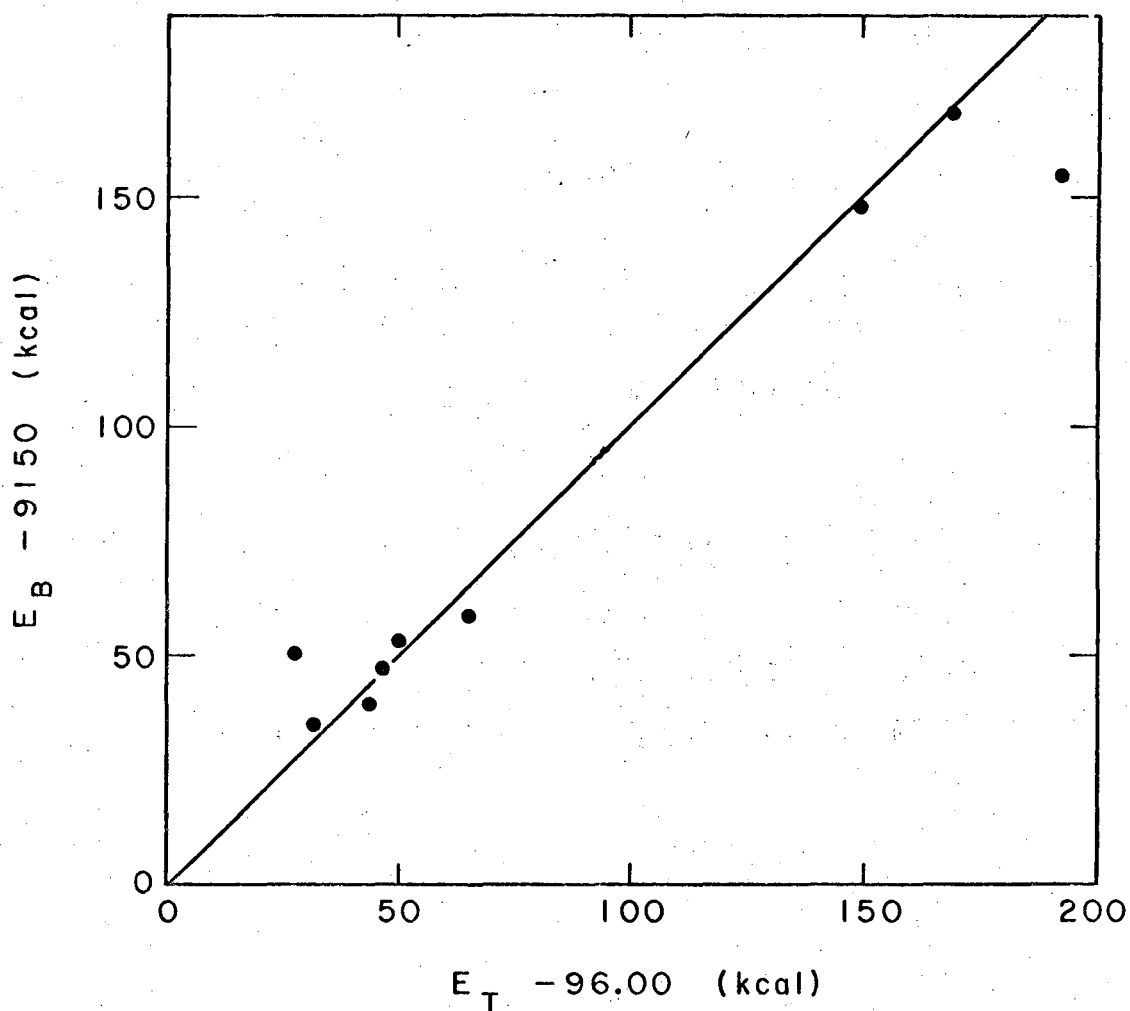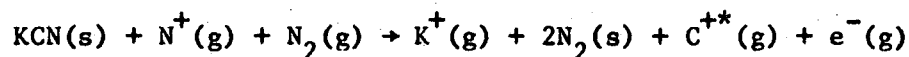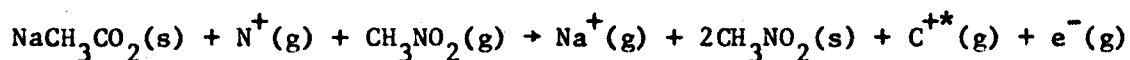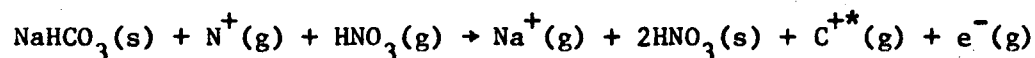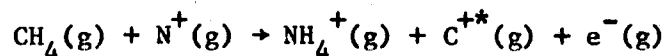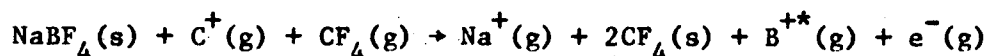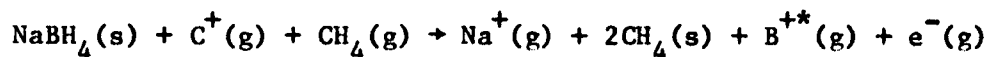
Figure 1. Nitrogen 1s binding energies (E_B) vs. the corresponding thermochemical energies (E_T). The E_B and E_T values have been reduced by 9150 and 96 kcal/mole, respectively, to make the best straight line pass through the origin.

state that changes in E_T are equal to the corresponding changes in E_B.

Extension to Other Elements. – Similar calculations can be carried out for the compounds of other elements for which both x-ray photoelectric data and the appropriate thermodynamic data are available. However the number and reliability of the data are not as great as in the case of nitrogen compounds. For carbon compounds, we may write the following thermo-equivalent reactions.

$$CH_4(g) + N^+(g) \rightarrow NH_4^+(g) + C^{+*}(g) + e^-(g)$$

$$NaHCO_3(s) + N^+(g) + HNO_3(g) \rightarrow Na^+(g) + 2HNO_3(s) + C^{+*}(g) + e^-(g)$$

$$NaCH_3CO_2(s) + N^+(g) + CH_3NO_2(g) \rightarrow Na^+(g) + 2CH_3NO_2(s) + C^{+*}(g) + e^-(g)$$

$$KCN(s) + N^+(g) + N_2(g) \rightarrow K^+(g) + 2N_2(s) + C^{+*}(g) + e^-(g)$$

$$CO_2(g) + N^+(g) \rightarrow NO_2^+ + C^{+*}(g) + e^-(g)$$

For boron compounds we may write the following thermo-equivalent reactions.

$$NaBH_4(s) + C^+(g) + CH_4(g) \rightarrow Na^+(g) + 2CH_4(s) + B^{+*}(g) + e^-(g)$$

$$NaBF_4(s) + C^+(g) + CF_4(g) \rightarrow Na^+(g) + 2CF_4(s) + B^{+*}(g) + e^-(g)$$

And for iodine compounds we may write the following thermo-equivalent reactions.

$$KI(s) + Xe^+(g) + Xe(g) \rightarrow K^+(g) + 2Xe(s) + I^{+*}(g) + e^-(g)$$

$$KIO_3(s) + Xe^+(g) + XeO_3(g) \rightarrow K^+(g) + 2XeO_3(s) + I^{+*}(g) + e^-(g)$$

$$KIO_4(s) + Xe^+(g) + XeO_4(g) \rightarrow K^+(g) + 2XeO_4(s) + I^{+*}(g) + e^-(g)$$
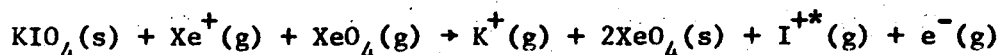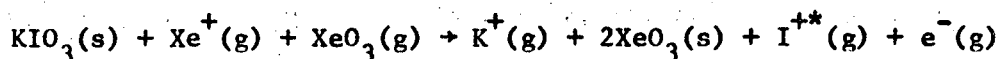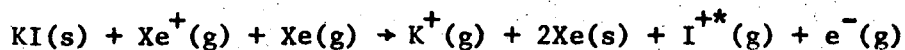
Values of E_B and E_T for compounds of boron, carbon, and iodine are listed in Table II. In Figure 2, we have plotted $E_B - \alpha$ against $E_T - \beta$, where α and β are arbitrary constants for each element, chosen such as to make the points fall on a line passing through the origin. It can be seen that E_B is a linear function of E_T for the compounds of Table II. Except for the boron-compound line, the lines through the points have slopes less than unity. However, perhaps the deviations from unit slope are insignificant in view of the paucity and relative inaccuracy of the data.

IV. <u>Electronic Relaxation</u>

<u>Lifetime of Core-Electron Hole.</u> - In the preceding discussion, we have assumed that a measured binding energy corresponds to the formation of an excited state in which a core electron has been removed from an atom. In other words, we have assumed that the x-ray photoelectric transition occurs in a time interval shorter

Table II.

Core-Electron Binding Energies (E_B) and the Corresponding
Thermochemical Energies (E_T) for Compounds of Boron, Carbon,
and Iodine.

Compound	E_B, kcal/mole	E_T, kcal/mole[c]
$NaBF_4$	4499[a]	339[d]
$NaBH_4$	4321[a]	170
CO_2	6745[a]	355[d]
$NaHCO_3$	6692[a]	317
$NaCH_3CO_2$	6660[a]	281
CH_4	6572[a]	160[d]
KCN	6572[a]	147
KIO_4	145[b]	370
KIO_3	122[b]	330
KI	0[b]	194

[a] 1s electron binding energies.

[b] Weighted average shifts for the core levels. Data from reference 6.

[c] E_T values were calculated from data in reference 22 except where otherwise indicated.

[d] See Section IX.
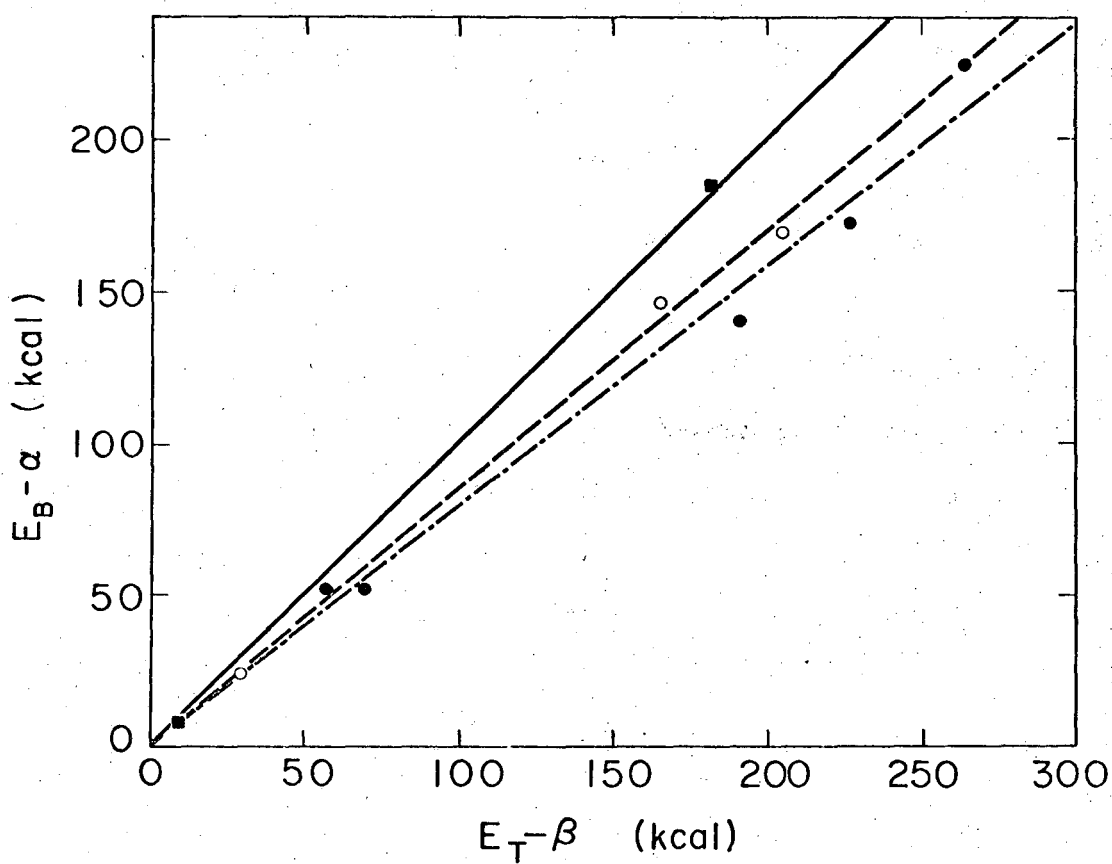
XBL 697-3179

Figure 2. Core-electron binding energies (E_B) vs. thermochemical
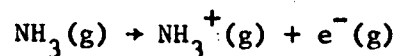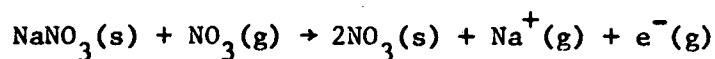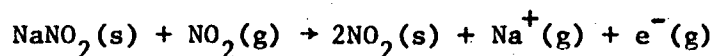
energies (E_T). The squares correspond to boron compounds

(α = 4314, β = 157); the filled circles correspond to

carbon compounds (α = 6544, β = 90); the open circles

correspond to iodine compounds (α = -24, β = 165).

than the lifetime of the core electron hole. This assumption seems

plausible because the photoelectric process is believed to occur

in a time interval around 10^{-18} sec, whereas x-ray states have

lifetimes around 10^{-16} sec.[10] However, we can actually test the

assumption using thermodynamic data. If the binding energies

corresponded to the formation of a state in which a valence electron

had fallen into the core-electron hole, the radical formed would

be of a type relatively familiar to chemists. Processes 1, 2 and 3

could be used to obtain a thermo-equivalent reaction, but the

asterisk would no longer have any meaning. The species X^{z+1*}

would refer to the radical in its ground state, and it would no

longer be appropriate to apply the concept of equivalent cores.

For the nitrogen $1\underline{s}$ binding energies in $NaNO_2(s)$, $NaNO_3(s)$, $NaCN(s)$

and $NH_3(s)$, we write the following reactions.

$$NaNO_2(s) + NO_2(g) \rightarrow 2NO_2(s) + Na^+(g) + e^-(g)$$

$$NaNO_3(s) + NO_3(g) \rightarrow 2NO_3(s) + Na^+(g) + e^-(g)$$

$$NaCN(s) + CN(g) \rightarrow 2CN(s) + Na^+(g) + e^-(g)$$

$$NH_3(g) \rightarrow NH_3^+(g) + e^-(g)$$

The calculated (or estimated) energies for these four reactions

(which we shall call E_T' values) and a set of seven similarly-calculated

E_T' values for carbon compounds (carbon $\underline{1s}$ binding energies) are given in Table III together with the corresponding E_B values. It is clear from these data that the measured binding energies do not correspond to the formation of ground-state radicals with complete cores. First, the E_B and E_T' values in Table III are of an entirely different order of magnitude. In order to make the E_T' values consistent with the E_B values it would be necessary to make the incredible assumption that the work functions (process 4) have values of several thousand kcal/mole. Second, there is no correlation whatsoever between the E_B and E_T' values, as was found between the E_B and E_T values.

Valence Electron Relaxation. - Although it is easy to show that an observed binding energy corresponds to the formation of a species lacking a core electron, it is considerably more difficult to show that the valence electrons have relaxed--that is, that they have adjusted to the increased core charge.

It will be remembered that when we calculated the E_T values, it was assumed that the valence electrons were relaxed. Consequently the fact that we observe the linear relationships between E_B and E_T shown in Figures 1 and 2 means that any unreleased electronic relaxation energy must be a linear function of E_B. In fact, because the line of Figure 1 has a slope of unity, any unreleased relaxation energy for nitrogen compounds must be a constant. These restrictions on the relaxation energy seem sufficiently improbable to us that we feel our assumption of complete relaxation is confirmed. However

Table III.

Values of E_B (1$\underline{s}$) and E_T' for Some Nitrogen
and Carbon Compounds.

Compound	E_B, kcal/mole	E_T' kcal/mole
NH_3	9196	234
NaCN	9203	269
$NaNO_2$	9318	230
$NaNO_3$	9395	255
CH_4	6572	300
KCN	6572	252
C_2H_6	6572	269
CS_2	6623	233
CH_2O	6639	251
CO_2	6745	318
CCl_4	6752	264

we have further confirmation in the form of estimated electronic relaxation energies. We have used the CNDO method to calculate the differences in the total valence electron energies for the following pairs of gaseous species: N_3^- and N_3*, CN^- and $CN*$, OCN^- and $OCN*$, and NO_2^- and NO_2*. The results were 482, 544, 641 and 773 kcal./mole, respectively.[11] When the E_T values for NaN_3, NaCN, KOCN and $NaNO_2$ are increased by these relaxation energies, they are no longer linearly related to the corresponding E_B values.

According to Koopmans' theorem[12] an E_B value would equal the calculated negative core electron eigenvalue $(-\epsilon)$ when we have the formation of an excited state with unrelaxed electrons. In Table IV we give, for a variety of species, the E_B values and the corresponding negative core electron energies $(-\epsilon)$ obtained from ab initio calculations. If Koopmans' theorem were valid in this situation, the E_B and $-\epsilon$ values would be equal. In fact, the E_B values are consistently smaller than the $-\epsilon$ values, and the differences (given in the third column of Table IV) are of the same magnitude as the values that we estimated for electronic relaxation energies.

V. Orientational Excitation Energy

Although measured core-electron binding energies correspond to the formation of species in which the valence electrons have probably relaxed, we believe (on the basis of the Born-Oppenheimer approximation) that the atoms in these species have not relaxed with respect

Table IV.

E_B Values and the Corresponding Ab Initio – Calculated
Energies for 1s Electrons.

Compound[a]	E_B, kcal/mole	$-\epsilon$, kcal/mole	$-\epsilon-E_B$, kcal/mole
$\underline{C}H_4$	6572	7033[b]	461
$\underline{C}F_3H$	6805	7374[b]	569
$\underline{C}O_2$	6745	7181[c]	436
$\underline{C}_2H_6$	6572	7036[d]	464
$H_2\underline{C}O$	6639	7123[e]	484
$C_5H_5\underline{N}$	9178	9837[f]	659
$\underline{N}H_3$	9196	9717[g]	521
K$\underline{C}$N	6572	6844[h]	272
KC$\underline{N}$	9201	9556[h]	355
Na($\underline{N}$NN)	9309	9706[i]	397
Na(N$\underline{N}$N)	9208	9549[i]	341
KS$\underline{C}$N	9189	9607[c]	418
KOC$\underline{N}$	9185	9579[c]	394

[a] The energies refer to the 1s electrons of the atoms indicated in bold-face type.

[b] Tae-Kyu Ha and L. C. Allen, International Journal of Quantum Chem., 1s, 199 (1962).

[c] A. D. McLean and M. Yoshimine, "Tables of Linear Molecule Wave

Functions", International Business Machines Corp. (1967).

[d] E. Clementi and D. R. Davis, J. Chem. Phys., 45, 2593 (1966).

[e] R. J. Buenker and J. L. Whitten (1967) in "Compendium of Ab Initio Calculations of Molecular Energies and Properties," M. Krauss, NBS Technical Note 438 (1967).

[f] E. Clementi, J. Chem. Phys. 46, 4731 (1967).

[g] P. Rajagopal, Z. Naturforsch. 20A, 1557 (1965).

[h] D. N. Hendrickson and P. M. Kuznesof, Theoret. Chim. Acta., to be published.

[i] S. D. Peyerimhoff and R. J. Buenker, J. Chem. Phys., 47, 1953 (1967).

to their relative positions. For example, we assume that the nitrogen 1$\underline{s}$ binding energy of cyanide ion corresponds to the formation of CN* radical with the same C-N bond distance as in the ground state of the cyanide ion (1.14Å). From the potential energy data for carbon monoxide[13] (r_{eq} = 1.128Å), we estimate the unreleased excitation energy to be about 1 kcal/mole. From the potential energy data for molecular nitrogen[14] (r_{eq} = 1.098Å), we estimate the excitation energy associated with the carbon 1$\underline{s}$ binding energy of cyanide to be about 3 kcal/mole. If the orientational excitation energies associated with all other core-electron binding energies are of the same general magnitude as these estimated values, i.e. 1-3 kcal/mole, then the error we have made by ignoring these excitation energies is less than the precision of the E_B values and is negligible.

VI. Lattice Shifts

Anions. - According to the approximate methods discussed in Section III, the binding energies for an atom in a particular -1 anion in a series of salts should differ only by the differences in the contributions from process 1, i.e., by the differences in the energy required to remove the anion from the lattice. In the case of salts with +1 cations, these differences should be equal to the differences in the lattice energies of the salts. Some idea of the accuracy of this postulate can be obtained from Table V, where E_B

Table V.

A Comparison of Relative Values of E_B and E_T for Nitrates, Nitrites and Cyanides.

Salt	Relative[a] E_B, kcal.	Relative[a] E_T, kcal.
$LiNO_3$	+ 8	+32
$NaNO_3$	0	0
KNO_3	− 5	− 7
NH_4NO_3	− 6	−18
$AgNO_3$	−14	+26
$NaNO_2$	0	0
KNO_2	−26	−20
$AgNO_2$	−19	+23
$NaCN$	0	0
KCN	− 2	−18

[a] Relative to the sodium salts.

and E_T values for nitrates, nitrites and cyanides (all _relative_

to the sodium salts) are tabulated. The several marked discrepancies

between the E_B and E_T values might suggest that the postulate has no

value. However, we believe that, except for the case of KCN, the

large discrepancies can be rationalized in terms of possibly

spurious E_B values. The tabulated E_B value for $LiNO_3$ may be low

because of hydration of the sample ($LiNO_3$ is very hygroscopic).

Hydration of the lithium ions would be expected to make it easier to

remove an anion from the lattice. The E_B values for $AgNO_3$ and

$AgNO_2$ may be low because of decomposition of the samples in the

x-ray beam. These samples, contrary to the others, became colored

upon irradiation. We have no explanation for the large discrepancy

in the case of KCN. We believe the data of Table V indicate that,

for a series of similar salts, the work function (the energy of

process 4) usually does not vary by more than 10 kcal/mole.

In the case of salts with cations having charges greater than

+1, the estimation of the energy of process 1 is considerably more

complicated. Consider the nitrogen 1s binding energy of a nitrate

of a +2 metal ion. The energy of removing a nitrate ion from an

$M(NO_3)_2$ lattice is some fraction _f_ of the energy of removing an

M^{2+} ion and two NO_3^- ions from the lattice. The latter energy can

be calculated from thermodynamic data (it is twice the lattice

energy), but _f_ is a quantity whose evaluation requires detailed

structural information. We have used binding energies and thermo-

dynamic data for a series of +2 metal nitrates to calculate _empirical_

values of $\underline{f}$. These data are presented in Table VI. The values of

$\underline{f}$ are remarkably similar; the average value is 0.159 ± 0.013. The

value of $\underline{f}$ can be estimated for the fluoride ion in calcium fluoride

if we make the reasonable assumption that the removal energies for

F^- and Ca^{2+} partition in the same ratio as the corresponding electro-

static energies. If we systematically delete half of the fluoride

ions in CaF_2 and change the charge on the remaining fluoride ions

to -2, we are left with a pseudo-zinc-blende structure.[15,16] Now

the energy of removing a Ca^{2+} ion from CaF_2 is equal to the energy

of removing a Ca^{2+} ion from the pseudo-zinc-blende structure, and

this energy is equal to the lattice energy of the pseudo-zinc-blende

structure.[9] Inasmuch as the lattice energies of the two structures

are proportional to the Madelung constants[17] times the product of

the ionic charges, we may calculate the quantity $1-2\underline{f}$ for CaF_2 as

follows,

$$1-2\underline{f} = 1.638/2.519 = 0.650$$

Thus we calculate $\underline{f} = 0.175$ for the fluoride ion in CaF_2. The value

is sufficiently close to the value empirically found for various

$M(NO_3)_2$ salts to suggest that it may be used as a rough value for

any MX_2 salt. The method has limited applicability to the calculation

of E_T values, however, because it requires the knowledge of the

heats of formation of gaseous anions (which are generally known

very inaccurately).

Table VI.

Nitrogen 1s Binding Energies for Nitrates of +2
Metal Ions and Empirically Evaluated f Values.

Salt	E_B, kcal/mole	f
$Mg(NO_3)_2$	9408	0.155
$Ca(NO_3)_2$	9406	0.170
$Ba(NO_3)_2$	9399	0.180
$Cd(NO_3)_2$	9378	0.130
$Pb(NO_3)_2$	9395	0.160

Potassium Salts. - Potassium core-electron binding energies have
been determined for a variety of potassium salts; the results are
given in the second column of Table VII. Probably the most remarkable
feature of these binding energies is the fact that they are essentially
constant on going from one salt to another. For the potassium halides,
we can use an approximate method for estimating the sum of the
energies of processes 1 and 3. The energy of process 1 is simply the
lattice energy of the salt, U. The energy of process 3 is the energy
of inserting a K^{2+*} ion (or, using the concept of equivalent cores,
a Ca^{2+} ion) into a cation vacancy in the potassium salt. We assert
that the energy of process 3 may be closely approximated by the Coulomb
lattice energy[18] ($-2U_c$) plus the energy of interaction of the K^{2+} ion
with the dipoles induced in the surrounding halide ions ($-U_p$).
We have estimated $-U_p$ using the known polarizabilities of the halide
ions and the assumption that the only charge-dipole forces of conse-
quence are those between the K^{2+*} ion and six halide ions octahedrally
arranged with a $K^{2+*} - X^-$ distance equal to the normal $K^+ - X^-$ distance
in the salt.[19] The calculated values of $U-2U_c-U_p$ are given in the
third column of Table VII; it can be seen that the values are
essentially constant. Thus the near constancy of the experimental
E_B values is in accord with theory. In fact if our values of
$U-2U_c-U_p$ are an accurate measure of the sum of the energies of pro-
cesses 1 and 3, we may ascribe the observed variations in E_B for
potassium salts to variations in the energy of process 4, the work
function.

Table VII.

Potassium 3p binding energies and some
values of $U-2U_c-U_p$. Values in kcal/mole.

| Salt	E_B	$U-2U_c-U_p$
KI	399	−298
KBr	374	−304
KCl	385	−301
KF	418	−301
KCN	392	
KNO$_3$	401	
KNO$_2$	393	
KOCN	396	

VII. The Prediction of Heats of Reaction

Suppose that a core-electron binding energy is known for an atom in a compound, but that it is not possible to calculate the corresponding thermochemical energy because the heat of formation of one of the species in the thermo-equivalent reaction is unknown. If a linear correlation between E_B and E_T has already been established for the element, one can estimate the E_T value using the correlation and then estimate the heat of formation of the species whose heat of formation is unknown.

For example, from the known 1s binding energy of the middle nitrogen atom in sodium azide (9309 kcal/mole) and Figure 1, we estimate E_T = 249 kcal/mole for the following thermo-equivalent reaction.

$$NaN_3(s) + NON(g) + O^+(g) \rightarrow 2NON(s) + Na^+(g) + N^{+*}(g) + e^-(g)$$

By estimating the sublimation energy of NON to be the same as that of CO_2, and by using the known heats of formation of $NaN_3(s)$ and $Na^+(g)$, we calculate ΔH_f° = 120 kcal/mole for NON(g). From this we calculate that ΔH° = -100 kcal/mole for the isomerization

$$NON(g) \rightarrow NNO(g)$$
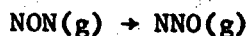
The heats of formation of various hydrogen-containing gaseous

cations can be estimated from E_B data, and these can be used to calculate proton affinities. For example from the carbon $\underline{1s}$ binding energy of chloroform (6683 kcal/mole) and Figure 2 we estimate $E_T = 265$ kcal/mole for the following thermo-equivalent reaction.

$$CHCl_3(g) + N^+(g) \rightarrow NHCl_3^+(g) + C^{+*}(g) + e^-(g)$$
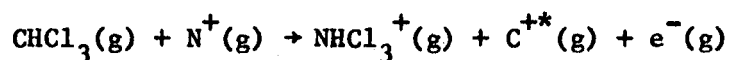
By combining this with the known heat of formation of gaseous chloroform we calculate $\Delta H_f^\circ = 240$ kcal/mole for $NHCl_3^+(g)$. When the latter quantity is combined with the heats of formation of $H^+(g)$ and $NCl_3(g)$, we obtain 190 kcal/mole for the proton affinity of NCl_3.

$$NCl_3(g) + H^+(g) \rightarrow HNCl_3^+(g) \quad \Delta H^\circ = -190 \text{ kcal/mole}$$
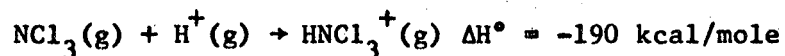
We have similarly calculated proton affinities for other species. These estimated values, as well as literature values for ammonia and water, are presented in Table VIII.

When thermodynamic data are available for the calculation of an E_T value for a compound for which no E_B value is known, it is possible to predict the E_B value. For example, we may write the following thermo-equivalent equation for sodium amide (nitrogen $\underline{1s}$ binding energy).

Table VIII.

Gas-Phase Proton Affinities Estimated from
Core-Electron Binding Energy Data.

Compound	Proton Affinity, kcal/mole
C_5H_5N	247
CH_3NH_2	247
CH_3CONH_2	239
NH_3	214[a]
CH_3NO_2	209
NH_2OH	208
$n-C_4H_9OH$	202
C_6H_5OH	192
NCl_3	190
H_2O	169[b]
NF_3	133

[a] Proton affinity taken from reference 26.

[b] Proton affinity taken from reference 24.

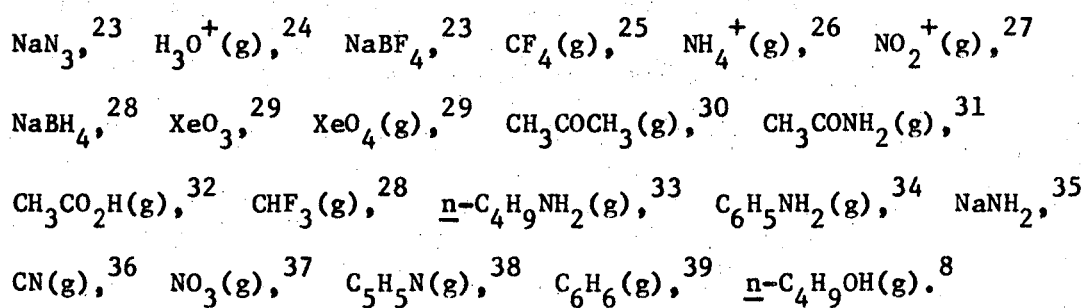$$NaNH_2(s) + O^+(g) + H_2O(g) \rightarrow 2H_2O(s) + Na^+(g) + N^{+*}(g) + e^-(g)$$
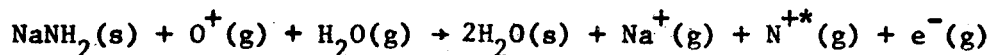
Available thermochemical data yield $E_T = 93$ kcal/mole; from Figure 1 we then predict the nitrogen 1s binding energy in sodium amide to be 9153 kcal/mole.

VIII. Core-Electron Binding Energies

Most of the core-electron binding energies were taken from the literature.[20] The carbon 1s binding energy of CHF_3 (6768 kcal/ mole) was recently determined by Professor Darrah Thomas, to whom we are grateful for this privileged information. Nitrogen 1s binding energies for $LiNO_3$, KNO_3, $Mg(NO_3)_2$, $Ca(NO_3)_2$, $Ba(NO_3)_2$, $Cd(NO_3)_2$, $Pb(NO_3)_2$, KNO_2, $AgNO_2$, and $NaCN$, potassium 3p binding energies for KF, KCl, KBr, KI, KNO_3 KNO_2, KOCN, and KCN, and boron 1s binding energies for KBH_4 and $NaBF_4$ were determined by us using $MgK\alpha$ x-radiation (1253.6 eV) and an iron-free double-focusing magnetic spectrometer of 50-cm radius.[21] A detailed description of the experimental aspects of x-ray photoelectron spectroscopy can be found in the review by Siegbahn et al.[1] The binding energy for each compound was measured at least three times. The carbon 1s line (arising from the film of pump oil on each sample) served as a convenient reference peak. The work function of the spectrometer material (aluminum) was assigned the value 4.0 eV. Powdered samples were mounted on an aluminum plate by means of double-faced con- ducting adhesive tape.
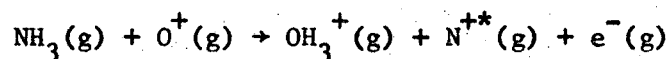
IX. Calculations

Most of the thermodynamic data were taken from U. S. National Bureau of Standards publications.[22] However some data were obtained from other sources. Heats of formation for the following compounds were taken from, or calculated from data in, the indicated references:

NaN_3,[23] $H_3O^+(g)$,[24] $NaBF_4$,[23] $CF_4(g)$,[25] $NH_4^+(g)$,[26] $NO_2^+(g)$,[27] $NaBH_4$,[28] XeO_3,[29] $XeO_4(g)$,[29] $CH_3COCH_3(g)$,[30] $CH_3CONH_2(g)$,[31] $CH_3CO_2H(g)$,[32] $CHF_3(g)$,[28] $\underline{n}\text{-}C_4H_9NH_2(g)$,[33] $C_6H_5NH_2(g)$,[34] $NaNH_2$,[35] $CN(g)$,[36] $NO_3(g)$,[37] $C_5H_5N(g)$,[38] $C_6H_6(g)$,[39] $\underline{n}\text{-}C_4H_9OH(g)$.[8] Ionization potentials for carbon compounds were taken from the compilation of Kiser.[41] In some cases heats of vaporization were estimated using Trouton's rule. Occasionally heats of sublimation were estimated by analogy; for example, the heat of sublimation of XeO_3 was assumed to be the same as that of $AsCl_3$.

The detailed calculations of nitrogen E_T values for $NH_3(s)$ and $NaNO_2(s)$ are given as examples. The thermo-equivalent reaction for $NH_3(s)$ is

$$NH_3(g) + O^+(g) \rightarrow OH_3^+(g) + N^{+*}(g) + e^-(g)$$

The standard heats of formation at 25° of $NH_3(g)$, $H_2O(g)$, $H^+(g)$, and $e^-(g)$ are -11.0, -57.8, 367.2, and 0 kcal/mole, respectively,[22] and the proton affinity of H_2O is 169 kcal/mole.[24] From these

data we calculate, for the thermochemical energy, E_T = -169 - 57.8 + 367.2 + 11.0 = 151 kcal/mole. The thermo-equivalent reaction for $NaNO_2(s)$ is

$$NaNO_2(s) + O^+(g) + O_3(g) \rightarrow 2O_3(s) + N^{+*}(g) + Na^+(g) + e^-(g)$$
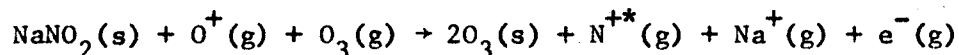
The standard heats of formation at 25° of $NaNO_2(s)$, $O_3(g)$, $Na^+(g)$, and $e^-(g)$ are -85.9, 34.0, 145.9, and 0 kcal/mole, respectively, and the sublimation energy of O_3 is 2.6 kcal/mole.[22] From these data we calculate E_T = -2x2.6 + 34.0 + 145.9 + 85.9 = 261 kcal/mole.

The calculation of the $U-2U_c-U_p$ values of Table VII is illustrated for the case of potassium iodide. From the heats of formation of $KI(s)$, $K^+(g)$, and $I^-(g)$ (-78.3, 123.0, and -47.0 kcal/mole, respectively[22]) we calculate U = 154.3 kcal/mole. From K - I distance in crystalline KI (3.526Å)[42] we calculate, using the Madelung expression, U_c = 164.6 kcal/mole. The polarization energy, U_p, is calculated from the following expression for a cation of charge q surrounded octahedrally at a distance $\underline{r}$ by six ions of polarizability α,[19]

$$U_p = \frac{6q\mu_i}{\underline{r}^2} - \frac{6(1.19)\mu_i^2}{\underline{r}^3} - \frac{6\mu_i^2}{2\alpha}$$

where $\mu_i = \dfrac{\alpha q}{\underline{r}^2 + 2.37\alpha/\underline{r}}$

By substituting q = 2, α = 6.45 X 10^{-24} cm^3,[43] and $\underline{r}$ = 3.526Å, we obtain U_p = 123.5 kcal/mole. Hence $U-2U_c-U_p$ = -298 kcal/mole.

References

(1) K. Siegbahn, C. Nordling, A. Fahlman, R. Nordberg, K. Hamrin, J. Hedman, G. Johansson, T. Bergmar, S.-E. Karlsson, I. Lindgren and B. Lindberg, "ESCA; Atomic Molecular and Solid State Structure Studied by Means of Electron Spectroscopy," Almqvist and Wiksells, Uppsala, 1967.

(2) J. M. Hollander, D. N. Hendrickson and W. L. Jolly, _J. Chem. Phys._, _49_, 3315 (1968).

(3) R. Nordberg, U. Celius, P. F. Hedén, J. Hedman, C. Nordling, K. Siegbahn and B. J. Lindberg, _Arkiv Kemi_.

(4) D. N. Hendrickson, J. M. Hollander and W. L. Jolly, to be published.

(5) Indeed, as will be shown later, there is no reason to expect a smooth correlation between binding energy and atomic charge for solid compounds. A smooth correlation would be expected only for isolated atoms – and in such cases the concept of fractional charge is hypothetical.

(6) C. S. Fadley, S. B. M. Hagstrom, M. P. Klein and D. A. Shirley, _J. Chem. Phys._, _48_, 3779 (1968).

(7) Waddington[8] has shown that uncertainties as great as ±30 kcal/mole are common when estimating the lattice energies of relatively simple binary compounds.

(8) T. C. Waddington, _Advances in Inorganic Chemistry and Radio-Chemistry_, _1_, 157 (1959).

(9) This statement is strictly true only for lattices in which interchange of the cations and anions yields an indistinguishable lattice, but this is a characteristic of most MX lattices.

(10) L. G. Parratt, Rev. Mod. Phys., 31, 616 (1959).

(11) A modified CNDO/1 version involving empirically evaluated repulsion integrals was used, as per P. M. Kuznesof and D. F. Shriver, J. Am. Chem. Soc., 90, 1683 (1968). Calculations were completed for each anion using the normal input parameters and also using contracted nitrogen $2s$ and $2p$ orbitals (the shielding parameter was decreased by 0.85, which is equivalent to removing the shielding of one nitrogen $1s$ electron). The difference in the total valence electron energies for these two cases is our estimated electronic relaxation energy. Neglect of core electron relaxation energies and charges in the valence electron bonding parameters and one-center kinetic and potential energies make this estimate very approximate.

(12) T. Koopmans, Physica, 1, 104 (1934); C. C. J. Roothaan, Rev. Mod. Phys., 23, 61 (1951).

(13) I. Tobias, R. J. Fallon, and J. T. Vanderslice, J. Chem. Phys., 33, 1638 (1960).

(14) S. Flügge, P. Walger, and A. Weiguny, J. Molec. Spec., 23, 243 (1967).

(15) This fact was pointed out to us by Professor D. H. Templeton. It is also discussed by Wells.[16]

(17) The Madelung constants for zinc-blende and CaF_2 are 1.638 and 2.519, respectively.

(18) The coulombic energy for inserting a +2 ion in a lattice is twice that for inserting a +1 ion in the same lattice.

(19) F. Basolo and R. G. Pearson, "Mechanisms of Inorganic Reactions," 2nd ed., John Wiley and Sons, Inc., New York, 1967, p. 62.

(20) Binding energies for the following elements were obtained from the indicated references; nitrogen,[1,2,4] carbon,[3] iodine.[6]

(21) J. M. Hollander, M. D. Holtz, T. Novakov, and R. L. Grahm, Arkiv. Fysik, 28, 375 (1965); T. Yamazaki and J. M. Hollander, Neuclear Physics, 84, 505 (1966).

(22) U. S. National Bureau of Standards Technical Notes 270-1 and 270-2 Gov. Printing Off., Washington, 1965 and 1966; U. S. National Bureau of Standards Circular 500, Gov. Printing Off., Washington, 1952.

(23) H. F. Halliwell and S. C. Nyburg, J. Chem. Soc., 4603 (1960).

(24) F. W. Lampe and F. H. Field, Tetrahedron, 7, 189 (1959); also see D. M. Bishop, J. Chem. Phys., 43, 4453 (1965).

(25) J. D. Cox, H. A. Gundry, and A. J. Head, Trans. Faraday Soc., 61, 1594 (1965).

(26) D. A. Johnson, "Some Thermodynamic Aspects of Inorganic Chemistry," Cambridge Univ. Press, 1968, p. 31

(27) M. I. Al-Jaboury and D. W. Turner, J. Chem. Soc., 4434 (1964); also see L. Burnelle, P. Beaudouin, and L. J. Schaad, J. Phys. Chem., 71, 2240 (1967) and P. Natalis and J. E. Collin, Chem. Phys. Letters, 2, 79 (1968).

(28) JANAF Thermochemical Tables prepared by the Joint Army-Navy-Air Force Thermochemical Panel under the Advanced Research Projects

Agency Program, U. S. Air Force.

(29) H. H. Claassen, "The Nobel Gases," D. C. Heath and Co., Boston, 1966, p. 56.

(30) R. Pennington and K. A. Kobe, _J. Am. Chem. Soc._, _79_, 300 (1957).

(31) M. Davies, A. H. Jones and G. H. Thomas, _Trans. Faraday Soc._, _55_, 1100 (1959).

(32) W. Weltner, Jr., _J. Am. Chem. Soc._, _77_, 3941 (1955).

(33) F. W. Evans, D. M. Fairbrother, and H. A. Skinner, _Trans. Faraday Soc._, _55_, 399 (1959).

(34) W. E. Halton, D. L. Hildenbrand, G. C. Sinke, and D. R. Stull, _J. Chem. Engr. Data_, _7_, 229 (1962).

(35) R. Juza, K. Fasold, and C. Haeberle, _Z. anorg. allgem. Chem._, _234_, 74 (1937).

(36) J. Berkowitz, W. A. Chupka, and T. A. Walter, _J. Chem. Phys._, _50_, 1497 (1969).

(37) I. C. Hisatsune, _J. Phys. Chem._, _65_, 2249 (1961).

(38) K. Li, _J. Phys. Chem._, _61_, 782 (1957).

(39) F. D. Rossini _et al_, "Selected Values of Physical Properties of Hydrocarbons and Related Compounds," Carnegie Press, Pittsburg, 1953.

(40) J. H. S. Green, _Chem. and Ind._, 12 15 (1960).

(41) R. W. Kiser, "Introduction to Mass Spectrometry and its Application," Prentice-Hall, Inc., Englewood Cliffs, N. J., 1965.

(42) A. F. Wells, "Structural Inorganic Chemistry," 3rd ed., Oxford, 1962, p. 357.

(43) J. A. A. Ketelaar, "Chemical Constitution," 2nd ed., Elsevier Publ. Co., Amsterdam, 1958, p. 91.

PART II.

AN INTERPRETATION OF THE PROTON
MAGNETIC RESONANCE SPECTRA OF PENTAAMMINES
OF COBALT(III), RHODIUM(III), AND IRIDIUM(III).

ABSTRACT

The proton magnetic resonance (pmr) spectra of some pentaammines of cobalt(III), rhodium(III), and iridium(III) have been studied in concentrated sulfuric acid. Only one non-solvent pmr peak was detected for rhodium and iridium pentaammines, whereas cobalt penta-ammines show two pmr peaks in the area ratio of four to one. Exchange with the solvent was eliminated as the explanation for the missing second pmr peak in the rhodium and iridium cases. This was accomplished by determining the "effective" proton concentration (by integration vs. a standard) of a certain rhodium pentaammine complex dissolved in concentrated sulfuric acid. Intramolecular proton exchange has also been excluded as the explanation for the missing rhodium and iridium pmr peaks by comparison of the temperature dependence of the widths of the pmr peaks observed for various cobalt, rhodium, and iridium ammine complexes. The loss of the 4:1 pmr pattern in the rhodium and iridium pentaammines, the trends in shifts observed for $Co(NH_3)_5X^{n+}$ as a function of X, and the additivity of effects observed for the cobalt complexes have been shown to be related to the magnitude and anisotropy of the "paramagnetic" shielding present in these complexes.

I. INTRODUCTION

Proton magnetic resonance (pmr) spectroscopy has been used to study some reactions of metal ammine complexes. Thus rates of proton-deuterium exchange on different ligands have been investigated in various solvents,[1,2] and the kinetics of solvolytic reactions of cobalt(III) ammines have been followed in sulfuric acid.[3] The mechanism of the aquation of the nitropentaamminecobalt(III) ion in sulfuric acid solutions has been conveniently studied by pmr coupled with visible spectrophotometry.[4] The base hydrolyses of trans-Co(NH$_3$)$_4$(^{15}NH$_3$)X^{2+} ions have been shown by pmr product analysis to involve a common intermediate.[5]

Applications of pmr to the identification of geometrical isomers of metal complexes have been reported.[6,7,8] The rates of conformational interchange of the ligand-metal rings in some cobalt ethylenediamine (en) complexes have been studied by pmr.[9] In the pmr spectra of cobalt(III) ammine complexes separate resonances have been observed for geometrically-different ammine groups.[1,3] For cobalt pentaammines the trans ammine protons generally occured upfield of the hexammine resonance, whereas the cis ammine protons were at lowfield. The chemical shift of a certain ammine proton in these complexes could be calculated assuming an additivity of five terms characteristic of the other five ligands and their geometric positions. Similar geometrical effects were found in the pmr spectra of bis (ethylenediamine) cobalt(III) complexes.[10]

In an attempt to understand the ammine proton chemical shifts in these cobalt(III) complexes, pmr studies were initiated on a series of rhodium(III) and iridium(III) pentaammines. Chemical shifts and line width-temperature data for some of these complexes are reported and interpreted in this work.

II. EXPERIMENTAL

Preparation of Complexes. - A sample of $[Rh(NH_3)_5Cl]Cl_2$ was prepared by a standard synthetic procedure.[11] Anal. Calcd for $[Rh(NH_3)_5Cl]Cl_2$: N, 23.79; H, 5.14; Cl, 36.13. Found: N, 23.96; H, 4.90; Cl, 36.06.

A sample of $[Rh(NH_3)_6](NO_3)_3$ was prepared by a modification of Jörgensen's recipe.[12] 1.09 g of $[Rh(NH_3)_5Cl]Cl_2$, dissolved in 20 ml. of concentrated aqueous ammonia, was sealed in a thick-walled (3mm) glass tube (volume $\approx$340 ml). This tube was held at 100° for 2 days in an oil bath; the yellow solution became colorless, and a white solid formed. The tube was opened; the mixture was added to water to dissolve the solid, and the resultant solution was boiled to eliminate excess ammonia. Addition of concentrated HNO_3 resulted in the immediate precipitation of the desired product. This white solid was recrystalized from a minimum of water, washed with ethanol and diethyl ether and air dried (1.13 g, 87% th. yield). Anal. Calcd for $[Rh(NH_3)_6](NO_3)_3$: N, 32.23; H, 4.64. Found: N, 32.48; H, 4.83.

A sample of $[Rh(NH_3)_5Br]Br_2$ was prepared by heating $[Rh(NH_3)_5 H_2O]Br_3$ at 110° for 3 hrs.[13] This later compound was obtained in a standard procedure.[14] Anal. Calcd for $[Rh(NH_3)_5Br]Br_2$: N, 16.37; H, 3.53; Br, 56.04. Found: N, 16.32; H, 3.70; Br, 56.42.

Samples of trans-$[Rh(NH_3)_4Cl_2]Cl$[15] and trans-$[Rh(en)_2Cl_2]NO_3$[15] were procured by standard synthetic procedures. In each case the

identity of the materials was determined by means of visible and ultraviolet absorption spectrophotometry.

The species $[M(NH_3)_5X]^{2+}$, $X = HSO_4^-$ or $ClSO_3^-$ and $M = Co$, Rh and Ir, were prepared in situ. The appropriate chloropentaammine chloride was treated with either concentrated H_2SO_4 or $ClSO_3H$; the reactions were easily followed by pmr.

A sample of $[Ir(NH_3)_5Cl]Cl_2$ was prepared by a modification of Palmaer's method.[16] An aqueous ammonia solution of $K_3(IrCl_6)\cdot3H_2O$ was heated in a sealed tube at $100°$ for ≈10 hours. The tube was cooled and opened. The desired product was obtained by evaporation of the excess ammonia from the solution and acidification with 12 $\underline{M}$ HCl. The resulting precipitate was washed with alcohol and ether and then oven dried (80% th. yield). Anal. Calcd for $[Ir(NH_3)_5$ $Cl]Cl_2$: Ir, 50.0; N, 18.25; H, 3.94; Cl, 27.76. Found: Ir, 50.1; N, 18.16; H, 4.07; Cl, 27.82.

Samples of $[Ir(NH_3)_5H_2O](ClO_4)_3$[16] and $[Ir(NH_3)_5NCS](ClO_4)_2$[17] were prepared by reported syntheses. Characterization of the materials was accomplished by ultraviolet spectrophotometry.[17]

A sample of $[Ru(NH_3)_5N_2](BF_4)_2$ was kindly provided by Dr. D. F. Harrison of Standford University.

Samples of $[Co(NH_3)_5CN](SO_4)$[18] and $[Co(NH_3)_5NCS](NCS)_2$[19] were prepared by reported syntheses.

Proton Resonance Measurements. – All measurements were made with a Varian A-60 spectrometer in either concentrated H_2SO_4 or $ClSO_3H$ solutions. Temperature studies were made using a Varian V-6040 unit;

15 minutes equilibration time was allowed at each temperature setting.

III. RESULTS

Chemical Shifts. - Proton chemical shifts vs. external TMS were
determined for a series of rhodium(III) and iridium(III) ammine
complexes dissolved in concentrated sulfuric acid. The results are
given in Table I along with previously determined chemical shift
values for the analogous cobalt(III) complexes. Two new cobalt
pentaammines are also included. As can be seen in Table I, only
one non-solvent pmr peak could be detected for rhodium and iridium
pentaammines, whereas the cobalt pentaammines typically show two
peaks in the ratio of four to one. The cobalt ammine resonances
(averaging the cis and trans values) occur at the highest field,
and the iridium ammine resonances occur at the lowest field.

Spectra of the $Ru(NH_3)_5N_2^{2+}$ ion dissolved in formamide and in
66 wt. % H_2SO_4 were obtained. In each case a 1:4 pattern was observed;
in 66 wt. % H_2SO_4 the two non-solvent peaks were observed at δ = -2.87
(cis ammine protons) and δ = -3.58 (trans ammine protons) vs.
external TMS. By rapid manipulation it was possible to observe a
similar 1:4 pattern in concentrated H_2SO_4 (δ = -2.62 and δ = -3.29).
It was possible to recover the nitrogen compound from both solvents;
identification was achieved by the characteristic N-N stretching
frequency in the ir spectrum.[20]

Solvolytic Reactions.- Dissolution of either $[Rh(NH_3)_5Cl]Cl_2$ or

TABLE I.

Proton Chemical Shifts of Some
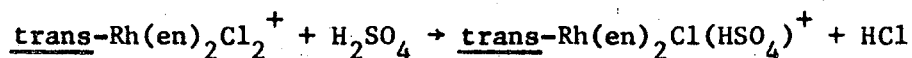### Ammine Complexes in Concentrated Sulfuric Acid

Complex	Chemical Shift(ppm) vs. ext. TMS		
	Co(III)	Rh(III)	Ir(III)
$M(NH_3)_6^{3+}$	-3.59[a]	-3.82	
$M(NH_3)_5HSO_4^{2+}$	-4.24 cis[a]	-4.13	4.80
	-2.75 trans		
$M(NH_3)_5H_2O^{3+}$	-4.16 cis[a]		-4.68
	-2.92 trans		
$M(NH_3)_5Cl^{2+}$	-3.76 cis[a]	-3.78	-4.55
	-3.10 trans		
$M(NH_3)_5Br^{2+}$	-3.65 cis[a]	-3.80	
	-3.17 trans		
$M(NH_3)_5NO_2^{2+}$	-3.59[a]		
$M(NH_3)_5NCS^{2+}$	-3.99 cis		-4.58
	-3.54 trans		
$M(NH_3)_5CN^{2+}$	-3.38 cis		
	-4.27 trans		
trans-$M(NH_3)_4Cl_2^{+}$	-3.93[a]	-3.85	
	-5.22 NH_2	-4.60 NH_2	
trans-$M(en)_2Cl_2^{+}$	-3.65 CH_2	-3.18 CH_2	

[a] See reference 3.

[Rh(NH$_3$)$_5$Br]Br$_2$ in concentrated H$_2$SO$_4$ gave solutions with one-peaked pmr spectra (excluding the solvent peak). When these solutions were kept for a few days, a second peak appeared to low field of the initial peaks. This latter peak occured at the same field (δ = -4.13 vs. external TMS) for both solutions and was assumed to be the resonance for Rh(NH$_3$)$_5$HSO$_4$$^{2+}$ in analogy with the cobalt complexes.[3] In the case of the Co(NH$_3$)$_5$Cl^{2+} ion, formation of the bisulfatopenta-ammine complex in concentrated H$_2$SO$_4$ was found to have a half-time of 4 hours at room temperature when dry air was bubbled through the solution.[3] In the case of the rhodium complex the solvolysis was so slow that it required $\approx$1 day of heating at 70° with dry air bubbling to complete the formation of the bisulfato complex. The chloropenta-ammineiridium complex required even higher temperatures and a longer time to effect completion.

The pmr spectrum of both trans-[Rh(NH$_3$)$_4$Cl$_2$]Cl and trans-[Rh(en)$_2$ Cl$_2$]Cl in concentrated H$_2$SO$_4$ as a function of time indicated that solvolytic reactions were occuring. In the case of the ethylenedi-amine complex the reaction was probably.

$$\text{trans-Rh(en)}_2\text{Cl}_2{}^+ + \text{H}_2\text{SO}_4 \rightarrow \text{trans-Rh(en)}_2\text{Cl(HSO}_4)^+ + \text{HCl}$$

A second "NH$_2$" peak appeared at δ = -4.89 while the "CH$_2$" peak at δ = -3.18 remained unchanged. Identification of the initial complex observed in the pmr was achieved by visible absorption spectroscopy. The identity of the solvolytic product was not definitely established.

It was found that the rate of solvolysis of trans- [Rh(en)$_2$Cl$_2$]Cl in concentrated H$_2$SO$_4$ (as measured by pmr) was acid catalyzed, the rate more than doubling by changing the weight percent of H$_2$SO$_4$ from 85 to 95%.

In the case of the trans-Rh(NH$_3$)$_4$Cl$_2$$^+$ ion in concentrated H$_2$SO$_4$ two solvolytic products were indicated by pmr. With time the pmr spectrum of this complex dissolved in concentrated H$_2$SO$_4$ showed a second peak at δ = -4.10 and eventually a third peak at δ = -4.53 vs. external TMS .

Exchange With the Solvent. - The missing second peak in a pmr spectra for rhodium and iridium pentaammines could be attributed to rapid exchange of the trans ammine hydrogens with the solvent. In that event the smaller peak (as observed in the cobalt case) would shift and merge with the large solvent peak. The probability of an increased trans-ammine-proton solvent exchange rate in going down the cobalt triad seems unlikely, for Palmer and Basolo[21] have found that for proton exchange with the solvent, the ratio of rates for Co(NH$_3$)$_6$$^{3+}$, Rh(NH$_3$)$_6$$^{3+}$, and Ir(NH$_3$)$_6$$^{3+}$ is approximately 100:15:1, respectively. To check this possibility, the "effective" proton concentration of a rhodium pentammine complex was determined. Solutions of measured amounts of [Rh(NH$_3$)$_5$Br]Br$_2$ (selected for its purity) and NH$_4$Br in concentrated H$_2$SO$_4$ were prepared. Integration of the single rhodium ammine peak vs. the NH$_4$$^+$ signal for 4 different solutions showed that all of the protons in the complex were accounted for in the single peak (the ratio of (H)$_{NH_4Br}$ to (H)$_{complex}$ was

observed to be 0.98 ±0.06 when the theoretical was set at 1.00 and

1.25 for the pentaammine and tetraammine cases, respectively).

Intramolecular Exchange. - Another conceivable explanation for

the loss of the second peak for the rhodium and iridium pentaammines

is intramolecular exchange of the protons and/or the ammonias

between the cis and trans sites. Experiments can be performed to

rule out intramolecular proton exchange. The pmr of a $Rh(^{15}NH_3)_5X^{n+}$

complex would be a check for the existence of exchange. The presence

of a doublet (due to coupling with the ^{15}N atom) in the pmr spectrum

of this complex would rule out intramolecular proton exchange,

but unfortunately the cost of preparing such a complex is prohibitive.

In this work, however, we elected to study the temperature dependence

of the line width of pmr peaks for various ammine complexes. The

line width of a metal ammine pmr peak is affected by various factors:

nuclear dipole-dipole interactions, nitrogen quadrupole interaction

and chemical exchange.[22] In the case of the cobalt(III) pentaammines

rapid intramolecular proton chemical exchange does not occur (as

shown by the 4:1 pattern). Comparison of the temperature dependence

of the width of the pmr peaks of these complexes with that obtained

for some of the analogous rhodium and iridium complexes can show

whether intramolecular proton chemical exchange is occuring in the

rhodium and iridium pentaammines.

The temperature dependence of the ammine proton line width is

shown in Figure 1 for concentrated H_2SO_4 and $ClSO_3H$ solutions of the

ions $Co(NH_3)_6^{3+}$ and $Rh(NH_3)_6^{3+}$. In both solvents the plots of log
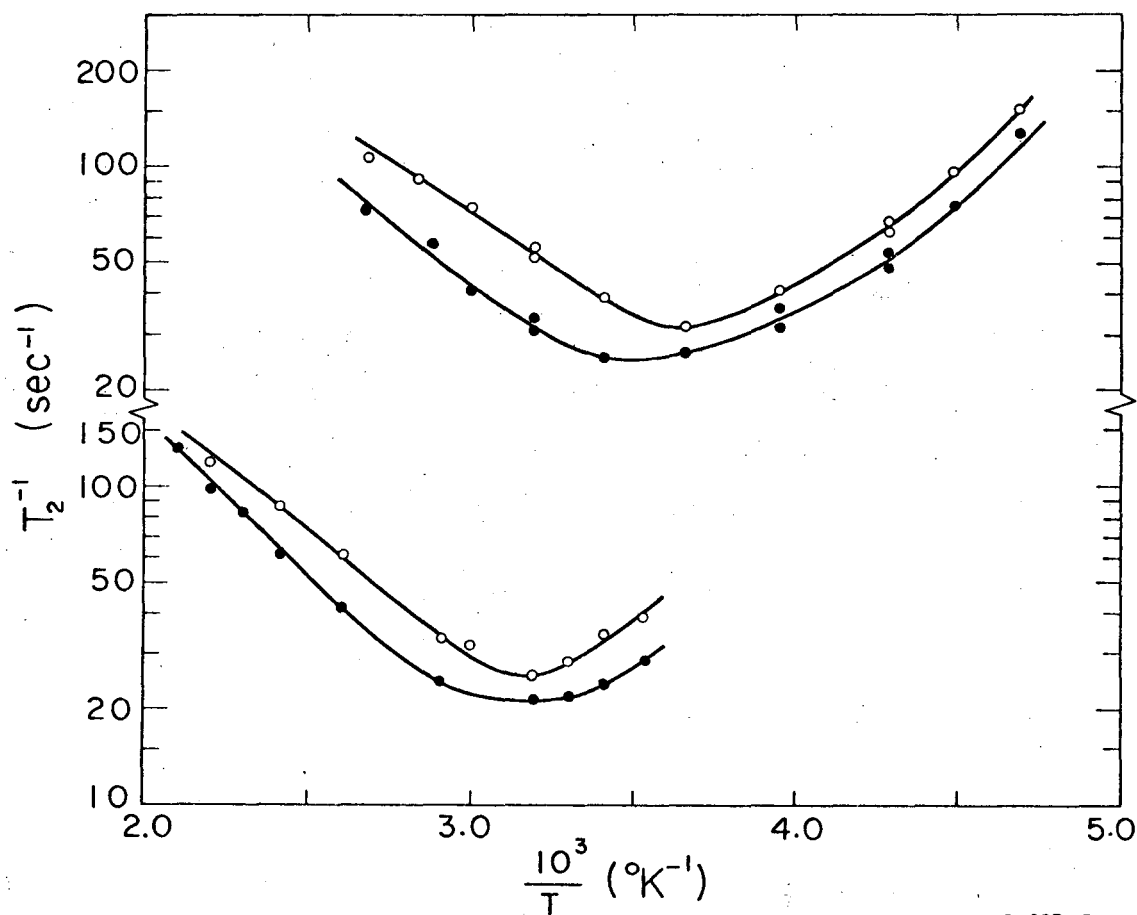
XBL697- 3182

Figure 1. The temperature dependence of log (T_2^{-1}) for solutions of $Co(NH_3)_6^{3+}$ and $Rh(NH_3)_6^{3+}$ in $ClSO_3H$ (upper curves) and concentrated H_2SO_4 (lower curves). The symbols ● and o refer to $Rh(NH_3)_6^{3+}$ and $Co(NH_3)_6^{3+}$, respectively.

T_2^{-1} (T_2^{-1} is the reciprocal of the effective spin-spin relaxation time, given by one-half the width of a peak at half-height in radians per sec.) vs. the reciprocal temperature seem to show two limiting regions. In the low-temperature region the width of a peak decreases as the temperature increases. This is the type of dependence expected for dipolar relaxation.[22] In the high-temperature region the width of a peak increases with increasing temperature. This type of temperature dependence is the expected one for a nitrogen proton when only a single peak is observed.[22,23] The increased molecular tumbling at higher temperature uncouples the nitrogen nuclear quadrupole moment from the electric field gradient; this results in a reduced probability of transition within the nitrogen spin system. The overall effect is that we start at lower temperatures with a single peak where the proton "sees" a rapidly flipping nitrogen spin system, the peak broadens as the probability of transition in the nitrogen spin system is reduced, and eventually at high enough temperatures a triplet is seen.[23]

The similarity of the pmr peak width vs. temperature curves for the $Co(NH_3)_6^{3+}$ and $Rh(NH_3)_6^{3+}$ ions tends to indicate that the same relaxation processes and interruptive mechanisms are operative. In the case of the bisulfato and chlorosulfato pentaammines of cobalt, rhodium and iridium the same type of temperature curves have been found (see Figures 2 and 3). It seems clear then that we cannot attribute the loss of the second peak in the rhodium and iridium pentaammines to intramolecular proton exchange. If this exchange
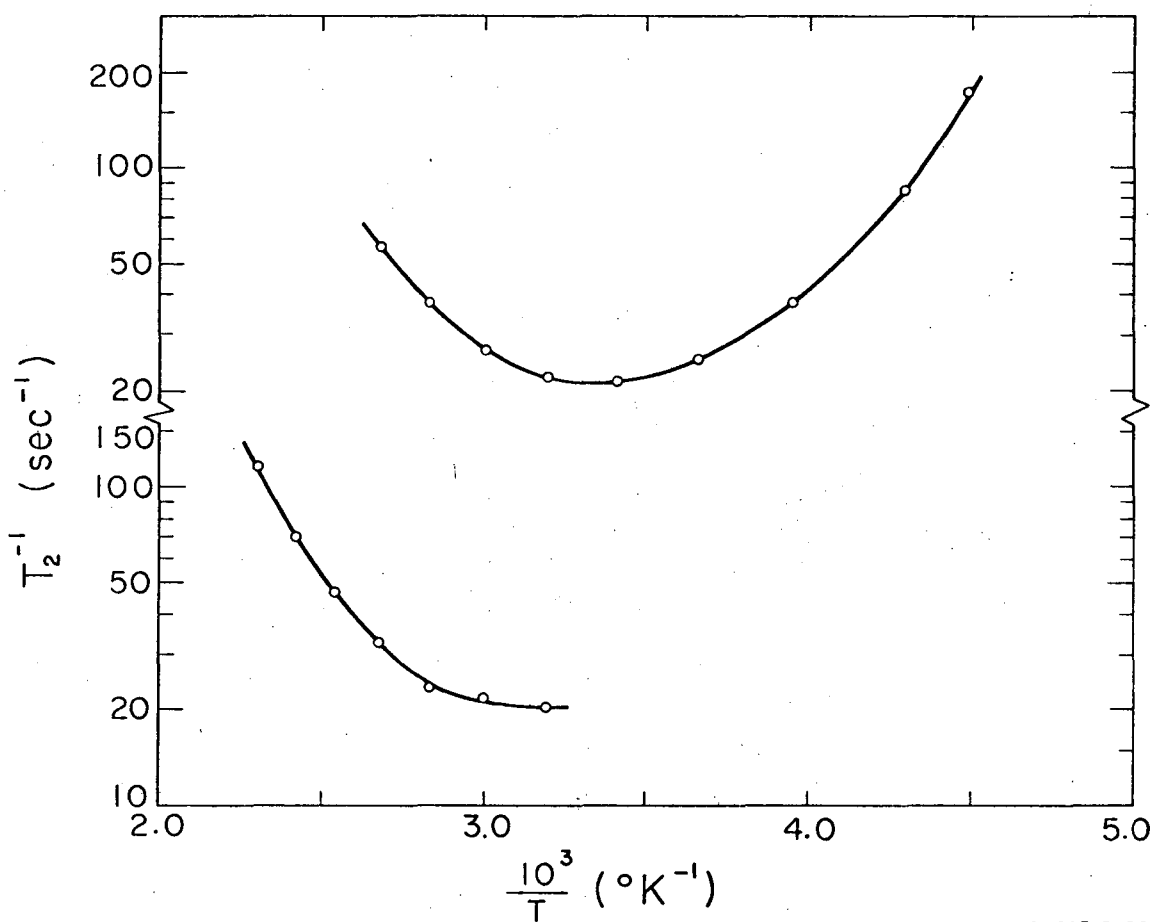
XBL697-3180

Figure 2. The temperature dependence of log (T_2^{-1}) for a $ClSO_3H$ solution (upper curve) of $Co(NH_3)_5(ClSO_3)^{2+}$ and for a concentrated H_2SO_4 solution (lower curve) of $Co(NH_3)_5(HSO_4).^{2+}$
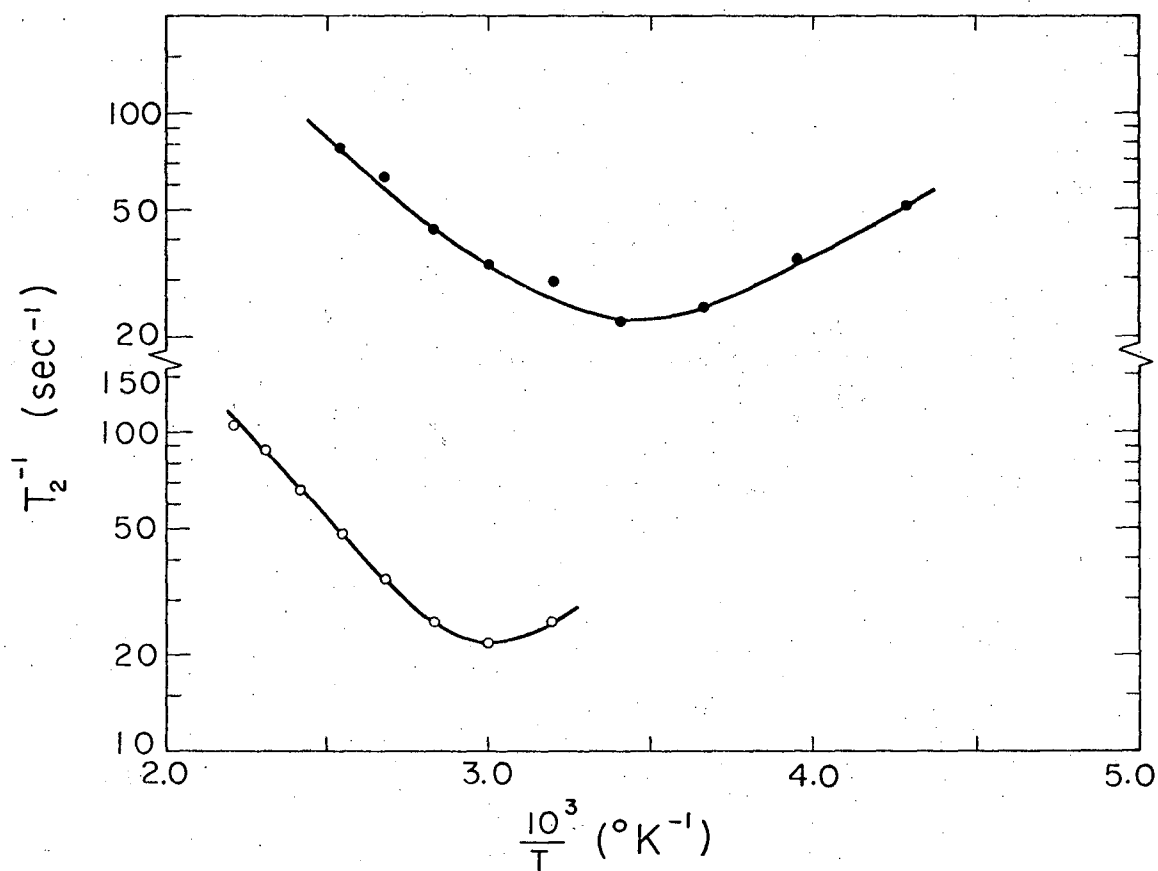
Figure 3. The temperature dependence of log (T_2^{-1}) for a $ClSO_3H$

solution (upper curve) of $Rh(NH_3)_5(ClSO_3)^{2+}$ and for a

concentrated H_2SO_4 solution (lower curve) of $Ir(NH_3)_5$

$(HSO_4).^{2+}$

were occuring at such a rate as to give only one peak, it would not be possible to observe broadening as the temperature is raised for the rhodium and iridium pentaammines. This would be true since raising the temperature would increase intramolecular proton exchange and the protons would still see only the averaged nitrogen spin system.

Another possible explanation for the loss of the second peak is intramolecular exchange of the NH_3 groups. The likelihood of intramolecular NH_3 group exchange in the rhodium and iridium penta- ammines is diminished somewhat by the reported isolation of cis and trans isomers of some rhodium and iridium tetraammine complexes. The temperature dependence of the line width as reported above could be evidence against intramolecular NH_3 exchange under certain conditions. If the exchange of an ammonia from a cis to the trans position in a pentaammine resulted in appreciably different shielding for the nitrogen atom, rapid exchange would increase the transition probability in the nitrogen spin system. Increasing the temperature would then tend to decrease the width of the peak for the proton attached to this nitrogen atom. In fact we have observed that increasing the temperature increases the width of the ammine-proton peaks of the rhodium and iridium complexes.

IV. DISCUSSION

Any interpretation of the pmr spectra of cobalt(III), rhodium (III), and iridium(III) pentaammines must explain the loss of the

4:1 pattern in the latter two cases. Also, trends in shifts observed for $Co(NH_3)_5X^{n+}$ as a function of X and the additivity of effects observed for the cobalt complexes[3] should be explained.

Proton exchange with the solvent has been shown not to occur in the rhodium and iridium pentaammines. The observed temperature dependence of the pmr line width for rhodium and iridium pentaammines excludes the possibility of _intramolecular_ proton exchange as an explanation for the loss of the 4:1 pmr pattern. _Intramolecular_ NH_3 group exchange seems improbable. It seems that the degeneracy of chemical shifts observed in these complexes is a manifestation of the electronic structure of the complexes.

It is well known that the effective magnetic field felt by a nucleus in a molecule which is in an external magnetic field is a function of electron densities in the various parts of the molecule. Using second-order perturbation theory, Ramsey obtained a two-term expression for the "shielding constant" σ.[24] In a solution where the molecule is rapidly tumbling, the shielding constant is given by

$$\sigma = \text{average}_\lambda \ \sigma_\lambda = \frac{e^2}{3mc^2} \ \langle o | \sum_k \frac{1}{r_k} | o \rangle$$

$$-2 \ \text{average}_\lambda \ \sum_n' \ (\frac{1}{E_n - E_o}) \ \langle o | \sum_k \frac{m_{zk}^2}{r_k^3} | n_\lambda \rangle$$

Here σ is an average over all orientations of some value σ_λ obtained for one particular orientation of the nuclear magnetic dipole σ and the static magnetic field H. The sums are over the k electrons in

the molecule and the excited state wave functions $\langle n|$. The operator m_{zk}° is the usual angular momentum operator.

$$m_{zk}^{\circ} = \frac{eh}{2mci} \left(x_k \frac{\partial}{\partial y_k} - y_k \frac{\partial}{\partial x_k} \right)$$

The first term in the shielding constant expression corresponds to the diamagnetic circulation of the electrons about the nucleus. This ground state term (i.e. $\langle o|$) represents the shielding of the nucleus by the nearby electron density; it would be sensitive to inductive effects of neighboring atoms as they influence the electron density about the nucleus of interest.

The second term in the expression for the shielding constant is called the "paramagnetic" term and is due to admixture of excited states $\langle n|$ with the ground state $\langle o|$ under the influence of the magnetic field. According to Ramsey this might physically correspond in part to the fact that the presence of attracting centers from several different massive nuclei prevents a simple diamagnetic circulation of electrons about any one nucleus. When there is a low-lying excited state (i.e. small $E_n - E_o$) of proper symmetry, the second term can dominate the shielding parameter as it probably does in the case of ^{19}F, ^{14}N, ^{17}O, etc.[25]

It is the intention of this discussion to indicate how the "paramagnetic" term in the shielding constant provides an explanation for the loss of the 4:1 pmr pattern for the rhodium and iridium pentaammines as well as other experimental observations. At the onset we note that <u>cobalt</u> chemical shifts measured for various

cobalt $\underline{d}^6$ complexes have been shown to be dominated by a paramagnetic contribution from the low-lying $^1T_{1g}$ excited state.[26] This same "paramagnetism" centered at the cobalt nucleus would be expected to influence the shielding for ammine protons in the cobalt pentaammines, but of course the greater electron distance (i.e. greater r_k in the second term) would result in a marked reduction in the shielding influence. Along similar lines the large upfield chemical shifts observed for hydridic protons in metal hydride complexes have been shown to be attributable to the "paramagnetism" induced in the metal atom by the static magnetic field.[27]

Fung[28] has shown that the proton chemical shift $\underline{vs.}$ free NH_3 for the $Co(NH_3)_6^{3+}$ ion is reasonable considering the estimated (via an M.O. calculation by Cotton and Haas[29]) electron density on the proton in this complex. If, as expected, coordination of NH_3 to Rh(III) and Ir(III) results in even a greater decrease of electron density around the hydrogen, then a shift to a field even lower than that observed for $Co(NH_3)_6^{3+}$ would result. Experimentally this is what is observed (see Table I). Recent results of nitrogen x-ray photoelectron spectroscopy[30] have indicated that the nitrogen atom in Rh(III) and Ir(III)-coordinated NH_3 has a somewhat more positive charge than that in the Co(III) ammine. It seems then that the chemical shifts of the cobalt triad hexammines can probably be understood by considering only the diamagnetic term in the shielding constant expression. However, the disappearance of the 4:1 pmr patterns in the rhodium and iridium pentaammines cannot be explained

with this same term; the influence of the "paramagnetic" term must be considered.

The "paramagnetic" term in the shielding constant expression is approximately proportional to the inverse of the ligand field stabilization energies (measured by $\Delta = 10Dq$) in the three different metal complexes and is also proportional to some magnetic moment integrals that depend on inverse cubes of distances. Thus in the case of iridium the Δ value (i.e. $E_n - E_o$) is the greatest and the $<o|\sum_k \frac{m_k^2}{r_k^3}|n>$ value the smallest; this results in very little contribution from the second term to the σ for iridium ammine protons. The values for the m_k^2/r_k^3 integrals are smallest in the iridium case, for the distance from the proton nucleus to the mainly-metal t_{2g} electron (i.e. r_k) is largest. The cis and trans ammine protons in an iridium pentaammine would only be affected by the diamagnetic term and therefore would probably occur at the same field position. These protons would only feel the sixth group X by inductive effects transferred through the iridium atom. In the case of the rhodium pentaammines the "paramagnetic" contribution to the proton shielding would still probably be negligible and as such we would only see a single peak.

When the "paramagnetic" term becomes important it would be possible to see any anisotropy in the term. The cis and trans ammine protons in a cobalt pentaammine could experience different effective magnetic fields due to the paramagnetic term. In an octahedral $\underline{d}^6$ cobalt complex the $^1T_{1g}$ state will be mixed with the $^1A_{1g}$ ground state under the influence of the magnetic field. Lowering the

symmetry to C_{4v} in a pentaammine splits the $^1T_{1g}$ to ^1E and $^1A_2$ states. Admixture of these two low-energy mainly-metal states with the ground state of the cobalt pentaammines will be the main source of the "paramagnetism". Whether or not a _trans_ proton resonates at higher field than a _cis_ proton in a particular $Co(NH_3)_5X^{n+}$ ion will depend on the difference in cobalt susceptibility when the magnetic field is directed parallel or perpendicular to the symmetry axis of the pentaammine.

The paramagnetic contribution to the shielding constant for a proton can be represented as some average $\sigma = \frac{1}{3}(\sigma_{xx} + \sigma_{yy} + \sigma_{zz})$.[22,27] In the pentaammines the ^1E state contributes to $\sigma_{x'x'}$ and $\sigma_{y'y'}$ whereas the $^1A_2$ state contributes to $\sigma_{z'z'}$ (x', y', z' are given here for local coordinates about the metal where the z' -axis is the symmetry axis of the pentaammine). In a series of complexes, $Co(NH_3)_5X^{n+}$, the energy of the ^1E state varies appreciably while that for the $^1A_2$ does not.[27] If we consider the _trans_ ammine protons in $Co(NH_3)_5X^{n+}$, variation of X will result in only $\sigma_{x'x'}$ and $\sigma_{y'y'}$ changing. The geometric position of the _trans_ ammine proton is such that both $\sigma_{x'x'}$ and $\sigma_{y'y'}$ will shield the proton. Thus the shielding should increase for the trans proton as the ligand field strength of X decreases [i.e. $E(^1E)-E(^1A_1)$ becomes smaller in the paramagnetic term]. This is what is observed in Table I.

Consideration of the shielding of the cobalt _cis_ ammine protons shows that when X is varied the same trend would not be expected. Here one of the directions perpendicular (i.e. the $\sigma_{x'x'}$ or $\sigma_{y'y'}$ term) to the Co-X axis will be directed along the Co-N bond for the partic-

ular cis proton. The paramagnetism induced in the metal center when the magnetic field is so oriented will produce deshielding at the cis ammine proton. If this deshielding outweighs the shielding, a chemical shift trend opposite to that observed for the trans protons would result-- the cis ammine protons would be expected to resonate at lower fields for weaker-field ligands X. This is the observed behavior (see Table I).

Predictions would then be that the trans protons resonate at higher field for weaker-field ligands X in $Co(NH_3)_5X$, whereas the opposite trend would be possible for the cis protons. In the case of the trans ammine protons in $Co(NH_3)_5X^{n+}$ the chemical shifts run from high field values for weak ligands (X = HSO_4^-, H_2O) to low field values for strong ligands (X = NO_2^-, SCN^-, and CN^-). It would be unreasonable to expect the cis and trans trends to exactly follow the "spectrochemical series" because in evaluating the integrals in the shielding expression the exponential behavior of the metal radial functions might vary. Similar variances were noted by Buckingham and Stephens in their analysis of metal hydride chemical shifts.[27] The overall result of the cis and trans trends is that we encounter a 4:1 pattern for weak-field X's and a 1:4 pattern for strong-field (i.e. back-bonding) X's.

The 1:4 pmr pattern observed for the $Ru(NH_3)_5N_2^{2+}$ ion perhaps gives some insight into the bonding characteristics of the N_2 ligand. The only other 1:4 pmr pattern observed was that for the $Co(NH_3)_5CN^{2+}$ ion. The CN^- ligand (isoelectronic with N_2) is supposedly a good

metal-to-ligand π back-bonding ligand. The fact that we do see two peaks in the case of this Ru(II) complex is not surprising, because Ru(II) would be expected to have low ligand field stabilization energies (relative to Rh(III) and Ir(III)) as does Co(III).[31]

Finally, the additivity of chemical shielding in the cobalt pentaammines and tetraammines[3] is probably just a manifestation of the average environment concept for ligand field splittings. Thus the ΔE (10Dq) value is just some additive function of the six ligands about the metal.

ACKNOWLEDGEMENTS

It is a pleasure to express my appreciation to the many people who have given me ideas and advice. In particular, I thank my advisor, Professor William L. Jolly, for his critical guidance throughout my graduate studies and especially for his introduction (albeit forceful) to the Sierra.

I owe a special debt of gratitude to Drs. Jack M. Hollander and Chuck S. Fadley for their encouragement and expert guidance in various experimental aspects.

The warmest thanks go to the Jolly groupers for providing many a springboard for certain non-academic activities.

Above all, I would like to express my deepest appreciation to my wife, Sherry, without whom this work would not have been possible.

REFERENCES TO PART II.

(1) P. Clifton and L. Pratt, Proc. Chem. Soc., 339 (1963).

(2) D. A. Buckingham, L. G. Marzailli, and A. M. Sargeson, J. Am. Chem. Soc., 90, 6028 (1968), and references therein.

(3) W. L. Jolly, A. D. Harris, and T. S. Briggs, Inorg. Chem., 4, 1064 (1965).

(4) A. D. Harris, R. Stewart, D. Hendrickson, and W. L. Jolly, ibid., 6, 1052 (1967).

(5) D. A. Buckingham, I. I. Olsen, and A. M. Sargeson, J. Am. Chem. Soc., 89, 5129 (1967).

(6) R. C. Fay and T. S. Piper, Inorg. Chem., 3, 348 (1964), and references therein.

(7) A. Chakrovorty and R. H. Holm, ibid., 3, 1521 (1964).

(8) J. I. Legg and D. W. Cooke, ibid., 4, 1577 (1965).

(9) B. M. Fung, J. Am. Chem. Soc., 89, 5788 (1967), and references therein.

(10) J. R. Lantzke and D. W. Watts, Aust. J. Chem., 20, 35 (1967).

(11) S. N. Anderson and F. Basolo, Inorg. Syn., 7, 216 (1963).

(12) S. M. Jøogensen, J. Prak. Chem., 44, 49 (1891).

(13) S. M. Jørgensen, ibid., 27, 453, 462 (1883).

(14) S. M. Jørgensen, ibid., 34, 399 (1886).

(15) S. N. Anderson and F. Basolo, Inorg. Syn., 7, 217, 218 (1963).

(16) W. Palmaer, Z. Anorg. Allgem. Chem., 10, 320 (1895).

(17) H.-H. Schmidtke, Inorg. Chem., 5, 1682 (1966).

(18) H. Siebert, _Z. Anorg. Allgem. Chem._, **327**, 63 (1964).

(19) A. Werner, _Z. Anorg. Allgem. Chem._, **22**, 91 (1900).

(20) A. D. Allen, F. Bottomley, R. O. Harris, V. P. Reinsalu and C. V. Senoff, _J. Am. Chem. Soc._, **89**, 5595 (1967).

(21) J. W. Palmer and F. Basolo, _J. Inorg. Nucl. Chem._, **15**, 279 (1960).

(22) J. A. Pople, W. G. Schneider and H. J. Bernstein, "_High-Resolution Nuclear Magnetic Resonance_," McGraw-Hill, New York, 1959. We will not consider the chemical anisotropy broadening, for it will probably be small.

(23) J. D. Roberts, _J. Am. Chem. Soc._, **78**, 4495 (1956).

(24) N. F. Ramsey, _Phys. Rev._, **78**, 699 (1950).

(25) For example see A. Saika and C. P. Slichter, _J. Chem. Phys._, **22**, 26 (1954).

(26) J. S. Griffith and L. E. Orgel, _Trans. Faraday Soc._, **53**, 601 (1957).

(27) A. D. Buckingham and P. J. Stephens, _J. Chem. Soc._, 2747 (1964).

(28) B. M. Fung, _J. Phys. Chem._, **72**, 4708 (1968).

(29) F. A. Cotton and T. E. Haas, _Inorg. Chem._, **3**, 1004 (1964).

(30) D. N. Hendrickson, J. M. Hollander, and W. L. Jolly, unpublished data.

(31) C. K. Jorgensen, "Absorption Spectra and Chemical Bonding in Complexes," Chapter 7, Pergamon Press (1962).